Supplementary Information

Surface phase structure evolution of the fcc MoC (001) surface in steam reforming atmosphere: systematic kinetic and thermodynamic investigations

Changqing Chu,*[ab] Chao Li,[cd] Xue Liu,[c] Hang Zhao,[c] Changning Wu,[b] Junguo Li,[b] Ke Liu*, [bc] Qi Li[e] and Daofan Cao*[f]

[a.] *Qingdao Univ Sci & Technol, Inst Climate Change & Energy Sustainable Dev, Qingdao 266061, Peoples R China E-mail: chucq@sustech.edu.cn*

[b.] *Academy for Advanced Interdisciplinary Studies, Southern University of Science and Technology, 1088 Xueyuan Avenue, Shenzhen 518055, P.R. China. E-mail: chucq@sustech.edu.cn*

[c.] *Department of Chemistry, College of Science, Southern University of Science and Technology, 1088 Xueyuan Avenue, Shenzhen 518055, P.R. China. E-mail: liuk@sustech.edu.cn*

[d.] *Harbin Institute of Technology, Harbin, 150080, China.*

[e.] *Shenzhen Gas Corporation Ltd., Shenzhen, 518049, PR China*

[f.] *Birmingham Centre for Energy Storage (BCES) & School of Chemical Engineering, University of Birmingham, UK B15 2TT. E-mail: dxc816@student.bham.ac.uk*

List of methods details, Figures and Tables

Fig. S17 Configurations of H_2O* (8/9 ML, based on number of surface Mo sites) and surface binding energy without ZPE correction. Gas phase H_2O and H_2 as reference

Fig. S18 Configurations of H_2O* (1 ML, based on number of surface Mo sites) and surface binding energy without ZPE correction. Gas phase H_2O and H_2 as reference

Fig. S19 Configurations of OH* (1/9 ML, based on number of surface Mo sites) and surface binding energy without ZPE correction. Gas phase H_2O and H_2 as reference.

Fig. S20 Configurations of OH* (2/9 ML, based on number of surface Mo sites) and surface binding energy without ZPE correction. Gas phase H_2O and H_2 as reference.

Fig. S21 Configurations of OH* (1/3 ML, based on number of surface Mo sites) and surface binding energy without ZPE correction. Gas phase H_2O and H_2 as reference.

Fig. S22 Configurations of OH* (4/9 ML, based on number of surface Mo sites) and surface binding energy without ZPE correction. Gas phase H_2O and H_2 as reference.

Fig. S23 Configurations of OH* (5/9 ML, based on number of surface Mo sites) and surface binding energy without ZPE correction. Gas phase H_2O and H_2 as reference

Fig. S24 Configurations of OH* (2/3 ML, based on number of surface Mo sites) and surface binding energy without ZPE correction. Gas phase H_2O and H_2 as reference

Fig. S25 Configurations of OH* (7/9 ML, based on number of surface Mo sites) and surface binding energy without ZPE correction. Gas phase H_2O and H_2 as reference

Fig. S26 Configurations of OH* (8/9 ML, based on number of surface Mo sites) and surface binding energy without ZPE correction. Gas phase H_2O and H_2 as reference

Fig. S27 Configurations of OH* (1 ML, based on number of surface Mo sites) and surface binding energy without ZPE correction. Gas phase H_2O and H_2 as reference

Fig. S28 Configurations of O* (1/9 ML, based on number of surface Mo sites) and surface binding energy without ZPE correction. Gas phase H_2O and H_2 as reference

Fig. S29 Configurations of O* (2/9 ML, based on number of surface Mo sites) and surface binding energy without ZPE correction. Gas phase H_2O and H_2 as reference

Fig. S30 Configurations of O* (1/3 ML, based on number of surface Mo sites) and surface binding energy without ZPE correction. Gas phase H_2O and H_2 as reference

Fig. S31 Configurations of O* (4/9 ML, based on number of surface Mo sites) and surface binding energy without ZPE correction. Gas phase H_2O and H_2 as reference

Fig. S32 Configurations of O* (5/9 ML, based on number of surface Mo sites) and surface binding energy without ZPE correction. Gas phase H_2O and H_2 as reference

Fig. S33 Configurations of O* (2/3 ML, based on number of surface Mo sites) and surface binding energy without ZPE correction. Gas phase H_2O and H_2 as reference

Fig. S34 Configurations of O* (7/9 ML, based on number of surface Mo sites) and surface binding energy without ZPE correction. Gas phase H_2O and H_2 as reference

Fig. S35 Configurations of O* (8/9 ML, based on number of surface Mo sites) and surface binding energy without ZPE correction. Gas phase H_2O and H_2 as reference

Fig. S36 Configurations of O* (1 ML, based on number of surface Mo sites) and surface binding energy without ZPE correction. Gas phase H_2O and H_2 as reference

Fig. S37 Configurations of H* (1/9 ML, based on number of surface Mo sites) and surface binding energy without ZPE correction. Gas phase H_2O and H_2 as reference

Fig. S38 Configurations of H* (2/9 ML, based on number of surface Mo sites) and surface binding energy without ZPE correction. Gas phase H_2O and H_2 as reference

Fig. S39 Configurations of H* (1/3 ML, based on number of surface Mo sites) and surface binding energy without ZPE correction. Gas phase H_2O and H_2 as reference

Fig. S40 Configurations of H* (4/9 ML, based on number of surface Mo sites) and surface binding energy without ZPE correction. Gas phase H_2O and H_2 as reference

Fig. S41 Configurations of H* (5/9 ML, based on number of surface Mo sites) and surface binding energy without ZPE correction. Gas phase H_2O and H_2 as reference

Fig. S42 Configurations of H* (2/3 ML, based on number of surface Mo sites) and surface binding energy without ZPE correction. Gas phase H_2O and H_2 as reference

Fig. S43 Configurations of H* (7/9 ML, based on number of surface Mo sites) and surface binding energy without ZPE correction. Gas phase H_2O and H_2 as reference

Fig. S44 Configurations of H* (8/9 ML, based on number of surface Mo sites) and surface binding energy without ZPE correction. Gas phase H_2O and H_2 as reference

Fig. S45 Configurations of H* (1 ML, based on number of surface Mo sites) and surface binding energy without ZPE correction. Gas phase H_2O and H_2 as reference

Fig. S46 Configurations of 8OH_1H_2O (mixed 8/9 ML OH and 1/9 ML H_2O) and surface energies without ZPE correction. Gas phase H_2O and H_2 as reference

Fig. S47 Configurations of 7OH_2H_2O (mixed 7/9 ML OH and 2/9 ML H_2O) and surface energies without ZPE correction. Gas phase H_2O and H_2 as reference

Fig. S48 Configurations of 6OH_3H_2O (mixed 2/3 ML OH and 1/3 ML H_2O) and surface energies without ZPE correction. Gas phase H_2O and H_2 as reference

Fig. S49 Configurations of 5OH_4H_2O (mixed 5/9 ML OH and 4/9 ML H_2O) and surface energies without ZPE correction. Gas phase H_2O and H_2 as reference

Fig. S50 Configurations of 4OH_5H_2O (mixed 4/9 ML OH and 5/9 ML H_2O) and surface energies without ZPE correction. Gas phase H_2O and H_2 as reference

Fig. S51 Configurations of 3OH_6H_2O (mixed 1/3 ML OH and 2/3 ML H_2O) and surface energies without ZPE correction. Gas phase H_2O and H_2 as reference

Fig. S52 Configurations of 2OH_7H_2O (mixed 2/9 ML OH and 7/9 ML H_2O) and surface energies without ZPE correction. Gas phase H_2O and H_2 as reference

Fig. S53 Configurations of 1OH_8H_2O (mixed 1/9 ML OH and 8/9 ML H_2O) and surface energies without ZPE correction. Gas phase H_2O and H_2 as reference

Fig. S54 Configurations of 7OH_1H_2O (mixed 7/9 ML OH and 1/9 ML H_2O) and surface energies without ZPE correction. Gas phase H_2O and H_2 as reference

Fig. S55 Configurations of 6OH_2H_2O (mixed 2/3 ML OH and 2/9 ML H_2O) and surface energies without ZPE correction. Gas phase H_2O and H_2 as reference

Fig. S56 Configurations of 5OH_3H_2O (mixed 5/9 ML OH and 1/3 ML H_2O) and surface energies without ZPE correction. Gas phase H_2O and H_2 as reference

Fig. S57 Configurations of 4OH_4H_2O (mixed 4/9 ML OH and 4/9 ML H_2O) and surface energies without ZPE correction. Gas phase H_2O and H_2 as reference

Fig. S58 Configurations of 3OH_5H_2O (mixed 1/3 ML OH and 5/9 ML H_2O) and surface energies without ZPE correction. Gas phase H_2O and H_2 as reference

Fig. S59 Configurations of 2OH_6H_2O (mixed 2/9 ML OH and 2/3 ML H_2O) and surface energies without ZPE correction. Gas phase H_2O and H_2 as reference

Fig. S60 Configurations of 1OH_7H_2O (mixed 1/9 ML OH and 7/9 ML H_2O) and surface energies without ZPE correction. Gas phase H_2O and H_2 as reference

Fig. S61 Configurations of 6OH_1H_2O (mixed 2/3 ML OH and 1/9 ML H_2O) and surface energies without ZPE correction. Gas phase H_2O and H_2 as reference

Fig. S62 Configurations of 5OH_2H_2O (mixed 5/9 ML OH and 2/9 ML H_2O) and surface energies without ZPE correction. Gas phase H_2O and H_2 as reference

Fig. S63 Configurations of 4OH_3H_2O (mixed 4/9 ML OH and 1/3 ML H_2O) and surface energies without ZPE correction. Gas phase H_2O and H_2 as reference

Fig. S64 Configurations of 3OH_4H_2O (mixed 1/3 ML OH and 4/9 ML H_2O) and surface energies without ZPE correction. Gas phase H_2O and H_2 as reference

Fig. S65 Configurations of 2OH_5H_2O (mixed 2/9 ML OH and 5/9 ML H_2O) and surface energies without ZPE correction. Gas phase H_2O and H_2 as reference

Fig. S66 Configurations of 1OH_6H_2O (mixed 1/9 ML OH and 2/3 ML H_2O) and surface energies without ZPE correction. Gas phase H_2O and H_2 as reference

Fig. S67 Configurations of 5OH_1H_2O (mixed 5/9 ML OH and 1/9 ML H_2O) and surface energies without ZPE correction. Gas phase H_2O and H_2 as reference

Fig. S68 Configurations of 4OH_2H_2O (mixed 4/9 ML OH and 2/9 ML H_2O) and surface energies without ZPE correction. Gas phase H_2O and H_2 as reference

Fig. S69 Configurations of 3OH_3H_2O (mixed 1/3 ML OH and 1/3 ML H_2O) and surface energies without ZPE correction. Gas phase H_2O and H_2 as reference

Fig. S70 Configurations of 2OH_4H_2O (mixed 2/9 ML OH and 4/9 ML H_2O) and surface energies without ZPE correction. Gas phase H_2O and H_2 as reference

Fig. S71 Configurations of 1OH_5H_2O (mixed 1/9 ML OH and 5/9 ML H_2O) and surface energies without ZPE correction. Gas phase H_2O and H_2 as reference

Fig. S72 Configurations of 4OH_1H_2O (mixed 4/9 ML OH and 1/9 ML H_2O) and surface energies without ZPE correction. Gas phase H_2O and H_2 as reference

Fig. S73 Configurations of 3OH_2H_2O (mixed 1/3 ML OH and 2/9 ML H_2O) and surface energies without ZPE correction. Gas phase H_2O and H_2 as reference

Fig. S74 Configurations of 2OH_3H_2O (mixed 2/9 ML OH and 1/3 ML H_2O) and surface energies without ZPE correction. Gas phase H_2O and H_2 as reference

Fig. S75 Configurations of 1OH_4H_2O (mixed 1/9 ML OH and 4/9 ML H_2O) and surface energies without ZPE correction. Gas phase H_2O and H_2 as reference

Fig. S76 Configurations of 3OH_1H_2O (mixed 1/3 ML OH and 1/9 ML H_2O) and surface energies without ZPE correction. Gas phase H_2O and H_2 as reference

Fig. S77 Configurations of 2OH_2H_2O (mixed 2/9 ML OH and 2/9 ML H_2O) and surface energies without ZPE correction. Gas phase H_2O and H_2 as reference

Fig. S78 Configurations of 1OH_3H_2O (mixed 1/9 ML OH and 1/3 ML H_2O) and surface energies without ZPE correction. Gas phase H_2O and H_2 as reference

Fig. S79 Configurations of 2OH_1H_2O (mixed 2/9 ML OH and 1/9 ML H_2O) and surface energies without ZPE correction. Gas phase H_2O and H_2 as reference

Fig. S80 Configurations of 1OH_2H_2O (mixed 1/9 ML OH and 2/9 ML H_2O) and surface energies without ZPE correction. Gas phase H_2O and H_2 as reference

Fig. S81 Configurations of 1OH_1H_2O (mixed 1/9 ML OH and 1/9 ML H_2O) and surface energies without ZPE correction. Gas phase H_2O and H_2 as reference

Fig. S82 Configurations of 3OH_5H_2O_1O (mixed 1/3 ML OH*, 5/9 ML H_2O* and 1/9 ML O*) and surface energies without ZPE correction. Gas phase H_2O and H_2 as reference

Fig. S83 Configurations of 4OH_4H_2O_1O (mixed 4/9 ML OH*, 4/9 ML H_2O* and 1/9 ML O*) and surface energies without ZPE correction. Gas phase H_2O and H_2 as reference.

Fig. S84 Configurations of 5OH_3H_2O_1O (mixed 5/9 ML OH*, 1/3 ML H_2O* and 1/9 ML O*) and surface energies without ZPE correction. Gas phase H_2O and H_2 as reference

Fig. S85 Configurations of 3OH_4H_2O_2O (mixed 1/3 ML OH*, 4/9 ML H_2O* and 2/9 ML O*) and surface energies without ZPE correction. Gas phase H_2O and H_2 as reference

Fig. S86 Configurations of 2OH_4H_2O_3O (mixed 2/9 ML OH*, 4/9 ML H_2O* and 1/3 ML O*) and surface energies without ZPE correction. Gas phase H_2O and H_2 as reference

Fig. S87 Configurations of 3OH_3H_2O_1O (mixed 1/3 ML OH*, 4/9 ML H_2O* and 1/9 ML O*) and surface energies without ZPE correction. Gas phase H_2O and H_2 as reference

Fig. S88 Configurations of 3OH_4H_2O_1O (mixed 1/3 ML OH*, 4/9 ML H_2O* and 1/9 ML O*) and surface energies without ZPE correction. Gas phase H_2O and H_2 as reference

Fig. S89 Configurations of 4OH_3H_2O_1O (mixed 4/9 ML OH*, 1/3 ML H_2O* and 1/9 ML O*) and surface energies without ZPE correction. Gas phase H_2O and H_2 as reference

Fig. S90 Configurations of 3OH_3H_2O_2O (mixed 1/3 ML OH*, 1/3 ML H_2O* and 2/9 ML O*) and surface energies without ZPE correction. Gas phase H_2O and H_2 as reference

Fig. S91 Configurations of 3OH_2H_2O_1O (mixed 1/3 ML OH*, 2/9 ML H_2O* and 1/9 ML O*) and surface energies without ZPE correction. Gas phase H_2O and H_2 as reference

Fig. S92 Configurations of 2OH_3H_2O_1O (mixed 2/9 ML OH*, 1/3 ML H_2O* and 1/9 ML O*) and surface energies without ZPE correction. Gas phase H_2O and H_2 as reference

Fig. S93 Configurations of 3OH_6H_2O_1H (mixed 1/3 ML OH*, 2/3 ML H_2O* and 1/9 ML H*) and surface energies without ZPE correction. Gas phase H_2O and H_2 as reference

Fig. S94 Configurations of 3OH_6H_2O_2H (mixed 1/3 ML OH*, 2/3 ML H_2O* and 2/9 ML H*) and surface energies without ZPE correction. Gas phase H_2O and H_2 as reference

Fig. S95 Configurations of 3OH_6H_2O_3H (mixed 1/3 ML OH*, 2/3 ML H_2O* and 1/3 ML H*) and surface energies without ZPE correction. Gas phase H_2O and H_2 as reference

Fig. S96 Configurations of 3OH_6H_2O_4H (mixed 1/3 ML OH*, 2/3 ML H_2O* and 4/9 ML H*) and surface energies without ZPE correction. Gas phase H_2O and H_2 as reference

Fig. S97 Configurations of 3OH_6H_2O_5H (mixed 1/3 ML OH*, 2/3 ML H_2O* and 5/9 ML H*) and surface energies without ZPE correction. Gas phase H_2O and H_2 as reference

Fig. S98 Configurations of 3OH_6H_2O_6H (mixed 1/3 ML OH*, 2/3 ML H_2O* and 2/3 ML H*) and surface energies without ZPE correction. Gas phase H_2O and H_2 as reference

Fig. S99 Configurations of 3OH_6H_2O_7H (mixed 1/3 ML OH*, 2/3 ML H_2O* and 7/9 ML H*) and surface energies without ZPE correction. Gas phase H_2O and H_2 as reference

Fig. S100 Configurations of 3OH_6H_2O_8H (mixed 1/3 ML OH*, 2/3 ML H_2O* and 8/9 ML H*) and surface energies without ZPE correction. Gas phase H_2O and H_2 as reference

Fig. S101 Configurations of 3OH_6H_2O_9H (mixed 1/3 ML OH*, 2/3 ML H_2O* and 1 ML H*) and surface energies without ZPE correction. Gas phase H_2O and H_2 as reference

Fig. S102 Configurations of 4OH_5H_2O_1H (mixed 4/9 ML OH*, 5/9 ML H_2O* and 1/9 ML H*) and surface energies without ZPE correction. Gas phase H_2O and H_2 as reference

Fig. S103 Configurations of 4OH_5H_2O_2H (mixed 4/9 ML OH*, 5/9 ML H_2O* and 2/9 ML H*) and surface energies without ZPE correction. Gas phase H_2O and H_2 as reference

Fig. S104 Configurations of 4OH_5H_2O_3H (mixed 4/9 ML OH*, 5/9 ML H_2O* and 1/3 ML H*) and surface energies without ZPE correction. Gas phase H_2O and H_2 as reference

Fig. S105 Configurations of 4OH_5H_2O_4H (mixed 4/9 ML OH*, 5/9 ML H_2O* and 4/9 ML H*) and surface energies without ZPE correction. Gas phase H_2O and H_2 as reference

Fig. S106 Configurations of 4OH_5H_2O_5H (mixed 4/9 ML OH*, 5/9 ML H_2O* and 5/9 ML H*) and surface energies without ZPE correction. Gas phase H_2O and H_2 as reference

Fig. S107 Configurations of 5OH_4H_2O_1H (mixed 5/9 ML OH*, 4/9 ML H_2O* and 1/9 ML H*) and surface energies without ZPE correction. Gas phase H_2O and H_2 as reference

Fig. S108 Configurations of 5OH_4H_2O_2H (mixed 5/9 ML OH*, 4/9 ML H_2O* and 2/9 ML H*) and surface energies without ZPE correction. Gas phase H_2O and H_2 as reference

Fig. S109 Configurations of 5OH_4H_2O_3H (mixed 5/9 ML OH*, 4/9 ML H_2O* and 1/3 ML H*) and surface energies without ZPE correction. Gas phase H_2O and H_2 as reference

Fig. S110 Configurations of 3OH_3H_2O_1H (mixed 1/3 ML OH*, 1/3 ML H_2O* and 1/9 ML H*) and surface energies without ZPE correction. Gas phase H_2O and H_2 as reference

Fig. S111 Configurations of 3OH_3H_2O_2H (mixed 1/3 ML OH*, 1/3 ML H_2O* and 2/9 ML H*) and surface energies without ZPE correction. Gas phase H_2O and H_2 as reference

Fig. S112 Configurations of 3OH_3H_2O_3H (mixed 1/3 ML OH*, 1/3 ML H_2O* and 1/3 ML H*) and surface energies without ZPE correction. Gas phase H_2O and H_2 as reference

Fig. S113 Configurations of 2OH_1H_2O_1H (mixed 2/9 ML OH*, 1/9 ML H_2O* and 1/9 ML H*) and surface energies without ZPE correction. Gas phase H_2O and H_2 as reference

Fig. S114 Configurations of 1OH_2H_2O_1H (mixed 1/9 ML OH*, 2/9 ML H_2O* and 1/9 ML H*) and surface energies without ZPE correction. Gas phase H_2O and H_2 as reference

Fig. S115 Configurations of 1OH_1H_2O_1H (mixed 1/9 ML OH*, 1/9 ML H_2O* and 1/9 ML H*) and surface energies without ZPE correction. Gas phase H_2O and H_2 as reference

Fig. S116 Surface phase structures of fcc MoC (001) surface under H_2O/H_2 environment at 473.15 K (only molecular H_2O adsorption structures were considered).

Fig. S117 Surface phase structures of fcc MoC (001) surface under H_2O/H_2 environment at 473.15 K (only surface OH* structures were considered).

Fig. S118 Surface phase structures of fcc MoC (001) surface under H_2O/H_2 environment at 473.15 K (only surface O* structures were considered).

Fig. S119 Surface phase structures of fcc MoC (001) surface under H_2O/H_2 environment at 473.15 K (only surface H* structures were considered).

Fig. S120 Surface phase structures of fcc MoC (001) surface under H_2O/H_2 environment at 473.15 K (only surface H_2* structures were considered). (a) showed that the adsorption of H_2 was thermodynamically unstable at the specified conditions; (b) showed that the surface energies for adsorption of H_2 on fcc MoC (001) surface were always higher than that of bare surface (referenced as 0).

Fig. S121 Surface phase structures of fcc MoC (001) surface under H_2O/H_2 environment at 473.15 K (only pure surface H_2O* and pure surface OH* structures were considered without considering their mixtures).

Fig. S122 Surface phase structures of fcc MoC (001) surface under H_2O/H_2 environment at 473.15 K (only pure surface H_2O*, pure surface OH* and pure surface O* structures were considered without considering their mixtures).

Fig. S123 Surface phase structures of fcc MoC (001) surface under H_2O/H_2 environment at 473.15 K (only pure surface H_2O*, pure surface OH*, pure surface O*, pure surface H* and pure surface H_2* structures were considered without considering their mixtures).

Fig. S124 Surface phase structures of fcc MoC (001) surface under H_2O/H_2 environment at 473.15 K (only pure surface H_2O*, pure surface OH*, pure surface O*, pure surface H*, pure surface H_2* and the mixtures of H_2O*/OH* structures were considered).

Fig. S125 Surface phase structures of fcc MoC (001) surface under H_2O/H_2 environment at 473.15 K (only pure surface H_2O*, pure surface OH*, pure surface O*, pure surface H*, pure surface H_2*, the mixtures of H_2O*/OH*, H_2O*/OH*/O*, H_2O*/OH*/H* structures were considered).

Fig. S126 The potential energy profiles for the transformation of top site O* to a bridge site O* on stable surface phases.

Fig. S127 The potential energy profiles for the H2O dissociation to generate surface OH* (a) and OH* direct deprotonation to generate O* (b) on 3OH_3H2O_1O surface structure.

Fig. S128 The potential energy profiles for the H2O dissociation to generate surface OH* (a) and OH* direct deprotonation to generate O* (b) on 4OH_4H2O_1O surface structure.

Fig. S129 The potential energy profiles for the H2O dissociation to generate surface OH* (a) and OH* direct deprotonation to generate O* (b) on 3OH_4H2O_2O surface structure.

Fig. S130 The potential energy profiles for the H2O dissociation to generate surface OH* (a) and OH* direct deprotonation to generate O* (b) on 3OH_3H2O surface structure.

Fig. S131 The potential energy profiles for the H2O dissociation to generate surface OH* (a) and OH* direct deprotonation to generate O* (b) on 4OH_5H2O surface structure.

Fig. S132 The potential energy profiles for the H2O dissociation to generate surface OH* (a) and OH* direct deprotonation to generate O* (b) on 3OH_6H2O surface structure.

Fig. S133 The potential energy profiles for the H2 dissociation to generate surface H* on 3OH_3H2O_1O surface structure.

Fig. S134 The potential energy profiles for the H2 dissociation to generate surface H* on 3OH_3H2O surface structure.

Table S1 Energetic aspects of surface H_2O^* dissociation with n adsorbing H_2O* (n = 1-9), $\Delta E_{TS,ZPE}^{\neq}$ and $\Delta E_{TS}^{\neq}$ were energy barriers of H_2O^* dissociation with or without ZPE correction, respectively; $\Delta E_{r,ZPE}$ and ΔE_r were reaction energies of H_2O^* dissociation with or without ZPE correction, respectively; σ_{TS}^{i} were imaginary frequencies of transition states for H_2O^* dissociation; $d_{O\cdots H}^{\neq}$ and $d_{C\cdots H}^{\neq}$ were the lengths of breaking O-H bond of $H_2O^*$and lengths of forming C-H bond of C site in the transition state, respectively. Energies were in eV with H_2O^* adsorption states as reference, distances were in Å and frequencies were in cm^{-1}

Table S2 Energetic aspects of surface H_2O^* dissociation with n adsorbing OH* (n = 1-8), $\Delta E_{TS,ZPE}^{\neq}$ and $\Delta E_{TS}^{\neq}$ were energy barriers of H_2O^* dissociation with or without ZPE correction, respectively; $\Delta E_{r,ZPE}$ and ΔE_r were reaction energies of H_2O^* dissociation with or without ZPE correction, respectively; σ_{TS}^{i} were imaginary frequencies of transition states for H_2O^* dissociation; $d_{O\cdots H}^{\neq}$ and $d_{C\cdots H}^{\neq}$ were the lengths of breaking O-H bond of $H_2O^*$and lengths of forming C-H bond of C site in the transition state, respectively. Energies were in eV with H_2O^* adsorption states as reference, distances were in Å and frequencies were in cm^{-1}

Table S3 Reaction rate constants k (s^{-1}) of elementary reactions at different surface coverage at 473.15 K; the reaction pathway with lowest energy barrier at each coverage was selected. (In order to cancel the error with low frequency mode in calculating the vibrational partition functions, frequencies below 200 cm^{-1} were shifted to 200 cm^{-1})

S-1. Detailed description on the elementary reaction rate constant calculation

The reaction rate constant k of each elementary step in surface reactions is calculated as below:

$$k = \frac{k_B T}{h} \frac{q_{\mathrm{TS,vib}}}{q_{\mathrm{IS,vib}}} e^{-\frac{\mathrm{E_a}}{k_B T}}$$

Where k_B is Boltzmann constant, T denotes the reaction temperature, h is the Planck constant, Ea stands for the zero-point energy corrected energy barrier for elementary reaction derived from DFT calculations, $q_{TS,vib}$ and $q_{IS,vib}$ are the vibrational partition functions for the transition states and the initial states, respectively. q_{vib} is calculated as below:

$$q_{\mathrm{vib}} = \prod_i \frac{1}{1-e^{\frac{-h\nu_i}{k_B T}}}$$

where ν_i is the vibrational frequency of each vibrational mode of the surface adsorbing species derived from DFT harmonic frequency calculations. In order to cancel the error with low frequency mode, frequencies below 50 cm^{-1} were shifted to 50 cm^{-1}.

S-2. Detailed description on the *ab initio* thermodynamic method

The stability of different surface configurations with i adsorbing species at temperature T and pressure p can be expressed as below:

$$\gamma_{\mathrm{T,p}} = G_{\mathrm{T,p}}^{slab,adsorbates} - G_{\mathrm{T,p}}^{slab} - \sum_i (\, n^i * \mu_{\mathrm{T,p}}^i) \qquad \text{(a)}$$

where $G_{\mathrm{T,p}}^{slab,adsorbates}$ is the Gibbs free energy of the catalyst model with adsorbates, $G_{\mathrm{T,p}}^{slab}$ is Gibbs free energy of the clean catalyst model and $\mu_{\mathrm{T,p}}^i$ is the chemical potential of isolated species i. A more negative $\gamma_{\mathrm{T,p}}$ denotes a more stable surface structure. For the condensed phases, the variation of vibrational energy and entropy contributions to the Gibbs free energy usually cancel to a large extent in the subtraction term $G_{T,p}^{slab,adsorbates} - G_{T,p}^{slab}$. With considering only the thermal correction to the adsorbates, the term $G_{T,p}^{slab,adsorbates} - G_{T,p}^{slab}$ can be replaced by $E_{0K,ZPE}^{slab,adsorbates} + \Delta G_T^{adsorbates} - E_{0K}^{slab}$, where the $E_{0K,ZPE}^{slab,adsorbates}$ and E_{0K}^{slab} are the total energies of catalyst model with adsorbates and clean catalyst model, respectively; $\Delta G_T^{adsorbates}$ is the thermal correction to the adsorbates which is calculated according to the following equation as implemented in VASPKIT software (V. Wang and N. Xu, VASPKIT: A pre- and post-processing program for the VASP code, http://vaspkit.sourceforge.net.):

$\Delta G_T^{adsorbates} = -RTln(q_{vib}^{ads})$, $q_{vib}^{ads} = \prod_{j=1}^{nmv} \frac{1}{1-\exp(-h\nu_j/k_B T)}$ is the vibrational partition functions for adsorbates, ν_j is the normal mode vibration (nmv) frequency of adsorbates, h is Plank constant and k_B is Boltzmann constant. Thus equation (a) can be simplified as below:

$$\gamma_{T,p} = E_{0K,ZPE}^{slab,adsorbates} + \Delta G_T^{adsorbates} - E_{0K}^{slab} - \sum_i (n^i * \mu_{T,p}^i) \qquad \text{(b)}$$

For gas phase (assuming ideal gas), the chemical potential of species i depending on temperature and pressure can be expressed below:

$$\mu_{T,p}^i = E_{0K,ZPE}^i + \mu_{T,p^0}^i + \mathrm{RTln}(\frac{p^i}{p^0}) \qquad \text{(c)}$$

where $E_{0K,ZPE}^i$ is the total energy of isolated species i with ZPE correction obtained from DFT calculation, μ_{T,p^0}^i is the energy difference between the chemical potential (temperature T and pressure 1 atm) and total energy at 0K for species i, p^i is the partial pressure of species i, p^0 is the standard atmospheric pressure, μ_{T,p^0}^i values are taken from the JANAF thermochemical tables (https://janaf.nist.gov/).

For liquid phase, the chemical potential of species i depending on temperature and pressure can be expressed below:

$$\mu^i_{T,p} = E^i_{0K,ZPE} + \mu^i_{T,p^0} + \mathrm{RTln}\left(\frac{p^i_{saturation}}{p^0}\right) + V_i(p^i - p^i_{saturation}) \quad \text{(d)}$$

where $p^i_{saturation}$ is the saturated vapor pressure of species i at temperature T, V_i is the unit volume of liquid phase i at temperature T.

Combining equation (b) and (c), the following expression can be obtained:

$$\gamma_{T,p} = E^{slab,adsorbates}_{0K,ZPE} + \Delta G^{adsorbates}_T - E^{slab}_{0K} - \sum_i(n^i * E^i_{0K,ZPE}) - \sum_i(n^i * \mu^i_{T,p^0}) - RT\sum_i(n^i * \ln(\frac{p^i}{p^0}))$$

(e)

where the surface stability with i number gas phase species can be evaluated.

Combining equation (b) and (d), the following expression can be obtained:

$$\gamma_{T,p} = E^{slab,adsorbates}_{0K,ZPE} + \Delta G^{adsorbates}_T - E^{slab}_{0K} - \sum_{i+j}(n^{i+j} * E^{i+j}_{0K,ZPE}) - \sum_{i+j}(n^{i+j} * \mu^{i+j}_{T,p^0}) -$$

$$RT\sum_i(n^i * \ln(\frac{p^i}{p^0})) - RT\sum_j(n^j * \ln(\frac{p^j_{saturation}}{p^0})) - \sum_j(n^j * V^j * (p^j - p^j_{saturation}))$$

(f)

where the surface stability with i number gas phase species and j number liquid phase species can be evaluated.

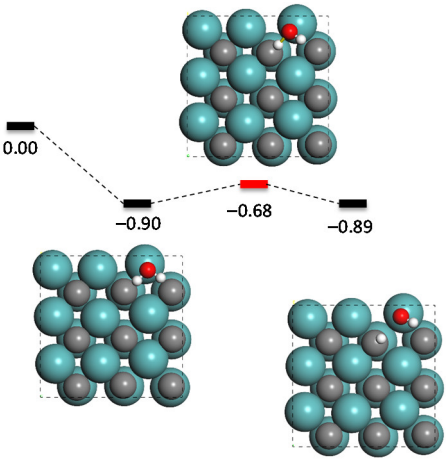
0.00
−0.90
−0.68
−0.89

(1)

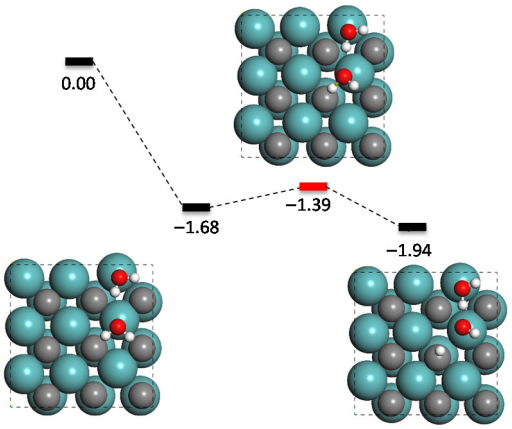
0.00
−1.68
−1.39
−1.94

(2-a)

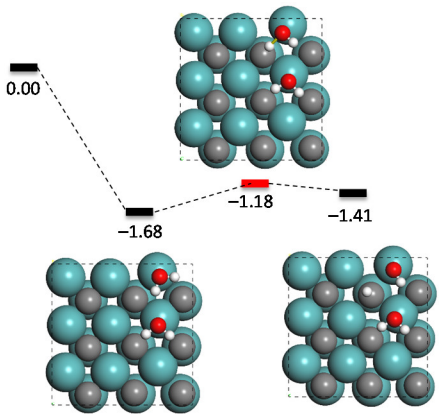
0.00
−1.68
−1.18
−1.41

(2-b)

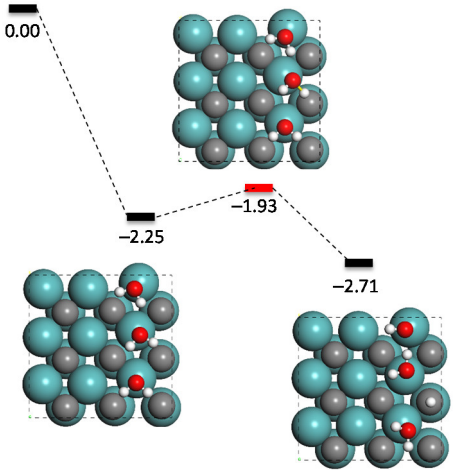
0.00
−2.25
−1.93
−2.71

(3-a)

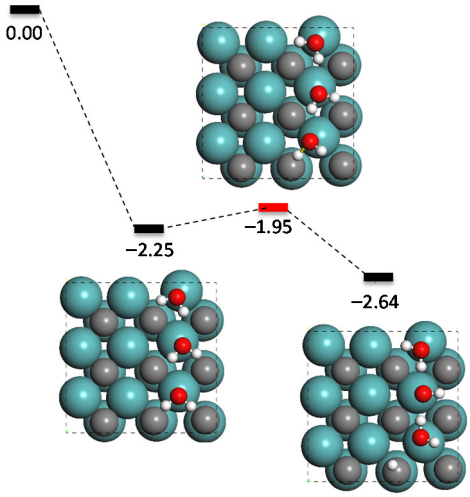
0.00
−2.25
−1.95
−2.64

(3-b)

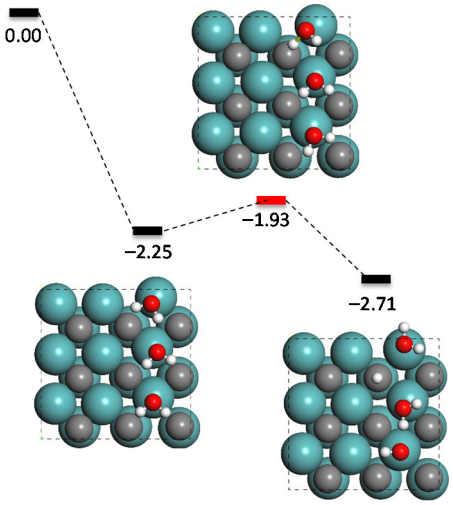
0.00
−1.93
−2.25
−2.71

(3-c)

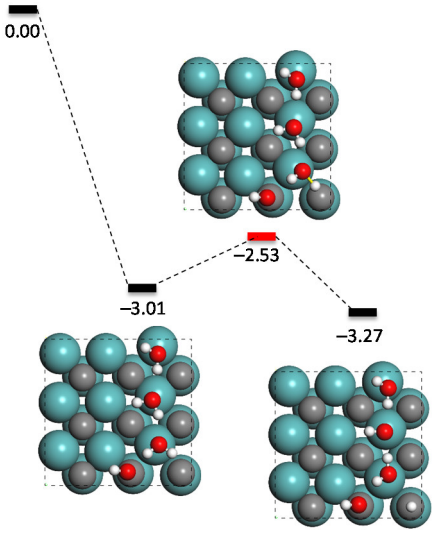
0.00
−2.53
−3.01
−3.27

(4-a)

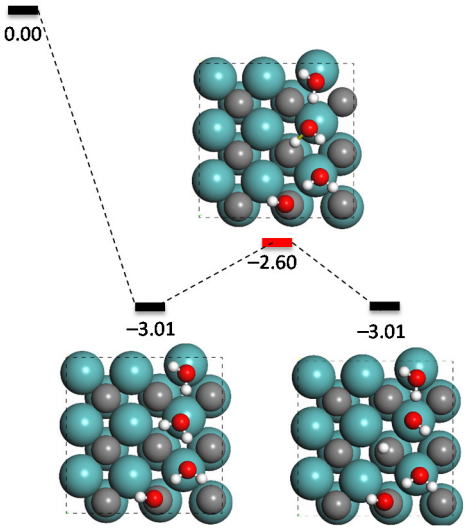
0.00
−2.60
−3.01
−3.01

(4-b)

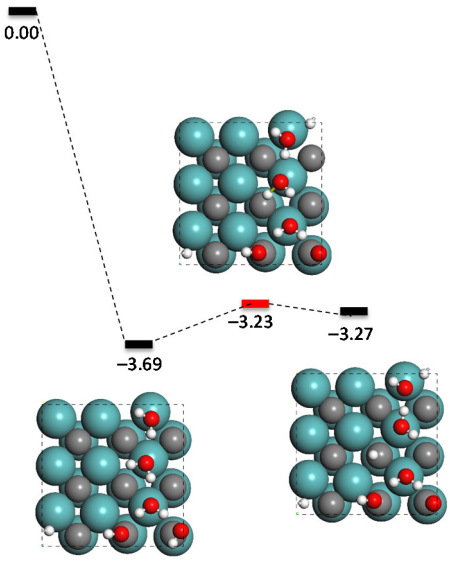
0.00
−3.23
−3.27
−3.69

(5-a)

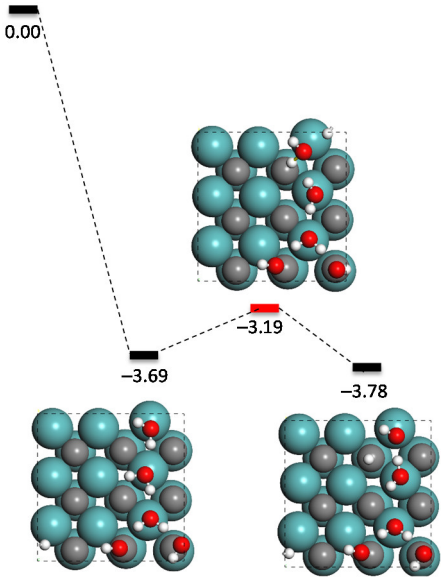
0.00
−3.19
−3.69
−3.78

(5-b)

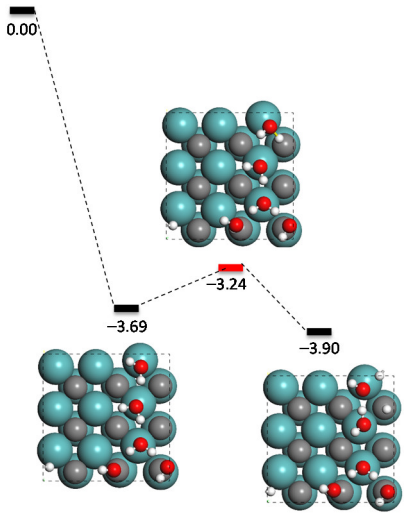
0.00
−3.24
−3.69
−3.90

(5-c)

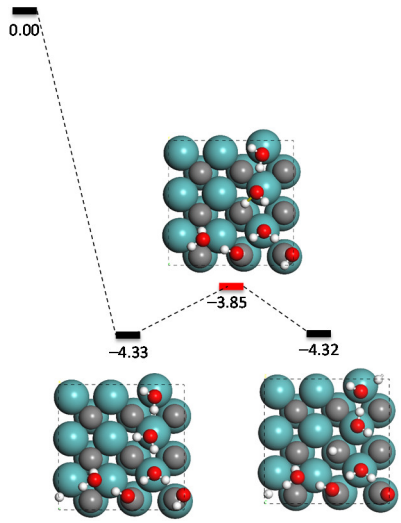
0.00
−3.85
−4.33
−4.32

(6-a)

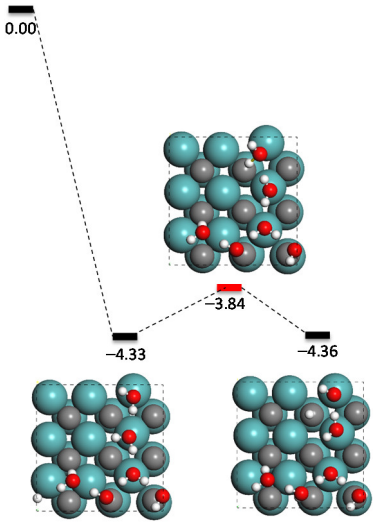
0.00
−3.84
−4.33
−4.36

(6-b)

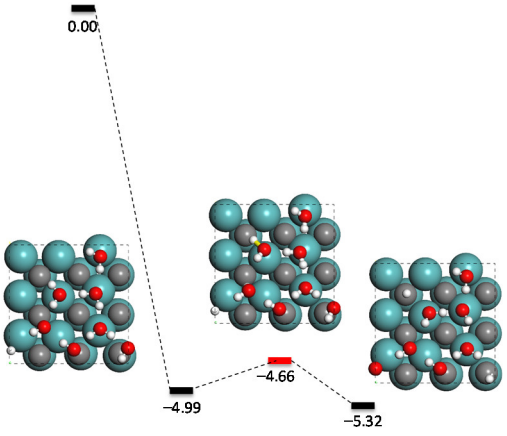
0.00
−4.66
−4.99
−5.32

(7-a)

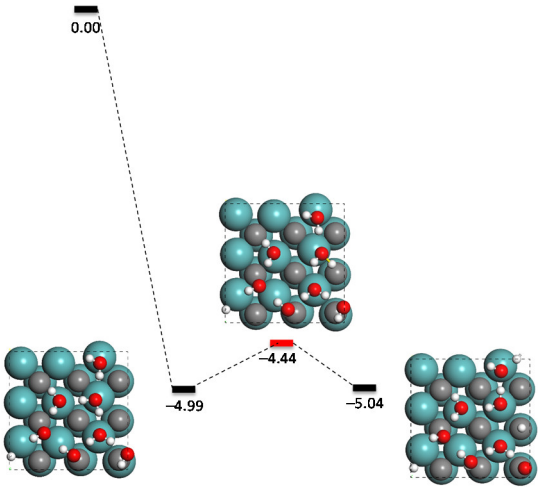
0.00
−4.44
−4.99
−5.04

(7-b)

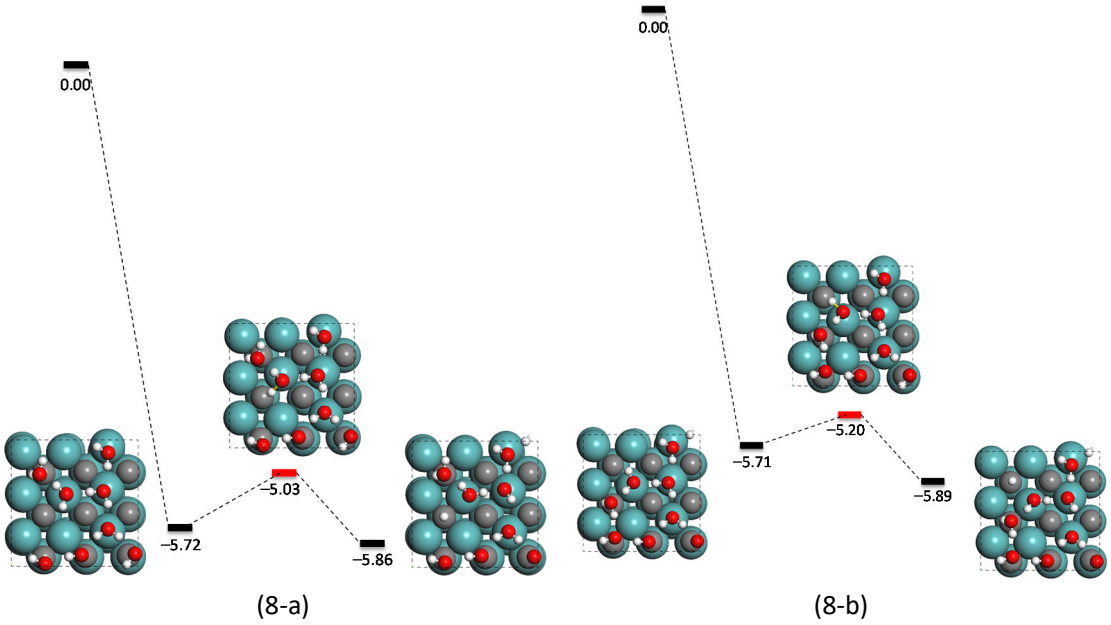

(8-a) (8-b)

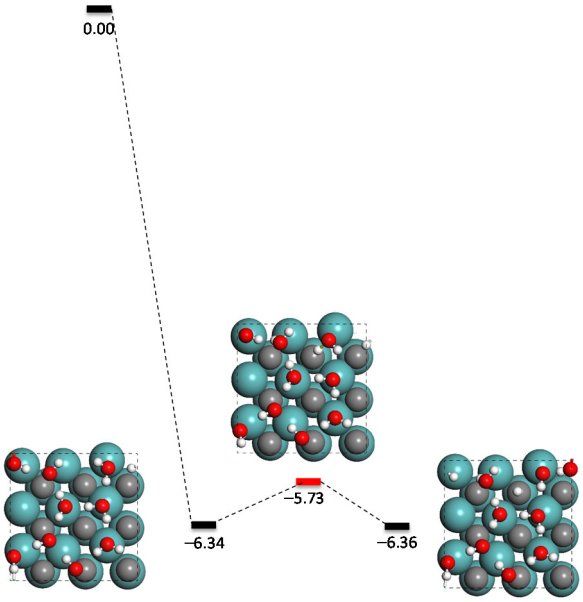

(9)

Fig. S1 The potential energy profiles with ZPE correction for H_2O* dissociation at different H_2O* coverage (For each H_2O* coverage, more than one site for H_2O dissociation may be considered, energies in eV with gas phase H_2O and H_2 as reference)

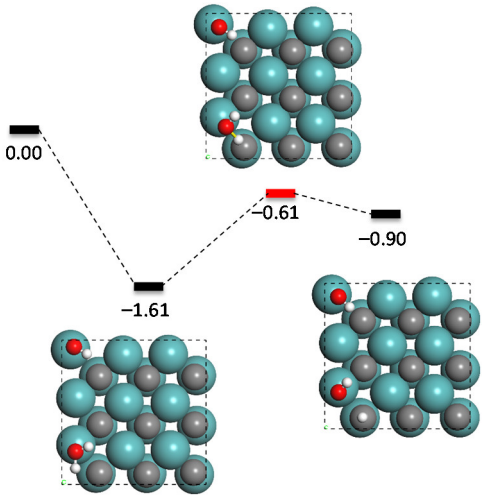
0.00
−0.61
−0.90
−1.61

(1-a)

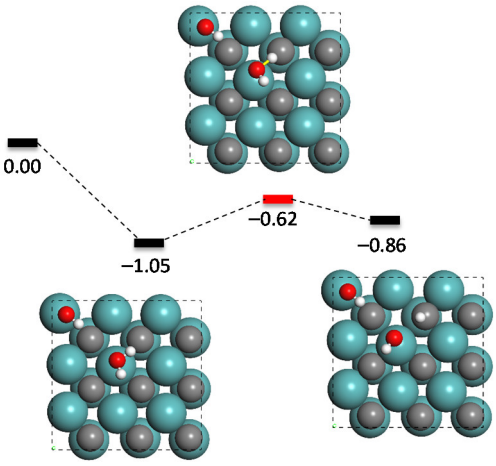
0.00
−0.62
−0.86
−1.05

(1-b)

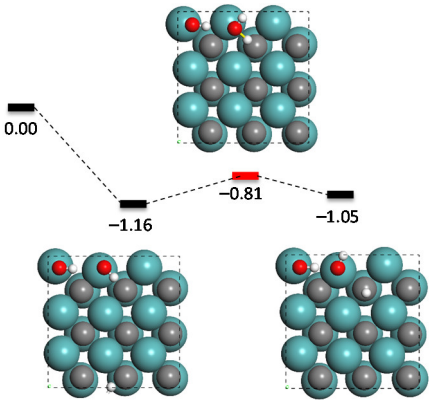
0.00
−0.81
−1.05
−1.16

(1-c)

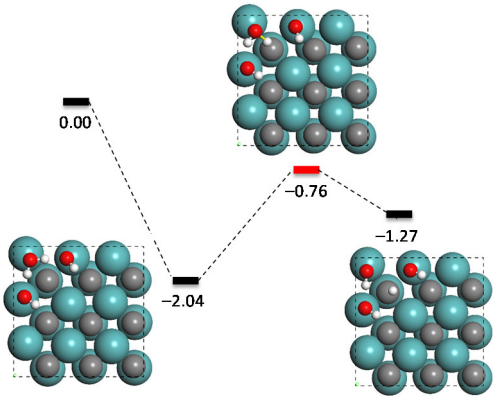
0.00
−0.76
−1.27
−2.04

(2-a)

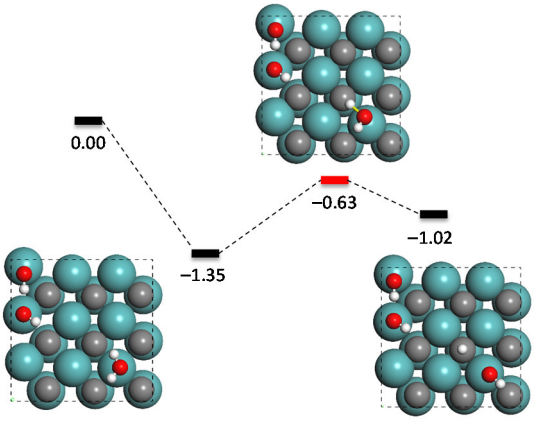
0.00
−0.63
−1.02
−1.35

(2-b)

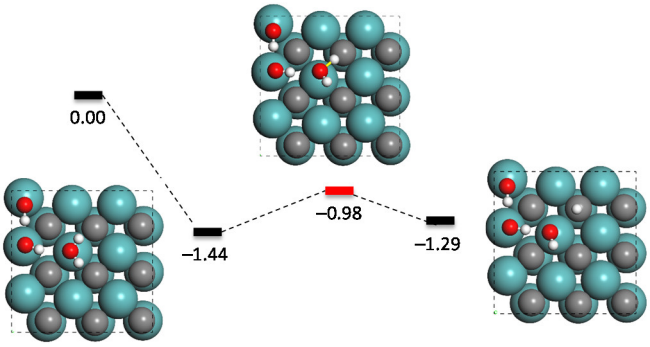

(2-c)

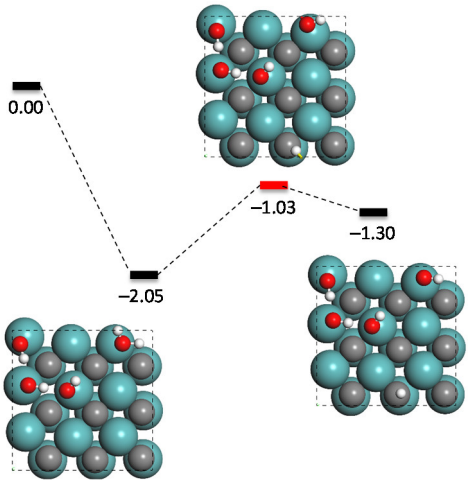

(3-a)

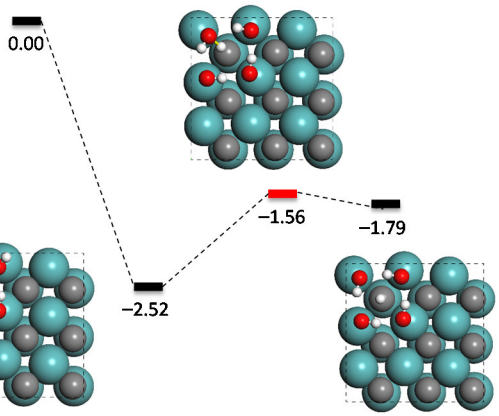

(3-b)

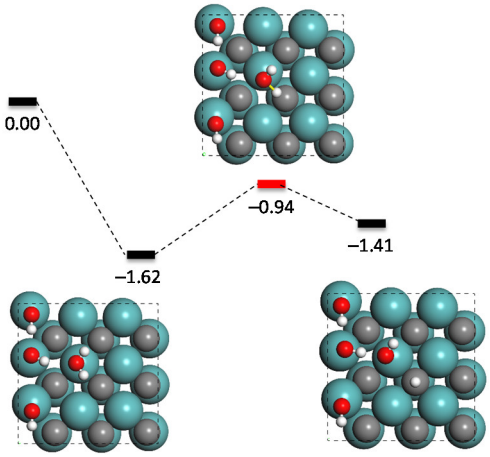

(3-c)

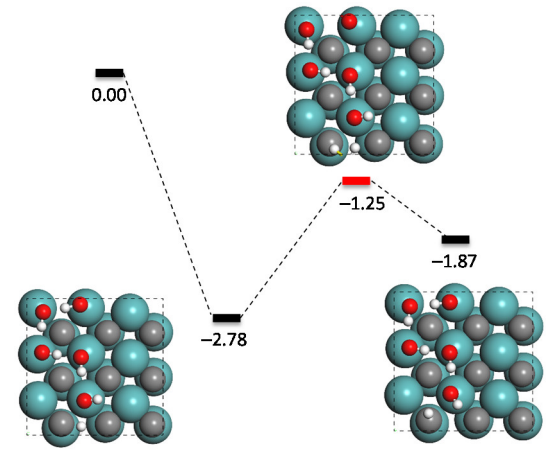
0.00
−1.25
−1.87
−2.78

(4-a)

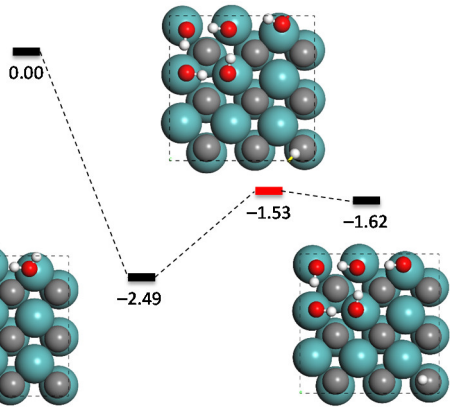
0.00
−1.53
−1.62
−2.49

(4-b)

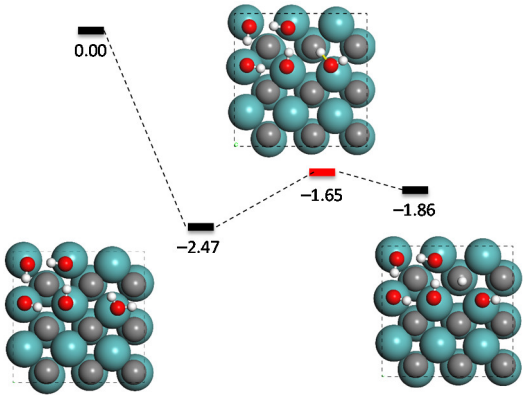
0.00
−1.65
−1.86
−2.47

(4-c)

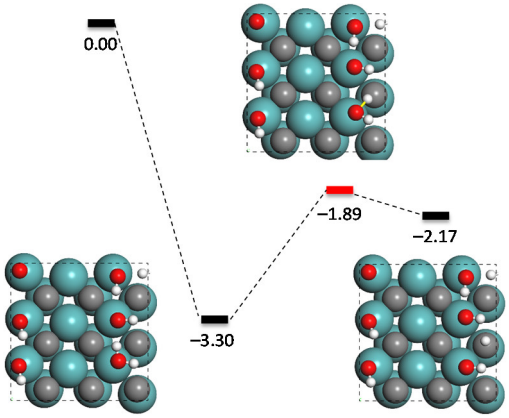
0.00
−1.89
−2.17
−3.30

(5-a)

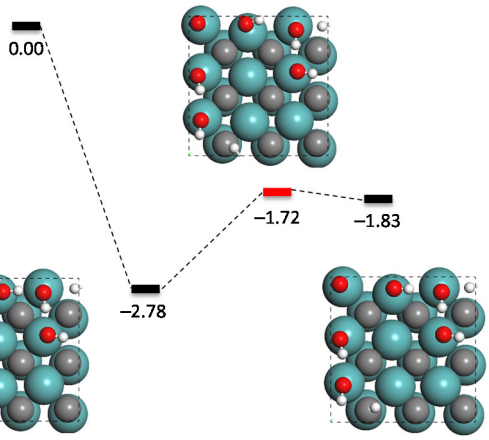
0.00
−1.72
−1.83
−2.78

(5-b)

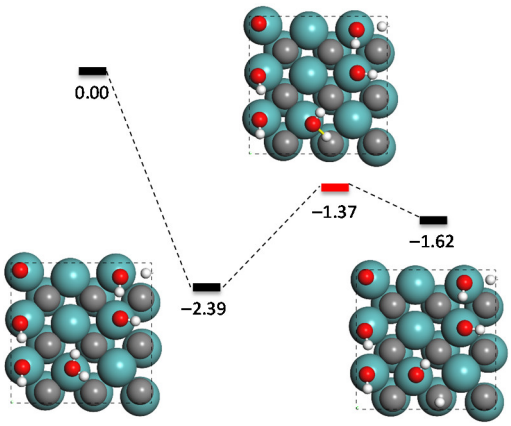

(5-c)

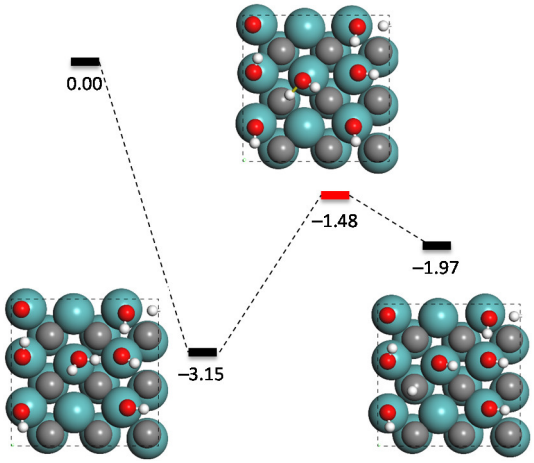

(6-a)

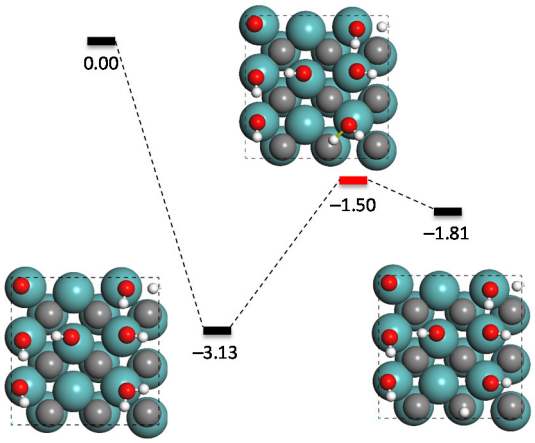

(6-b)

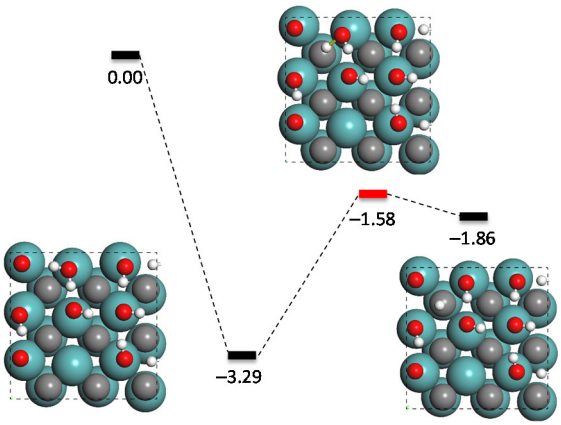

(7)

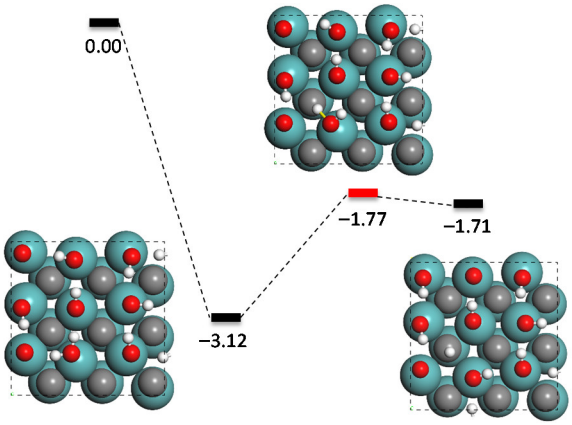

(8)

Fig. S2 The potential energy profiles with ZPE correction for H_2O* dissociation at different OH* coverage (For each OH* coverage, more than one site for H_2O dissociation may be considered, energies in eV with gas phase H_2O and H_2 as reference)

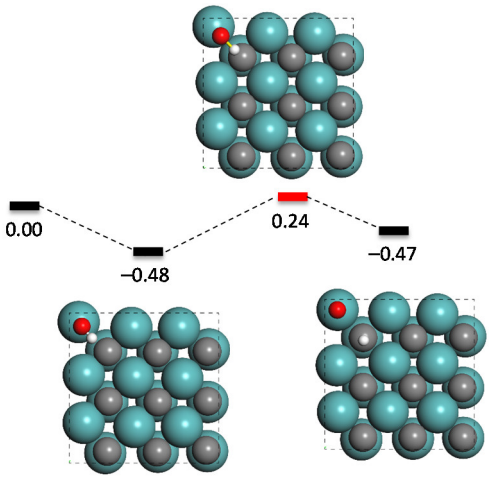

(1)

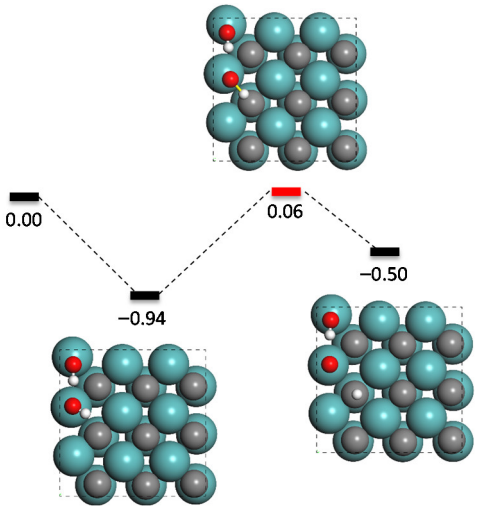

(2)

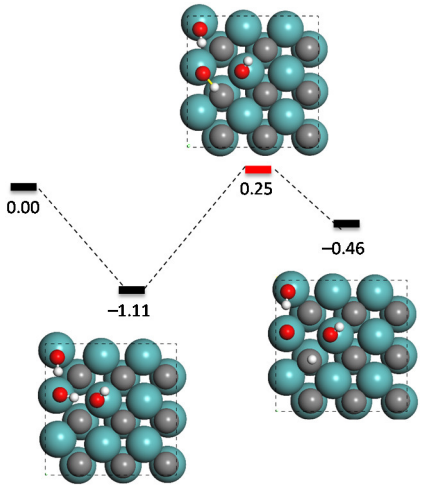
0.00
0.25
−0.46
−1.11

(3)

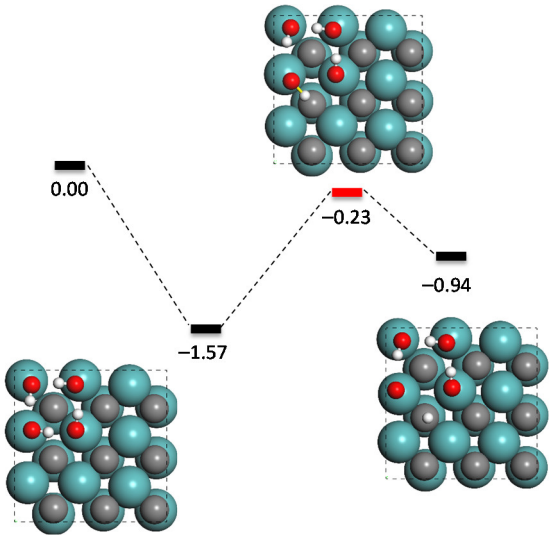
0.00
−0.23
−0.94
−1.57

(4)

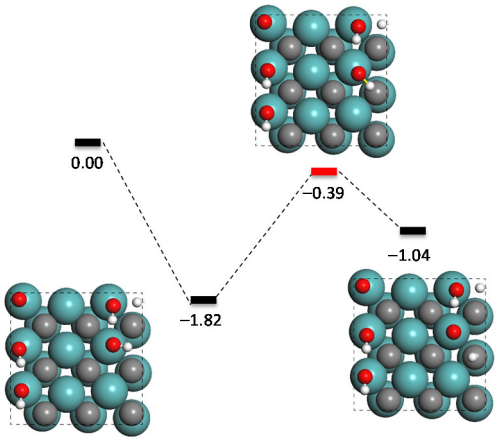
0.00
−0.39
−1.04
−1.82

(5)

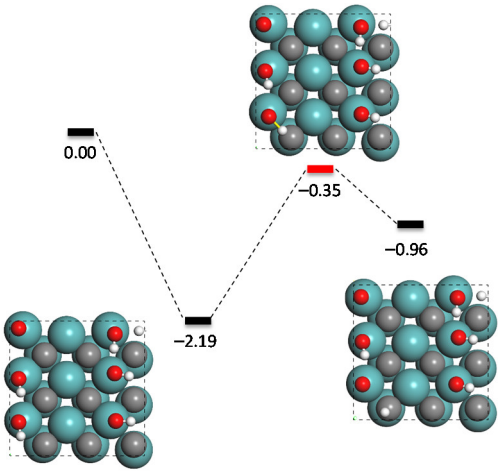
0.00
−0.35
−0.96
−2.19

(6)

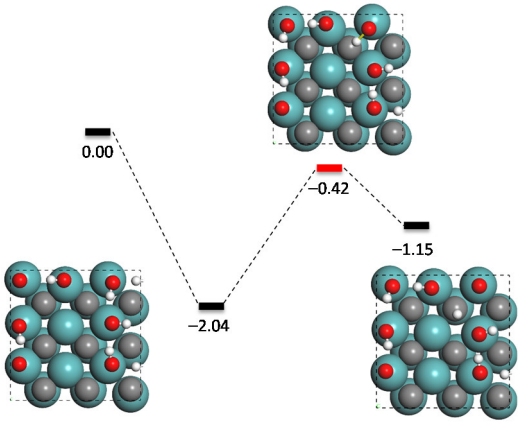
0.00
−0.42
−1.15
−2.04

(7)

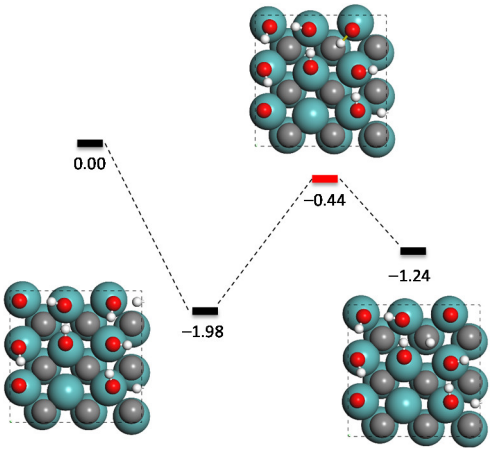
0.00
−0.44
−1.24
−1.98

(8)

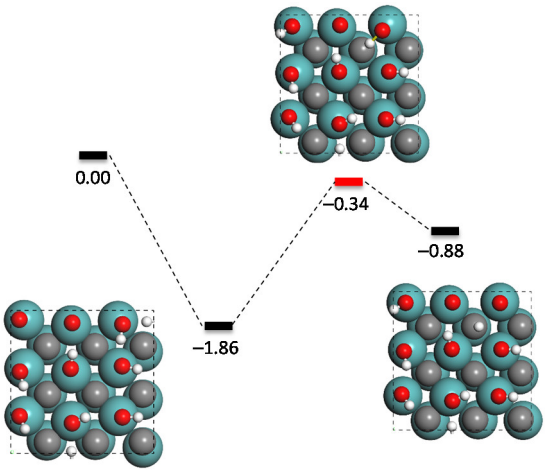

(9)

Fig. S3 The potential energy profiles with ZPE correction for direct deprotonation of single OH* at different OH* coverage (Energies in eV with gas phase H_2O and H_2 as reference)

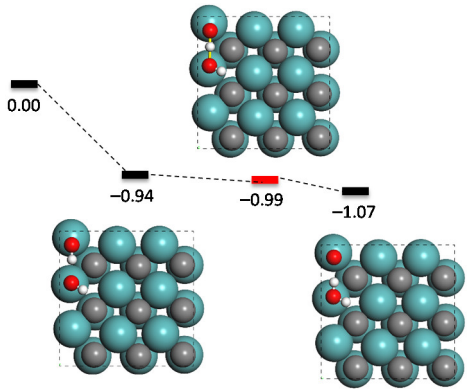

(1)

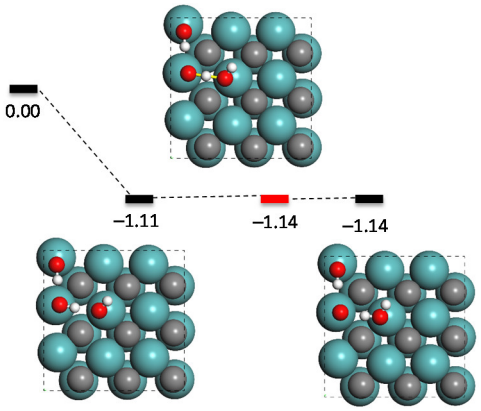

(2)

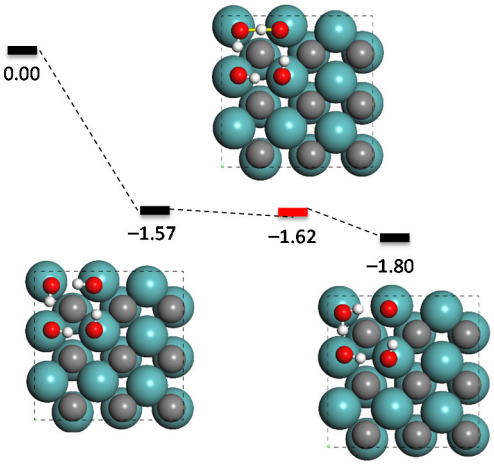

(3)

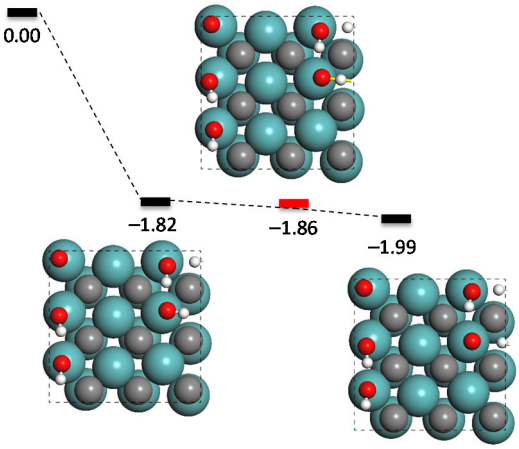

(4)

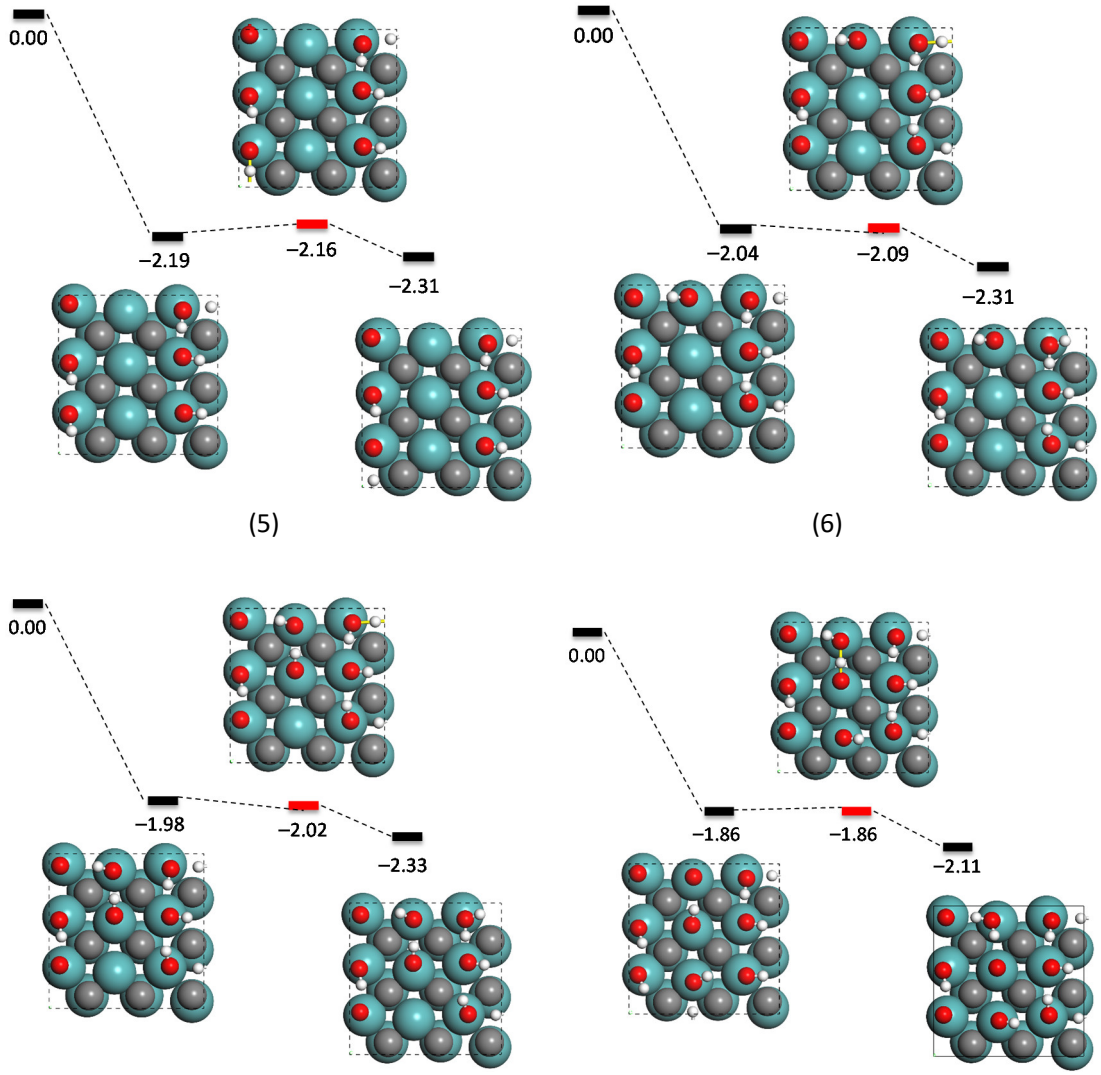

Fig. S4 The potential energy profiles with ZPE correction for hydroxyls condensation at different OH* coverage (Energies in eV with gas phase H_2O and H_2 as reference)

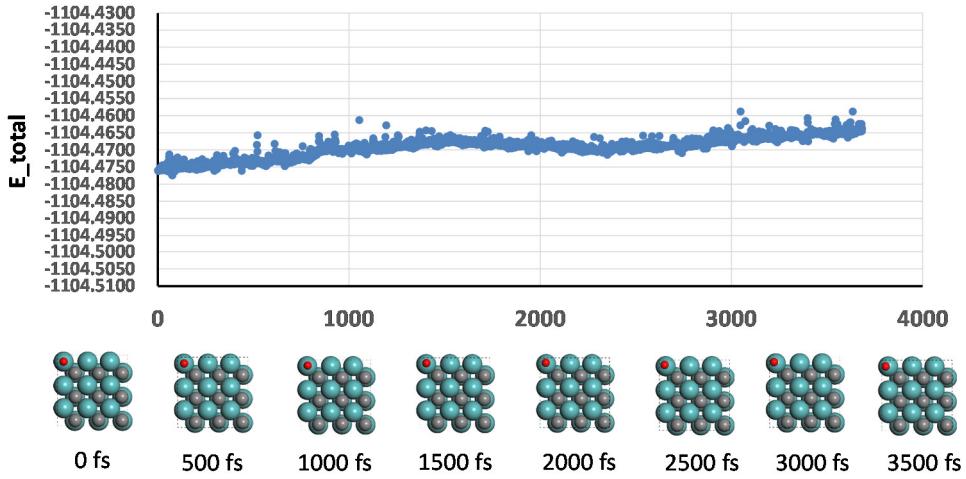

Fig. S 5 Structure evolution of surface O* at 1/9 ML coverage with time scale of 1-3700 femtoseconds at temperature of 473.15K. A canonical ensemble with Nosé-Hoover thermostats was employed in the *ab initio* molecular dynamics (AIMD), and the time step was set to 1 fs.

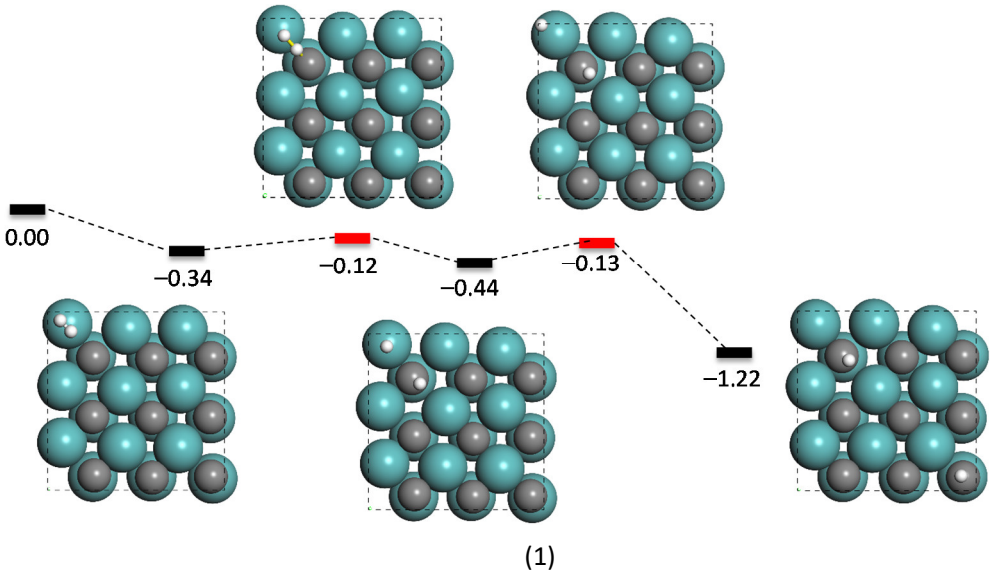

(1)

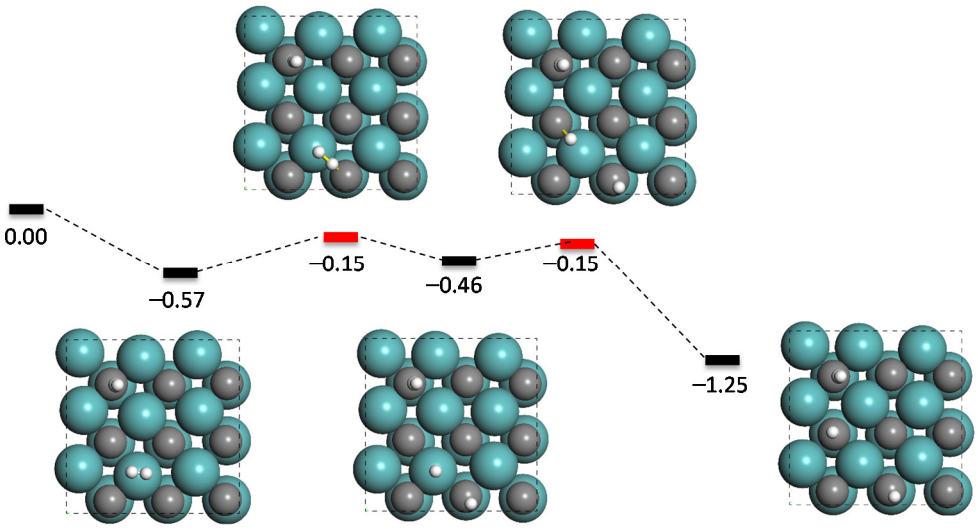

(2)

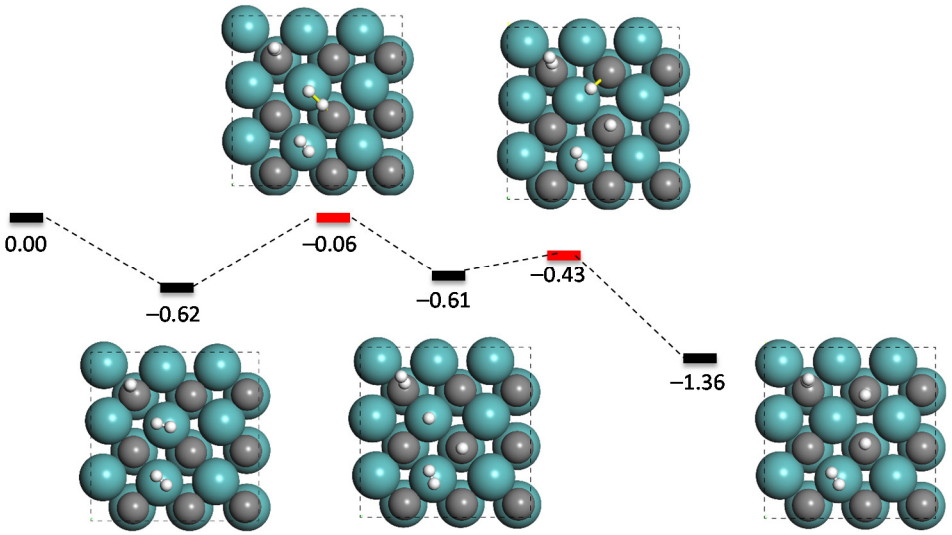
0.00
−0.62
−0.06
−0.61
−0.43
−1.36

(3)

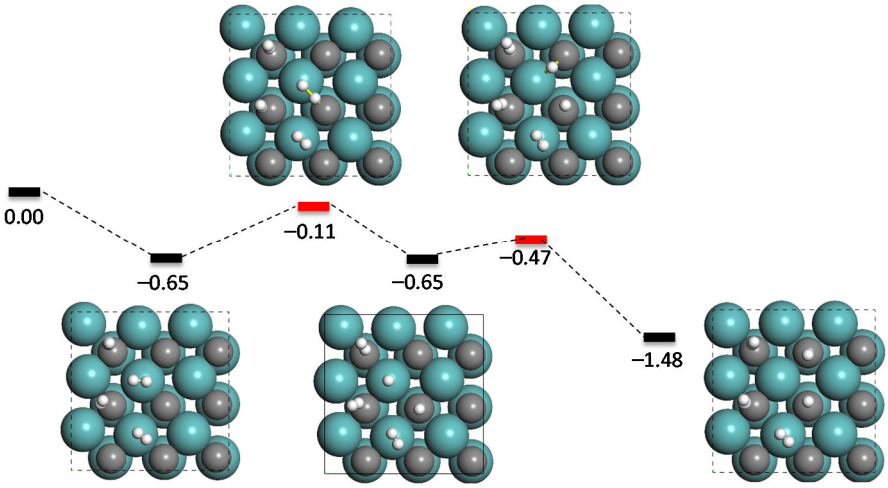
0.00
−0.65
−0.11
−0.65
−0.47
−1.48

(4)

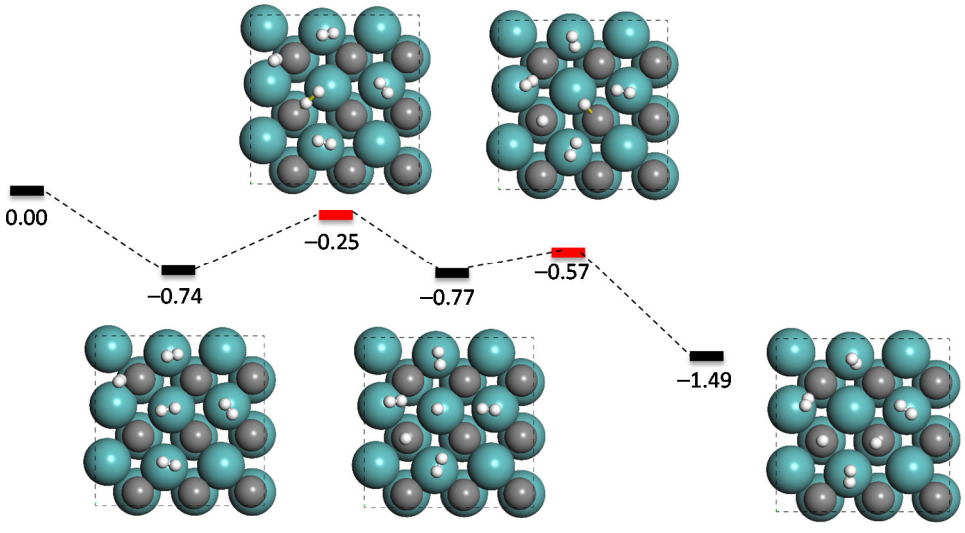
0.00
−0.74
−0.25
−0.77
−0.57
−1.49

(5)

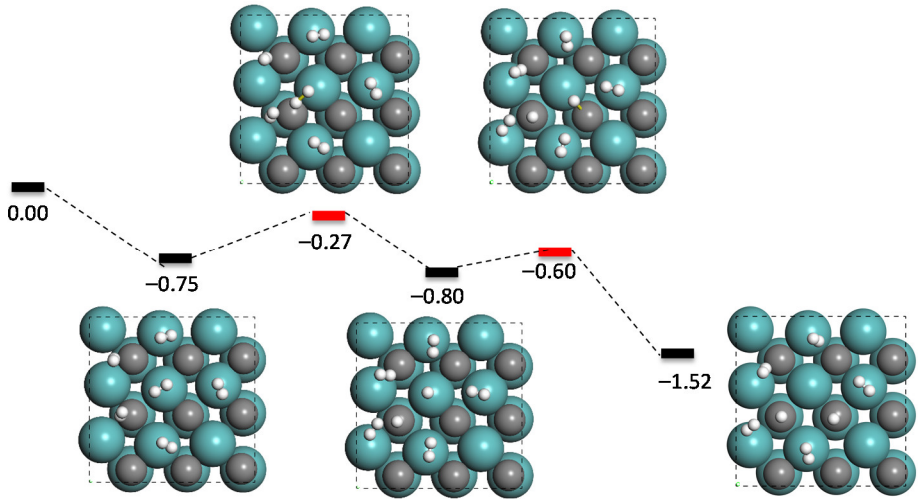
0.00
−0.75
−0.27
−0.80
−0.60
−1.52

(6)

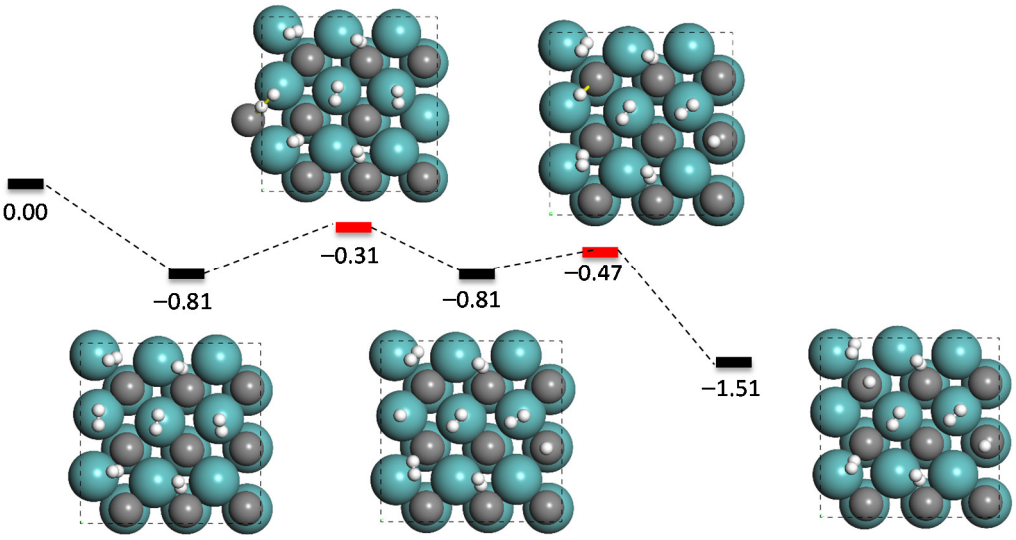
0.00
−0.81
−0.31
−0.81
−0.47
−1.51

(7)

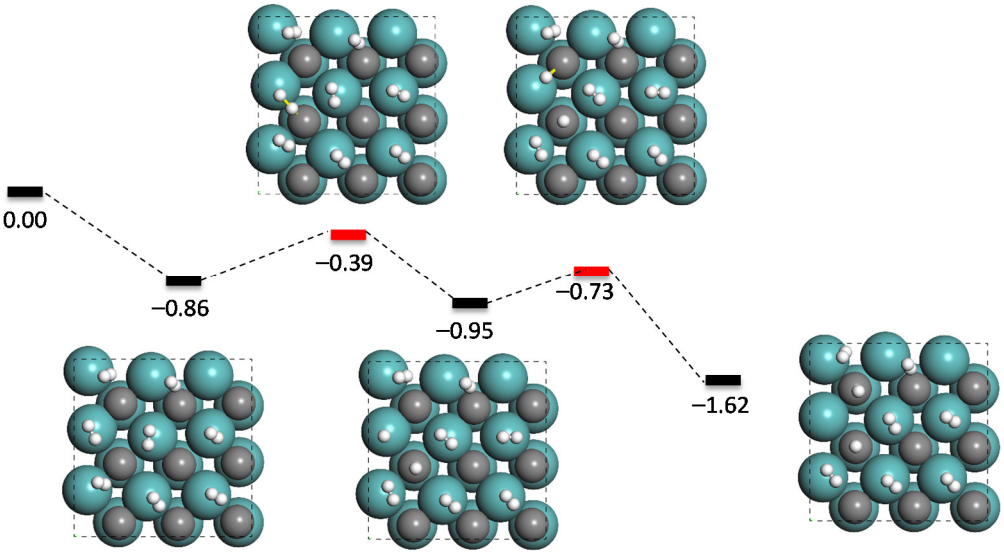
0.00
−0.86
−0.39
−0.95
−0.73
−1.62

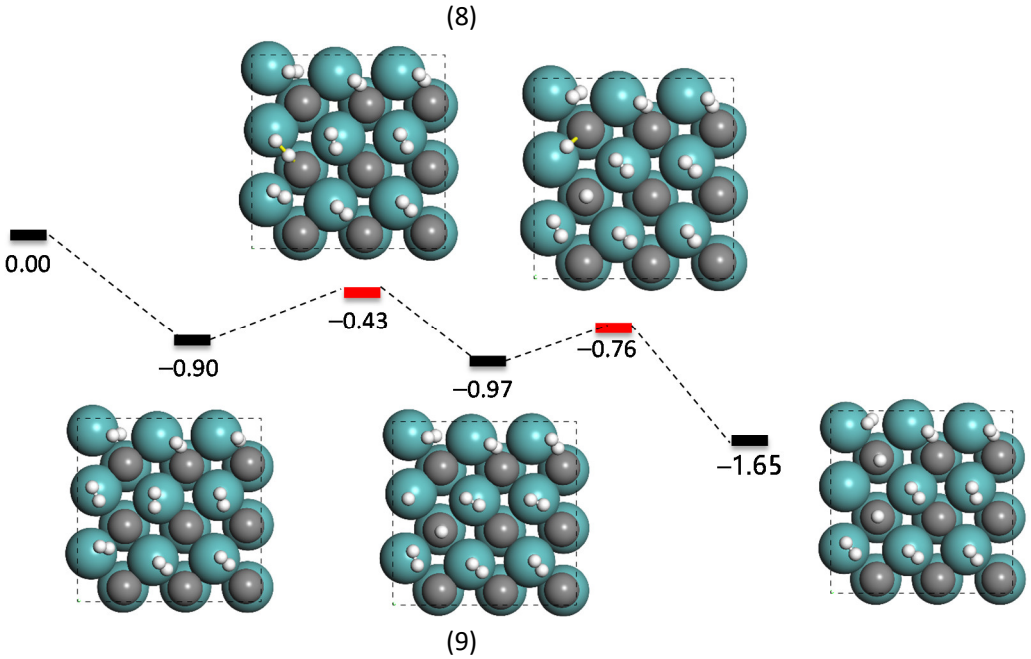

Fig. S6 The potential energy profiles with ZPE correction for H-H bond breaking and H transfer at different H_2* coverage. Energies in eV with gas phase H_2O and H_2 as reference.

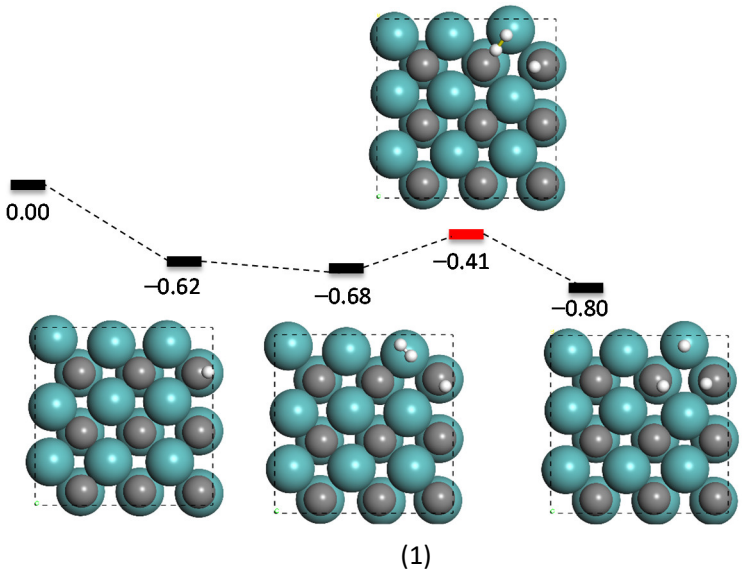

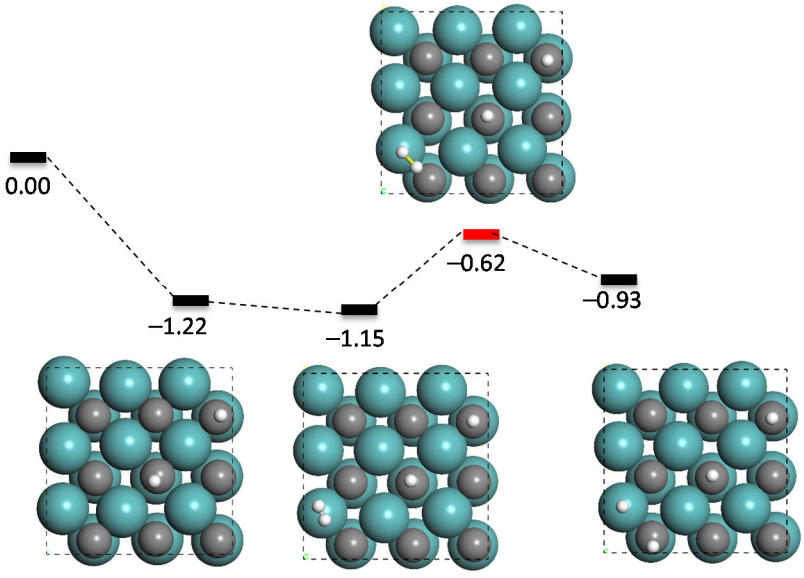

(2)

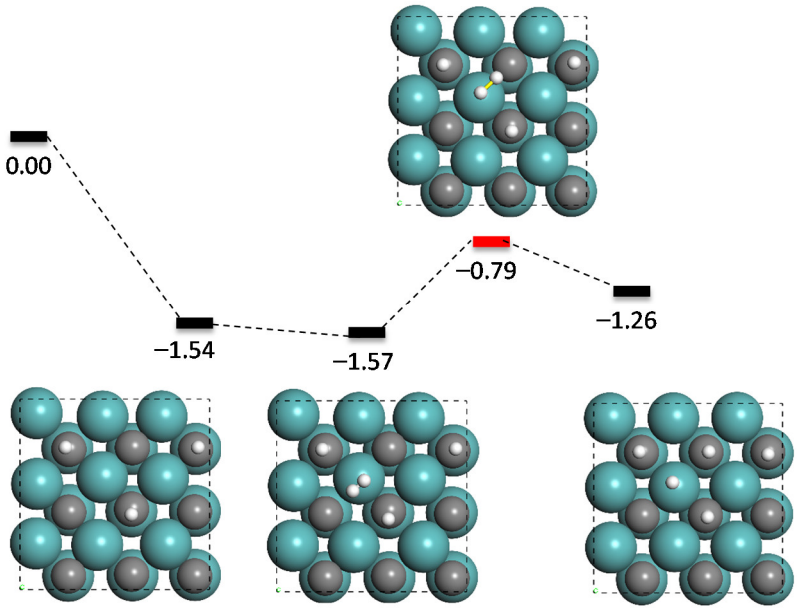

(3)

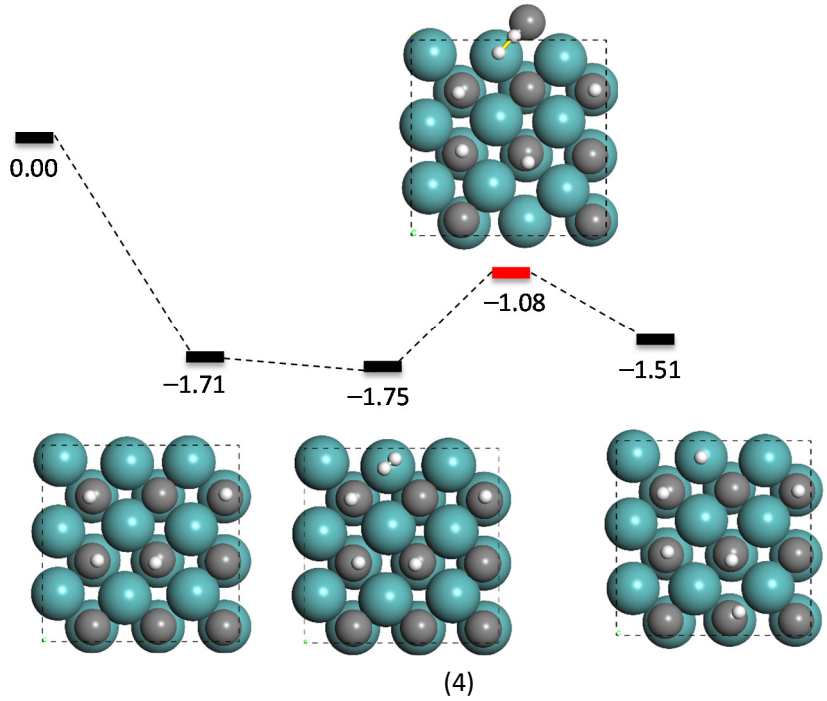

(4)

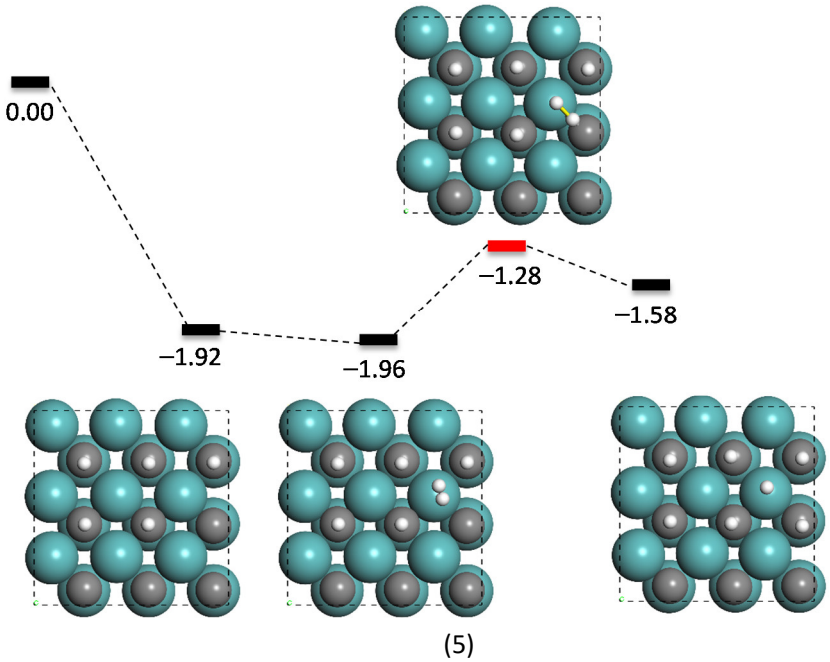

(5)

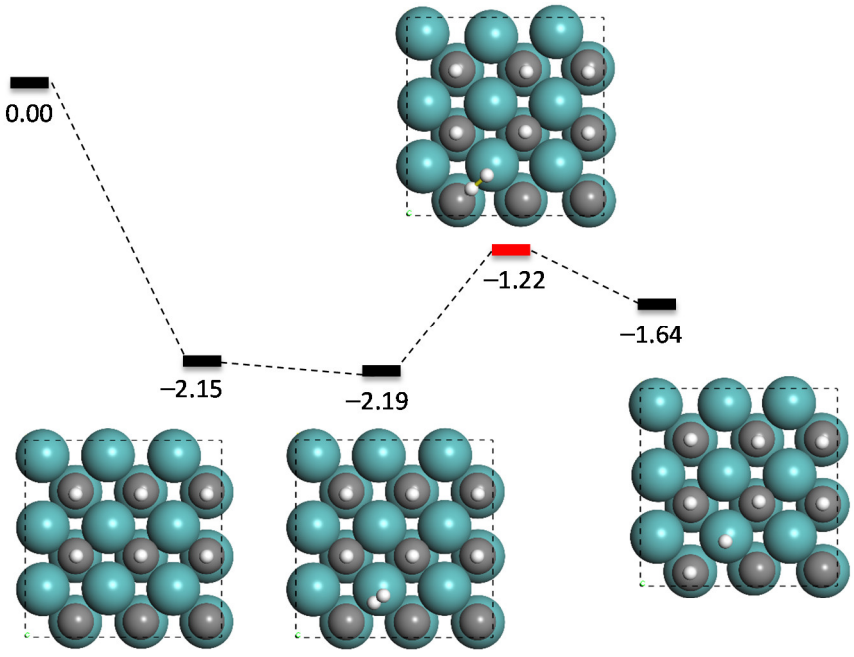

(6)

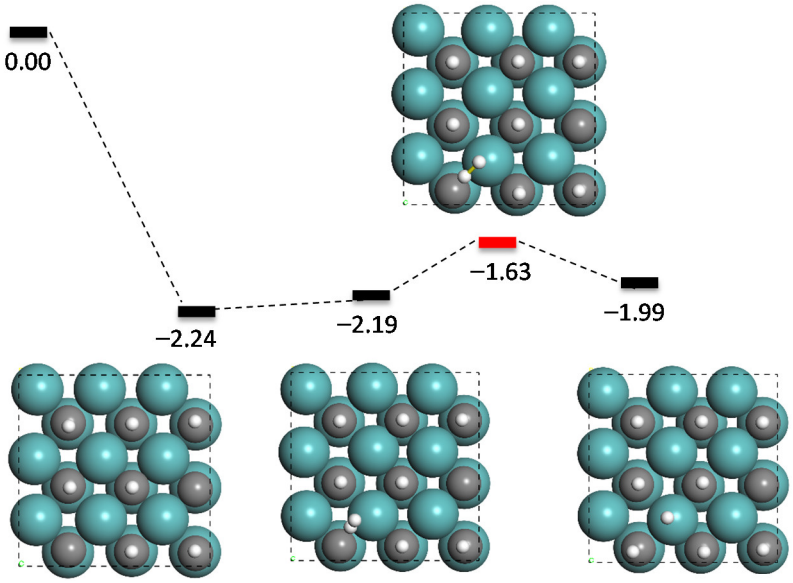

(7)

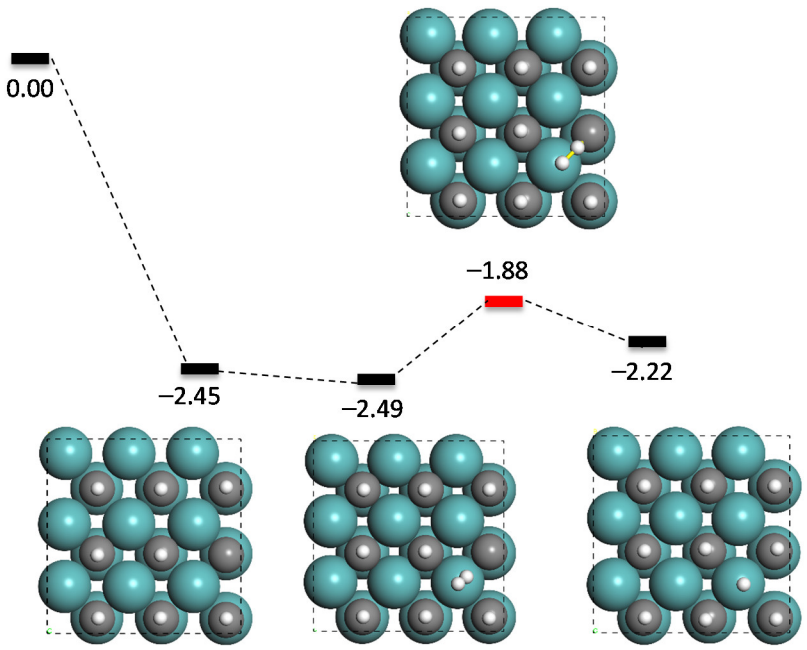

(8)

Fig. S7 The potential energy profiles with ZPE correction for H-H bond breaking at different H* coverage. Energies in eV with gas phase H_2O and H_2 as reference.

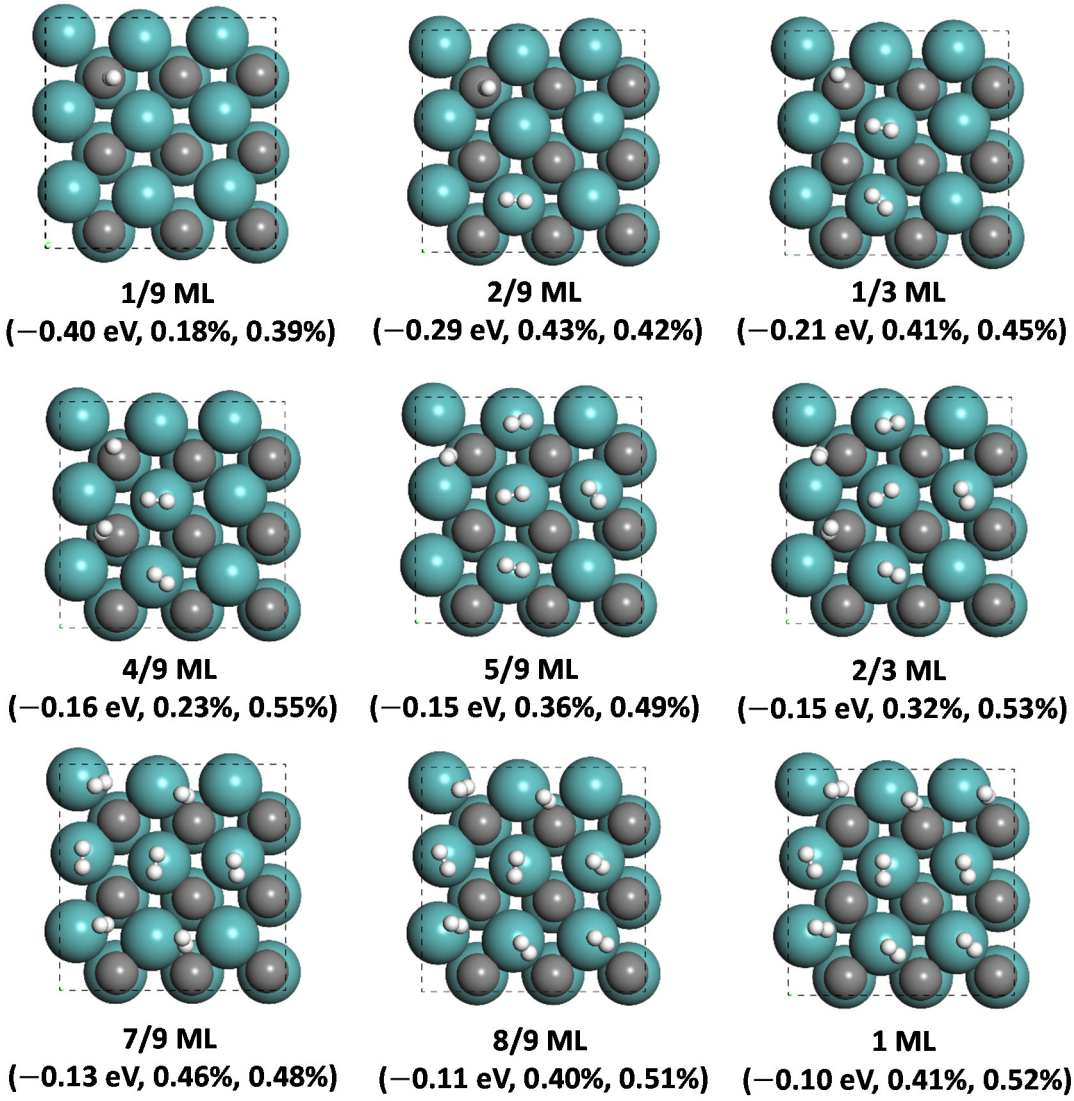

Fig. S8 Configurations of H_2 adsorption, values in the parentheses from left to right represent average binding energies of H_2 ($E_{AVG,n}^{H2O}$, n = 1-9), surface oxidation degree of Mo sites (OX_{Mo}) and surface oxidation degree of C sites (OX_C) at different coverage (1/9 – 1 ML, based on number of surface Mo sites) on fcc MoC (001) surface, respectively. Gaseous H_2 as energy reference.

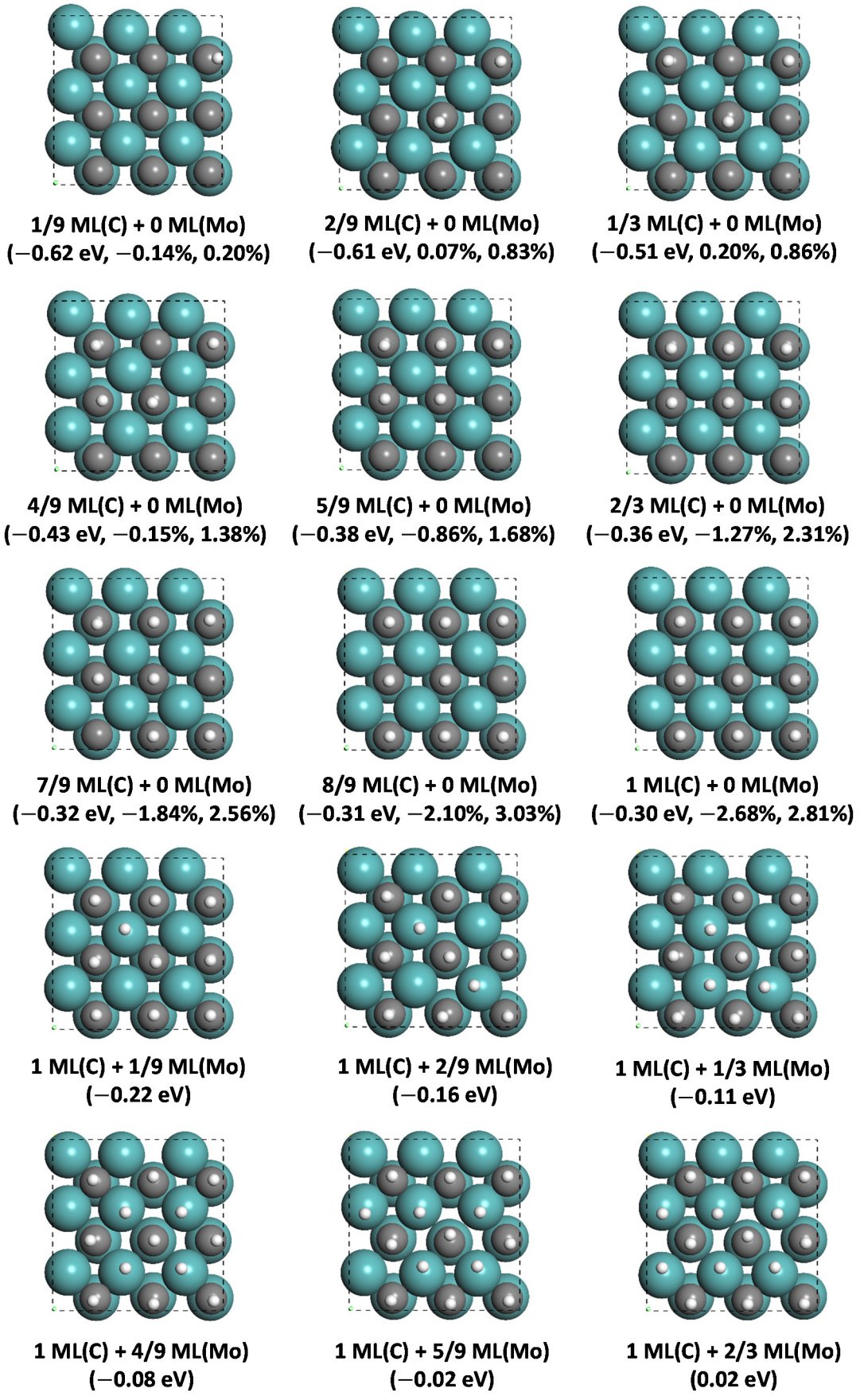

Fig. S9 Configurations of H* species, values in the parentheses from left to right represent average

binding energies of H_2 ($E_{AVG,n}^{H2O}$, n = 1-9), surface oxidation degree of Mo sites (OX_{Mo}) and surface oxidation degree of C sites (OX_C) at different coverage (1/9 – 1 ML, based on number of surface C and Mo sites, respectively) on fcc MoC (001) surface, respectively. Gaseous H_2 as energy reference.

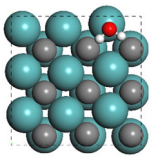

(1)
−1.00 eV

Fig. S10 Configurations of H_2O* (1/9 ML, based on number of surface Mo sites) and surface binding energy without ZPE correction. Gas phase H_2O and H_2 as reference

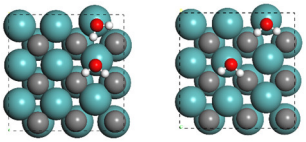

(1)
−0.94 eV

(2)
−0.81 eV

Fig. S11 Configurations of H_2O* (2/9 ML, based on number of surface Mo sites) and surface binding energy without ZPE correction. Gas phase H_2O and H_2 as reference

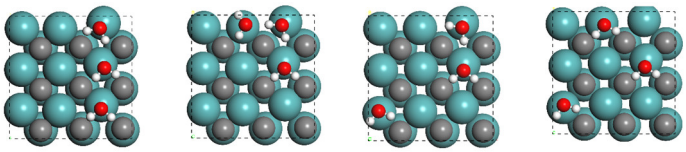

(1)
−0.85 eV

(2)
−0.84 eV

(3)
−0.80 eV

(4)
−0.74 eV

Fig. S12 Configurations of H_2O* (1/3 ML, based on number of surface Mo sites) and surface binding energy without ZPE correction. Gas phase H_2O and H_2 as reference

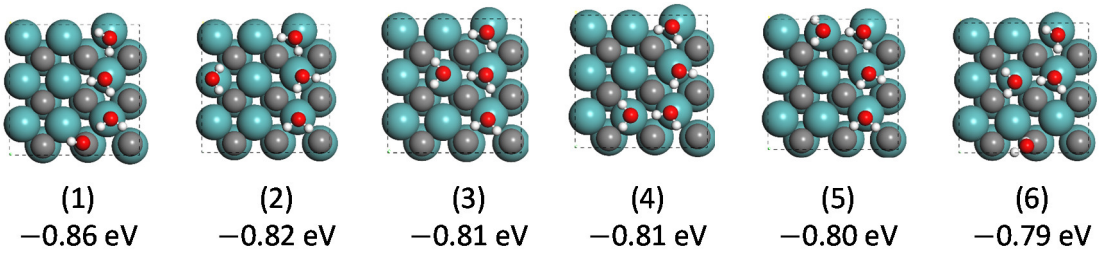

(1)
−0.86 eV

(2)
−0.82 eV

(3)
−0.81 eV

(4)
−0.81 eV

(5)
−0.80 eV

(6)
−0.79 eV

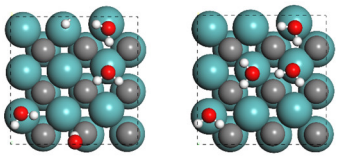

(7)
−0.77 eV

(8)
−0.76 eV

Fig. S13 Configurations of H_2O* (4/9 ML, based on number of surface Mo sites) and surface

binding energy without ZPE correction. Gas phase H_2O and H_2 as reference

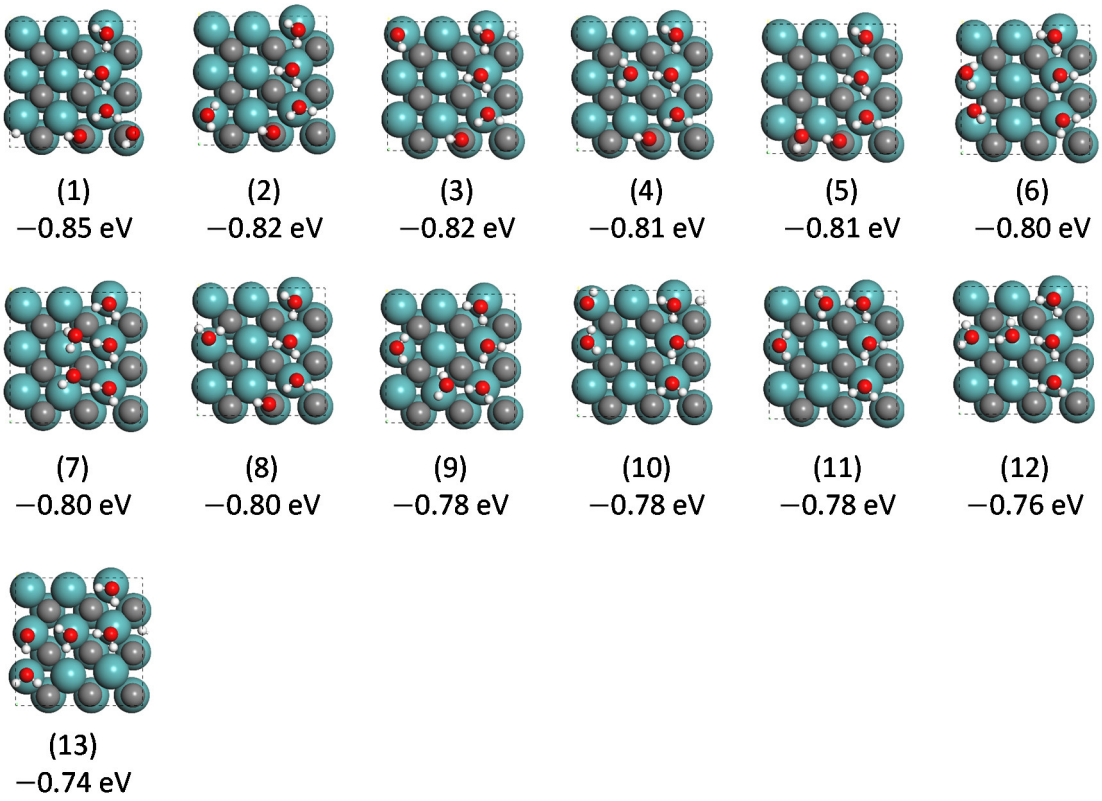

Fig. S14 Configurations of H_2O* (5/9 ML, based on number of surface Mo sites) and surface binding energy without ZPE correction. Gas phase H_2O and H_2 as reference

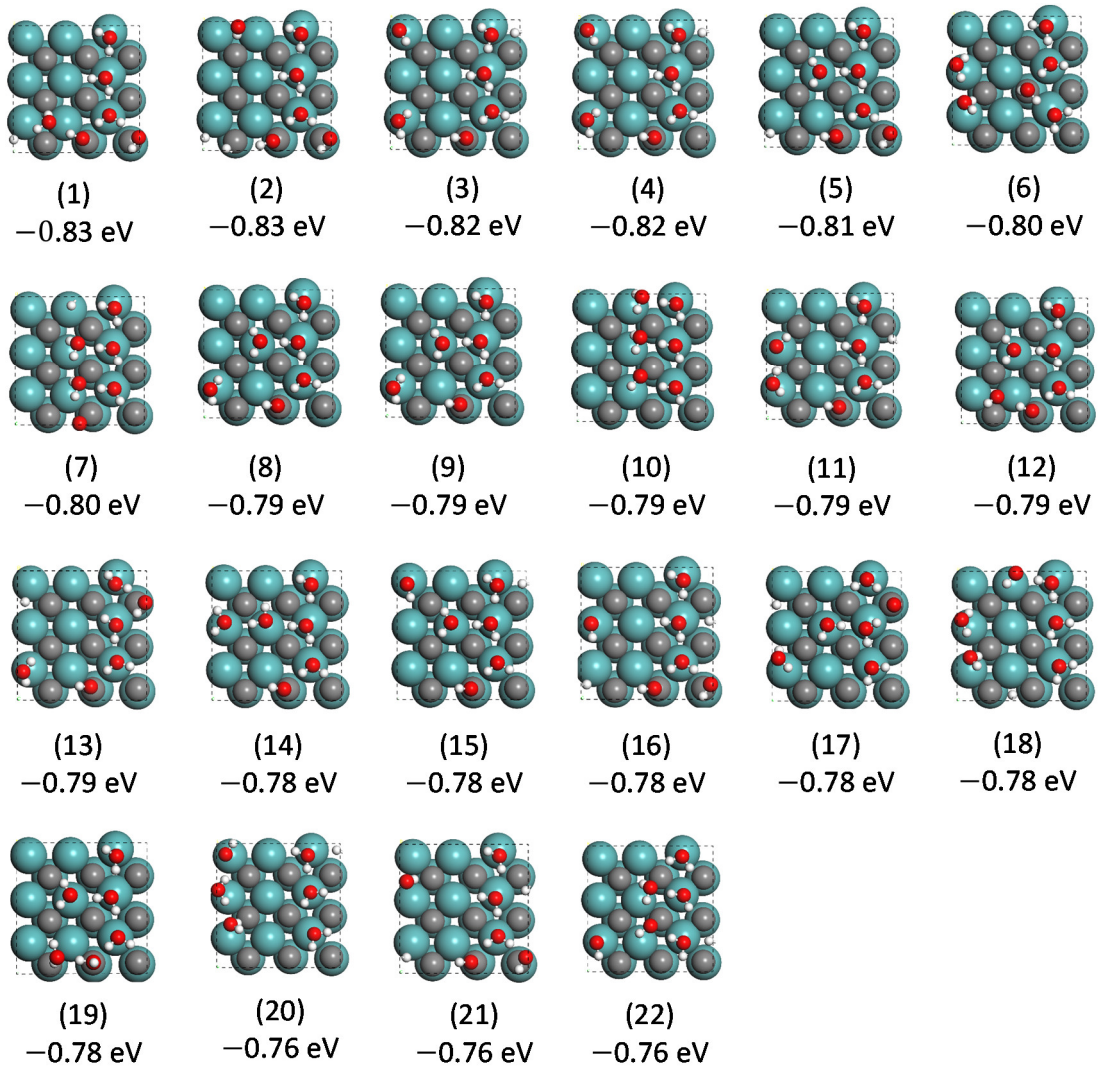

Fig. S15 Configurations of H_2O* (2/3 ML, based on number of surface Mo sites) and surface binding energy without ZPE correction. Gas phase H_2O and H_2 as reference

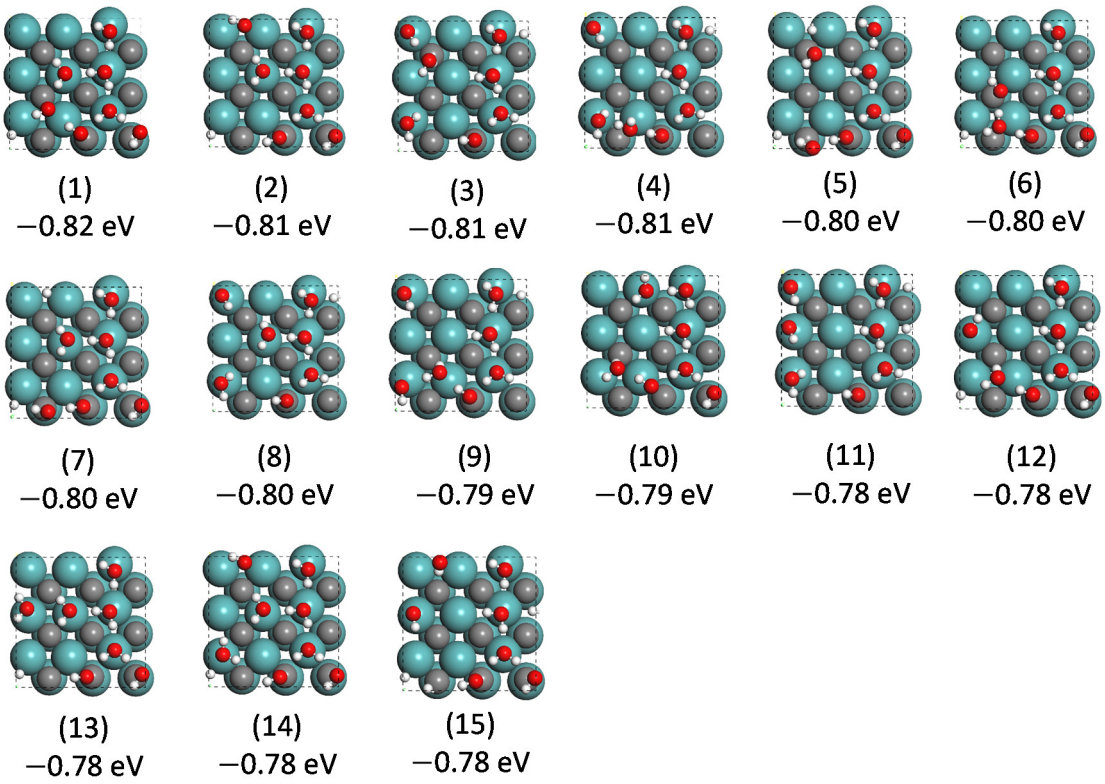

Fig. S16 Configurations of H_2O* (7/9 ML, based on number of surface Mo sites) and surface binding energy without ZPE correction. Gas phase H_2O and H_2 as reference

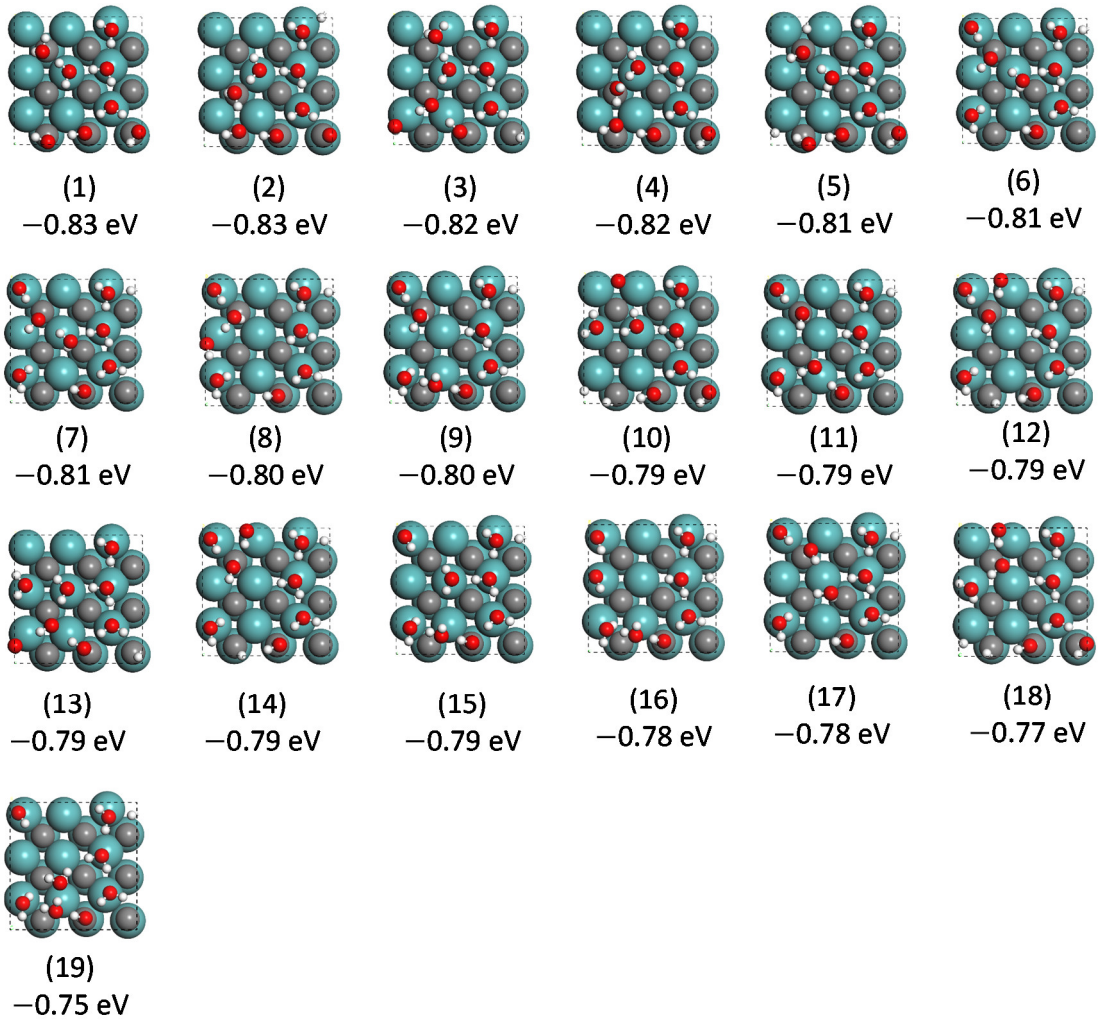

Fig. S17 Configurations of H_2O* (8/9 ML, based on number of surface Mo sites) and surface binding energy without ZPE correction. Gas phase H_2O and H_2 as reference

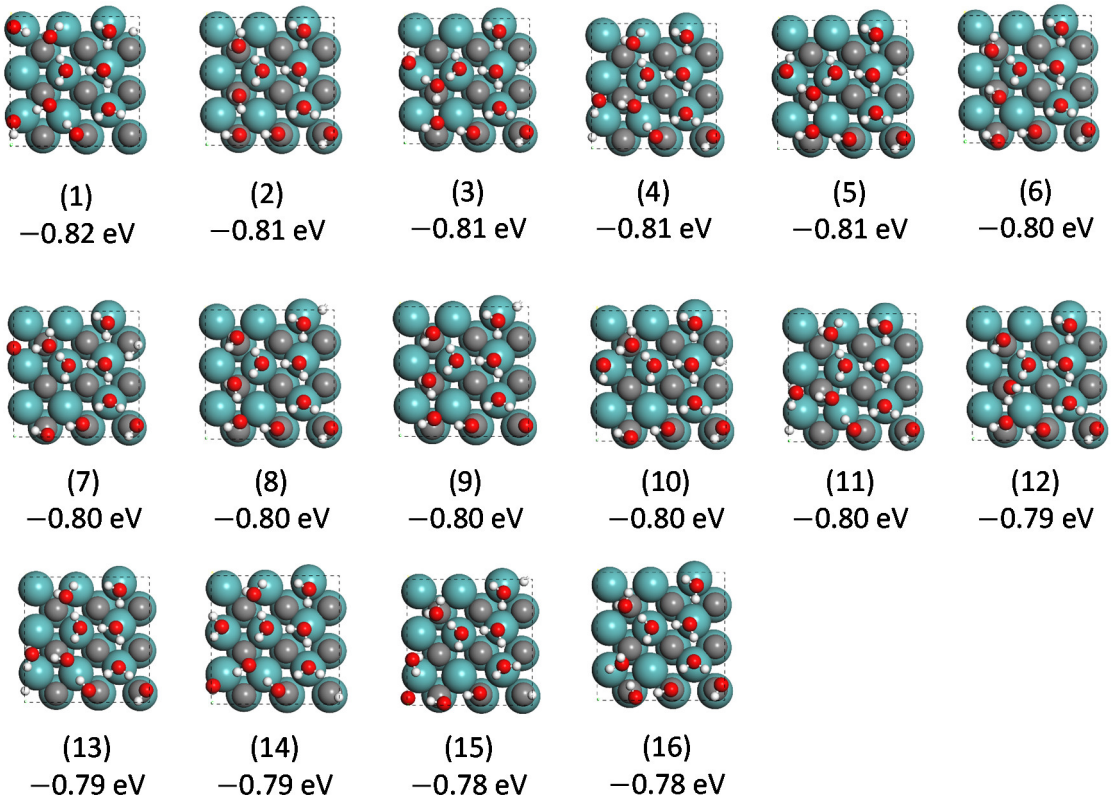

Fig. S18 Configurations of H_2O* (1 ML, based on number of surface Mo sites) and surface binding energy without ZPE correction. Gas phase H_2O and H_2 as reference

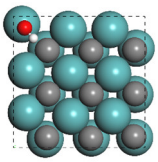

(1)
0.40 eV

Fig. S19 Configurations of OH* (1/9 ML, based on number of surface Mo sites) and surface binding energy without ZPE correction. Gas phase H_2O and H_2 as reference.

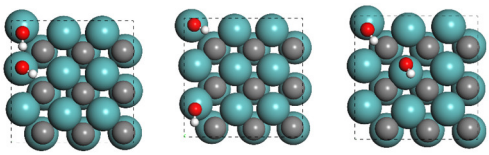

(1)
−0.78 eV

(2)
−0.74 eV

(3)
−0.46 eV

Fig. S20 Configurations of OH* (2/9 ML, based on number of surface Mo sites) and surface binding energy without ZPE correction. Gas phase H_2O and H_2 as reference.

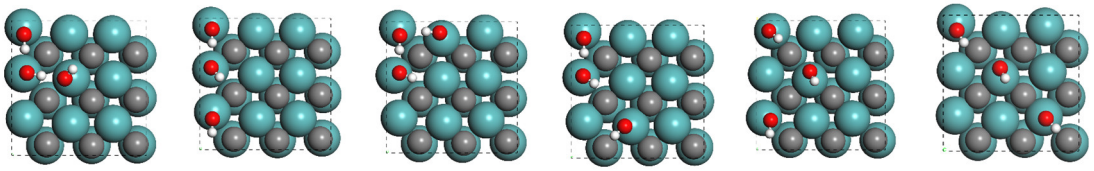

(1)
−0.89 eV

(2)
−0.89 eV

(3)
−0.83 eV

(4)
−0.72 eV

(5)
−0.51 eV

(6)
−0.32 eV

Fig. S21 Configurations of OH* (1/3 ML, based on number of surface Mo sites) and surface binding energy without ZPE correction. Gas phase H_2O and H_2 as reference.

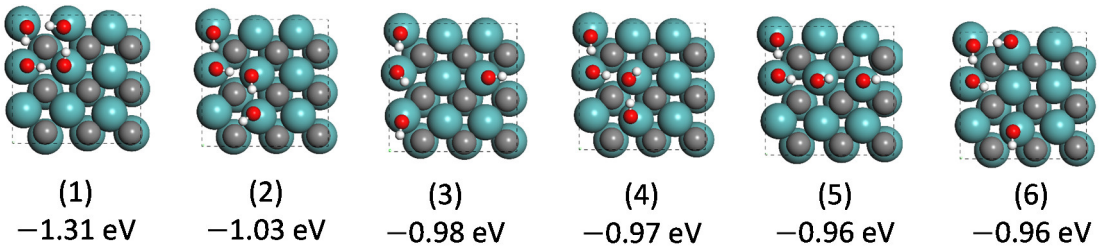

(1)
−1.31 eV

(2)
−1.03 eV

(3)
−0.98 eV

(4)
−0.97 eV

(5)
−0.96 eV

(6)
−0.96 eV

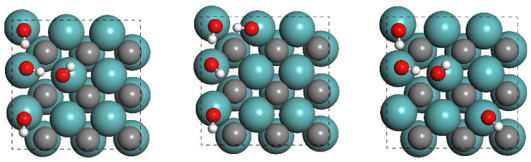

(7)
−0.93 eV

(8)
−0.88 eV

(9)
−0.61 eV

Fig. S22 Configurations of OH* (4/9 ML, based on number of surface Mo sites) and surface binding energy without ZPE correction. Gas phase H_2O and H_2 as reference.

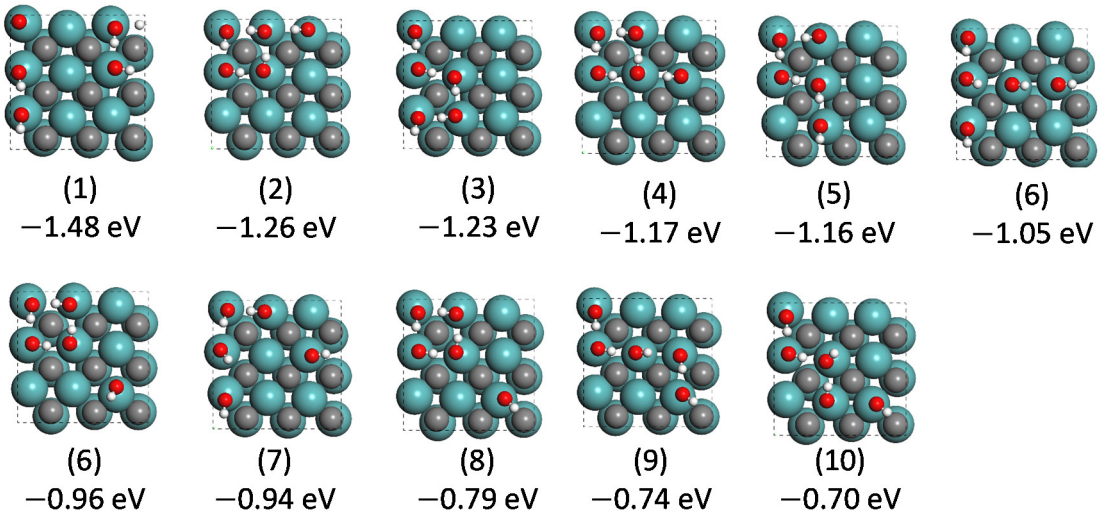

Fig. S23 Configurations of OH* (5/9 ML, based on number of surface Mo sites) and surface binding energy without ZPE correction. Gas phase H_2O and H_2 as reference

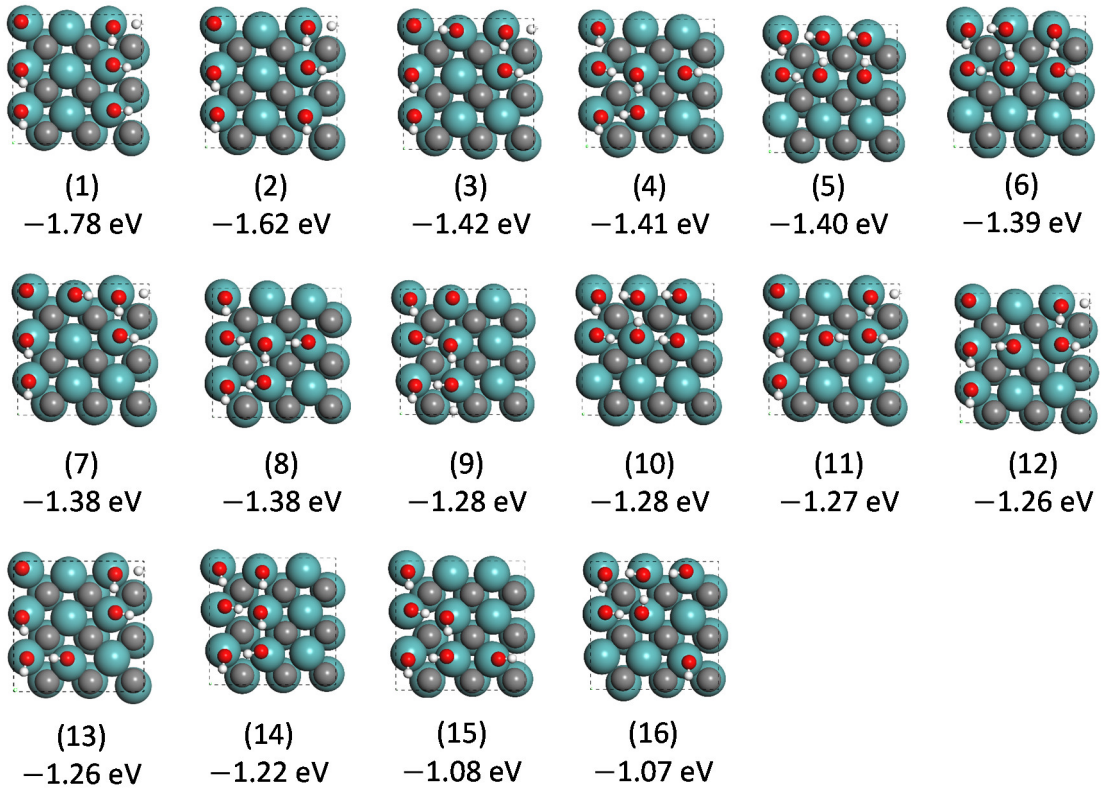

Fig. S24 Configurations of OH* (2/3 ML, based on number of surface Mo sites) and surface binding energy without ZPE correction. Gas phase H_2O and H_2 as reference

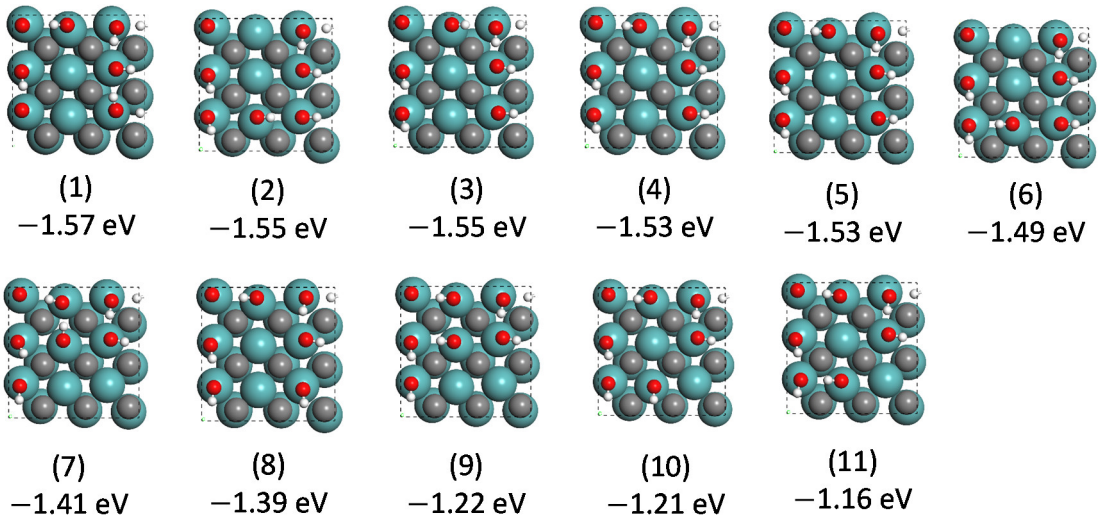

Fig. S25 Configurations of OH* (7/9 ML, based on number of surface Mo sites) and surface binding energy without ZPE correction. Gas phase H_2O and H_2 as reference

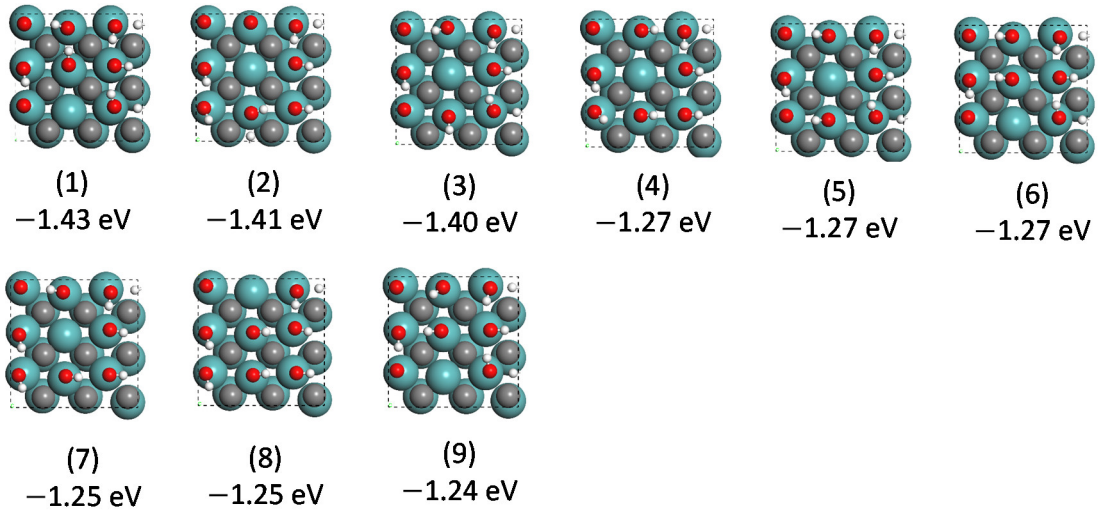

Fig. S26 Configurations of OH* (8/9 ML, based on number of surface Mo sites) and surface binding energy without ZPE correction. Gas phase H_2O and H_2 as reference

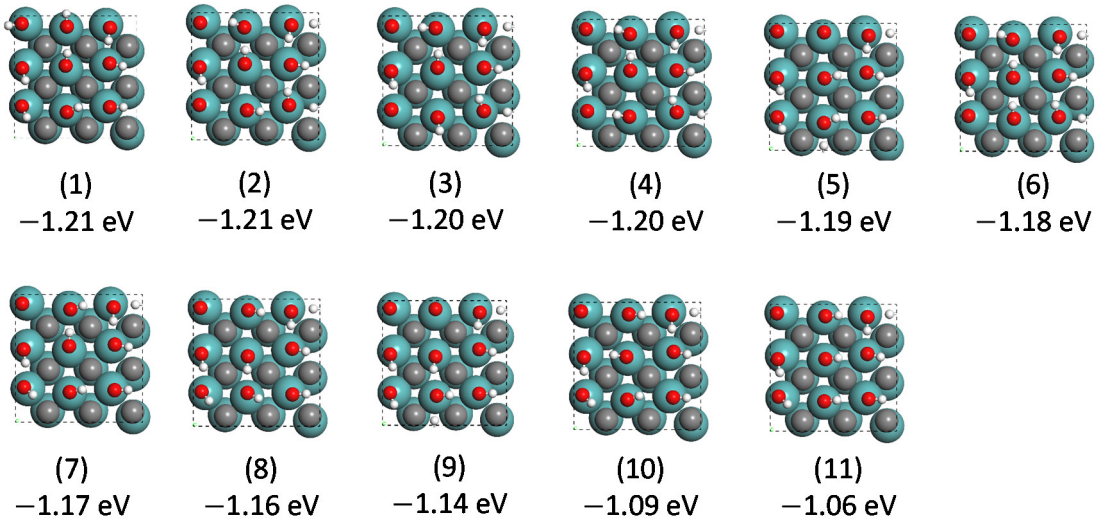

Fig. S27 Configurations of OH* (1 ML, based on number of surface Mo sites) and surface binding

energy without ZPE correction. Gas phase H_2O and H_2 as reference

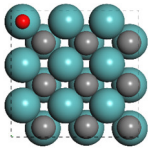

(1)
0.17 eV

Fig. S28 Configurations of O* (1/9 ML, based on number of surface Mo sites) and surface binding energy without ZPE correction. Gas phase H_2O and H_2 as reference

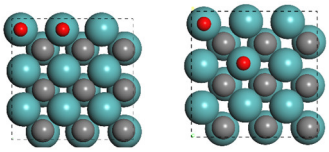

(1)
0.20 eV

(2)
0.22 eV

Fig. S29 Configurations of O* (2/9 ML, based on number of surface Mo sites) and surface binding energy without ZPE correction. Gas phase H_2O and H_2 as reference

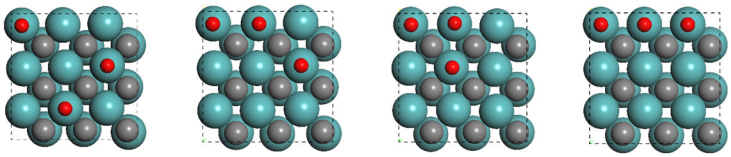

(1)
0.28 eV

(2)
0.32 eV

(3)
0.37 eV

(3)
0.38 eV

Fig. S30 Configurations of O* (1/3 ML, based on number of surface Mo sites) and surface binding energy without ZPE correction. Gas phase H_2O and H_2 as reference

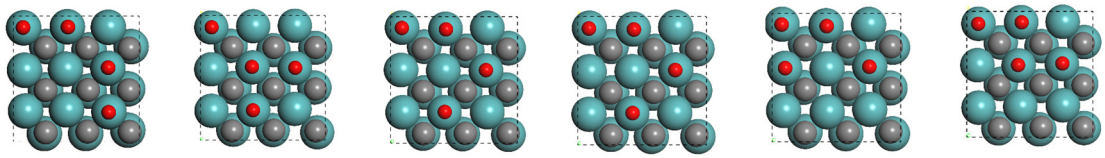

(1)
0.39 eV

(2)
0.40 eV

(3)
0.40 eV

(4)
0.40 eV

(5)
0.42 eV

(6)
0.42 eV

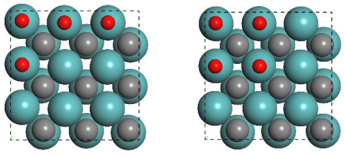

(7)
0.45 eV

(8)
0.47 eV

Fig. S31 Configurations of O* (4/9 ML, based on number of surface Mo sites) and surface binding energy without ZPE correction. Gas phase H_2O and H_2 as reference

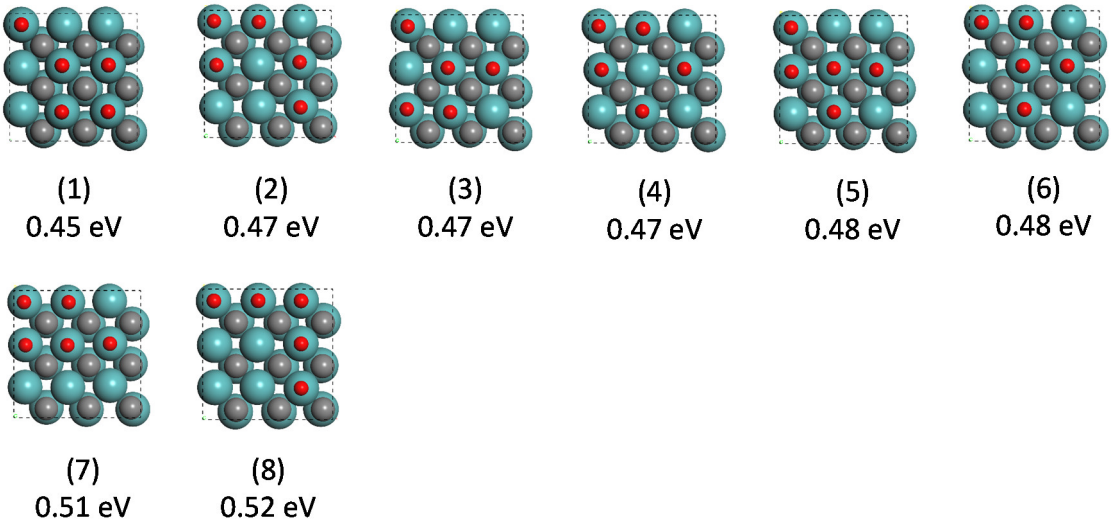

Fig. S32 Configurations of O* (5/9 ML, based on number of surface Mo sites) and surface binding energy without ZPE correction. Gas phase H_2O and H_2 as reference

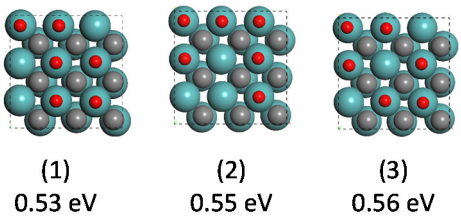

Fig. S33 Configurations of O* (2/3 ML, based on number of surface Mo sites) and surface binding energy without ZPE correction. Gas phase H_2O and H_2 as reference

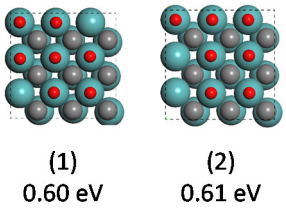

Fig. S34 Configurations of O* (7/9 ML, based on number of surface Mo sites) and surface binding energy without ZPE correction. Gas phase H_2O and H_2 as reference

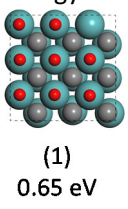

Fig. S35 Configurations of O* (8/9 ML, based on number of surface Mo sites) and surface binding energy without ZPE correction. Gas phase H_2O and H_2 as reference

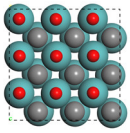

(1)
0.72 eV

Fig. S36 Configurations of O* (1 ML, based on number of surface Mo sites) and surface binding energy without ZPE correction. Gas phase H_2O and H_2 as reference

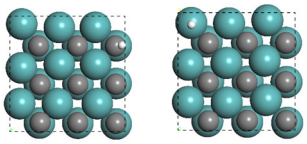

(1)
−0.73 eV

(2)
−0.07 eV

Fig. S37 Configurations of H* (1/9 ML, based on number of surface Mo sites) and surface binding energy without ZPE correction. Gas phase H_2O and H_2 as reference

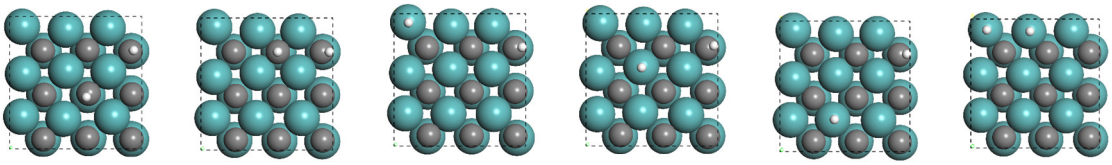

(1)
−0.73 eV

(2)
−0.52 eV

(3)
−0.31 eV

(4)
−0.24 eV

(5)
−0.22 eV

(6)
0.03 eV

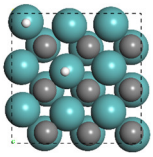

(6)
0.05 eV

Fig. S38 Configurations of H* (2/9 ML, based on number of surface Mo sites) and surface binding energy without ZPE correction. Gas phase H_2O and H_2 as reference

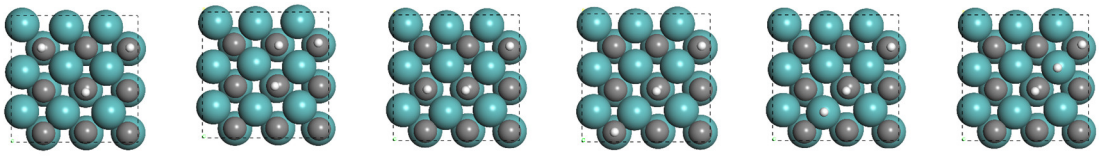

(1)
−0.63 eV

(2)
−0.62 eV

(3)
−0.62 eV

(4)
−0.57 eV

(5)
−0.38 eV

(6)
−0.37 eV

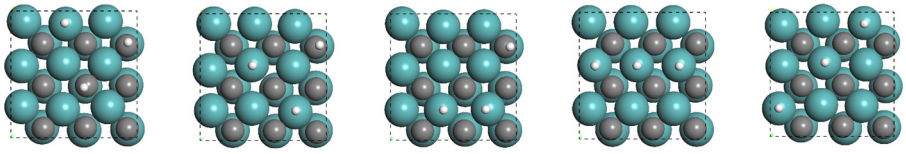

(7)
−0.35 eV

(8)
−0.14 eV

(9)
−0.11 eV

(10)
0.10 eV

(11)
0.12 eV

Fig. S39 Configurations of H* (1/3 ML, based on number of surface Mo sites) and surface binding energy without ZPE correction. Gas phase H_2O and H_2 as reference

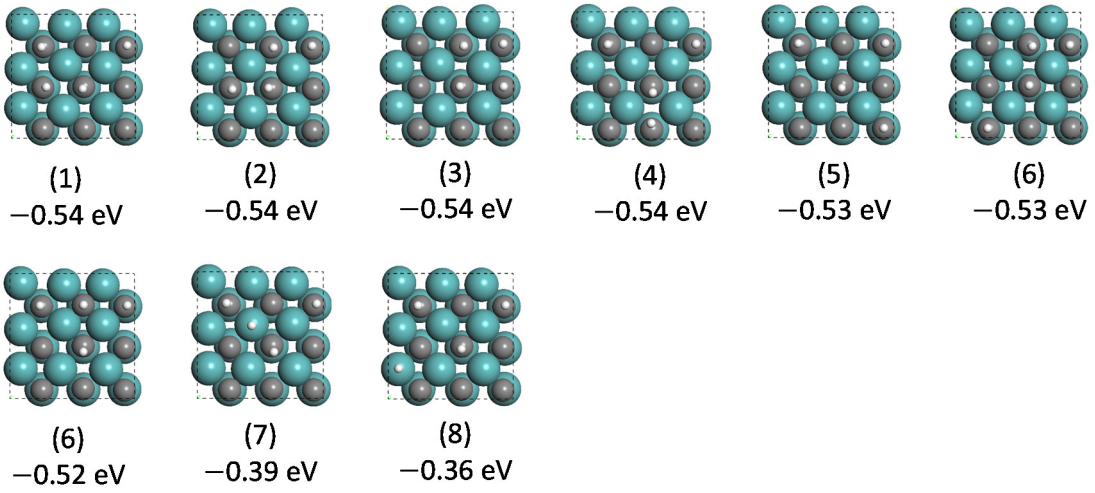

Fig. S40 Configurations of H* (4/9 ML, based on number of surface Mo sites) and surface binding energy without ZPE correction. Gas phase H_2O and H_2 as reference

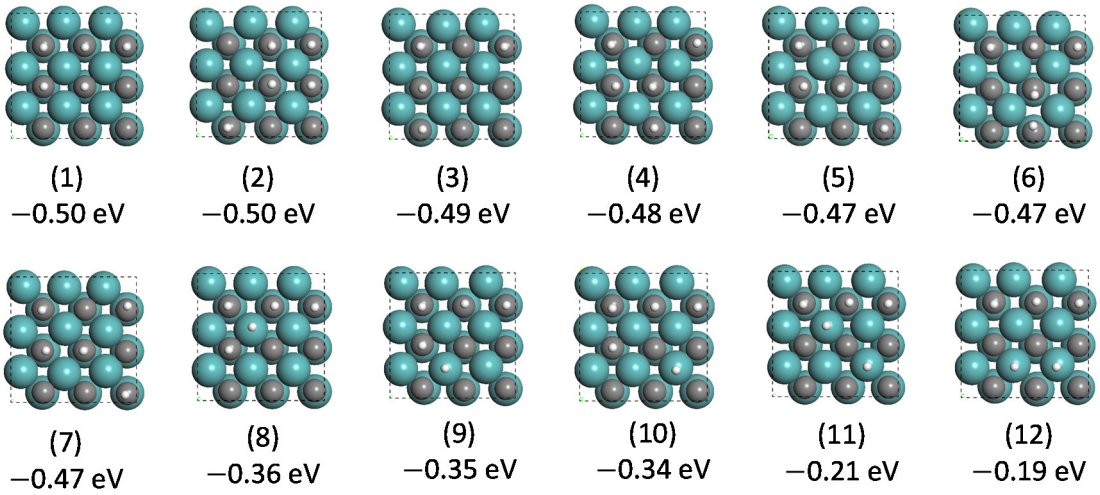

Fig. S41 Configurations of H* (5/9 ML, based on number of surface Mo sites) and surface binding energy without ZPE correction. Gas phase H_2O and H_2 as reference

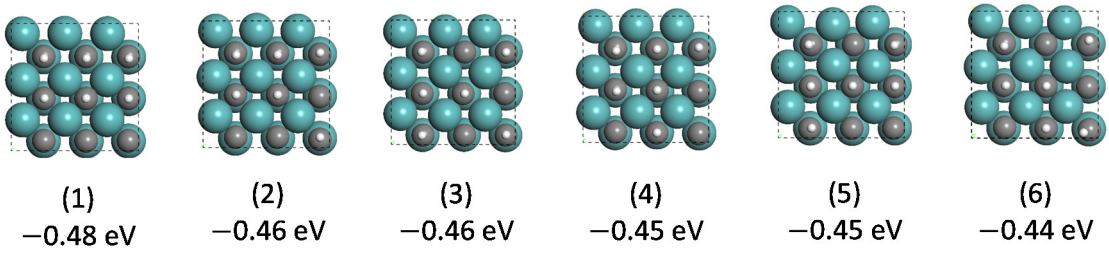

Fig. S42 Configurations of H* (2/3 ML, based on number of surface Mo sites) and surface binding energy without ZPE correction. Gas phase H_2O and H_2 as reference

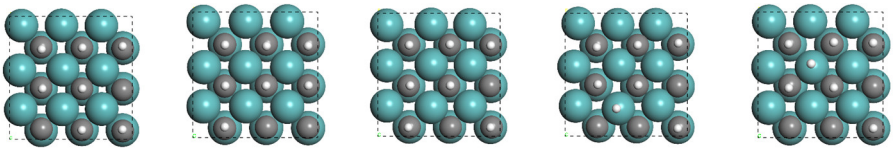

Fig. S43 Configurations of H* (7/9 ML, based on number of surface Mo sites) and surface binding energy without ZPE correction. Gas phase H_2O and H_2 as reference

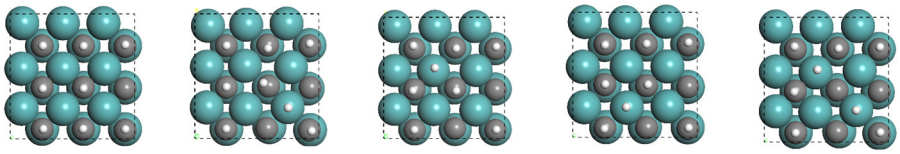

Fig. S44 Configurations of H* (8/9 ML, based on number of surface Mo sites) and surface binding energy without ZPE correction. Gas phase H_2O and H_2 as reference

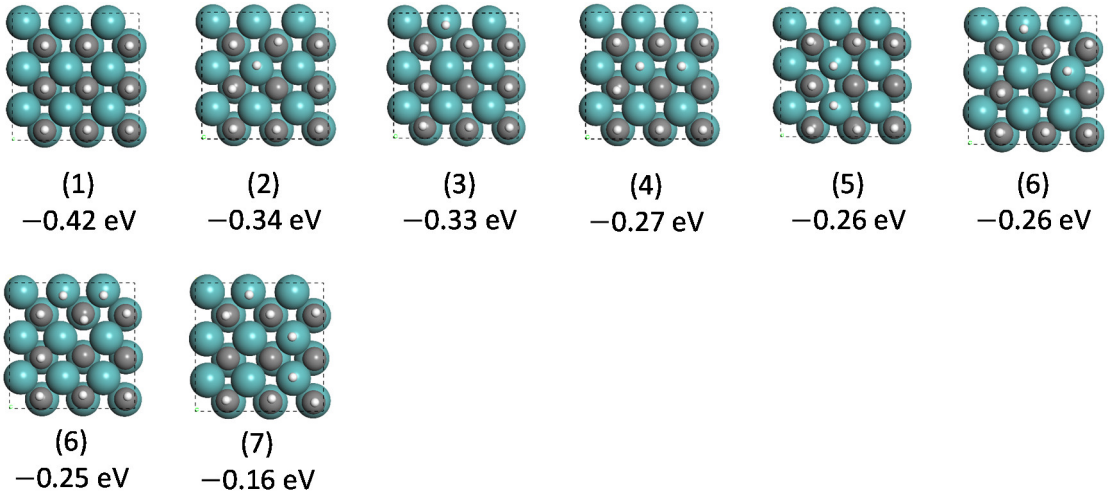

Fig. S45 Configurations of H* (1 ML, based on number of surface Mo sites) and surface binding energy without ZPE correction. Gas phase H_2O and H_2 as reference

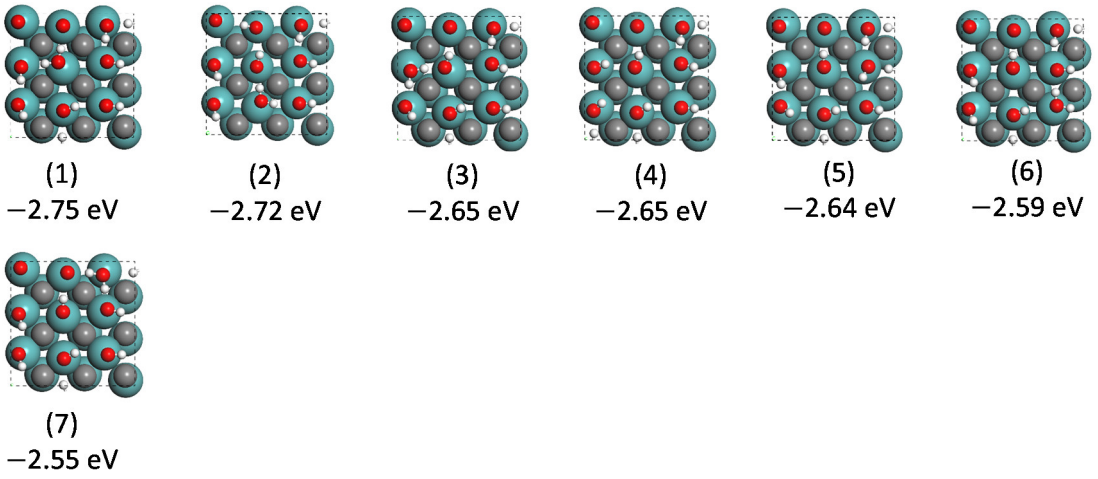

Fig. S46 Configurations of 8OH_1H_2O (mixed 8/9 ML OH and 1/9 ML H_2O) and surface energies without ZPE correction. Gas phase H_2O and H_2 as reference

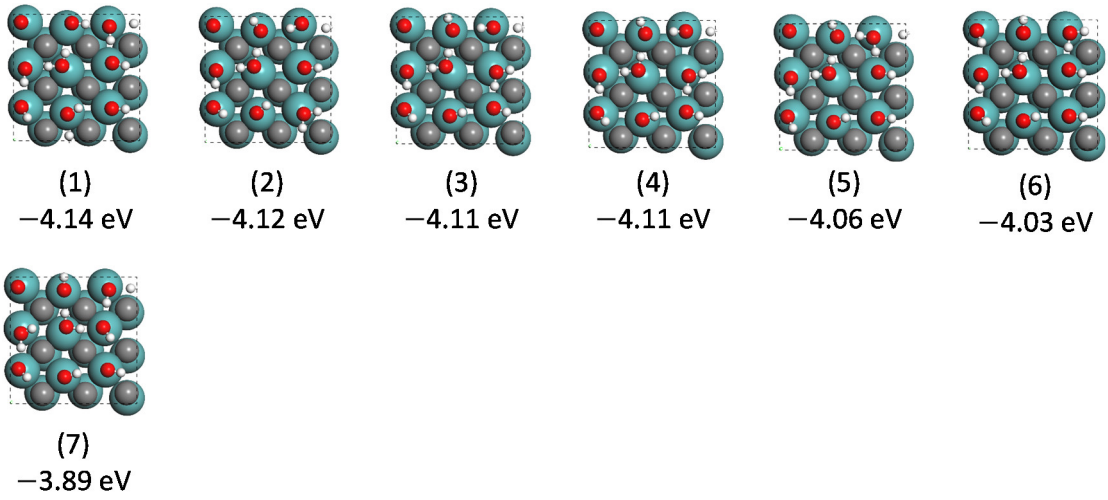

Fig. S47 Configurations of 7OH_2H_2O (mixed 7/9 ML OH and 2/9 ML H_2O) and surface energies without ZPE correction. Gas phase H_2O and H_2 as reference

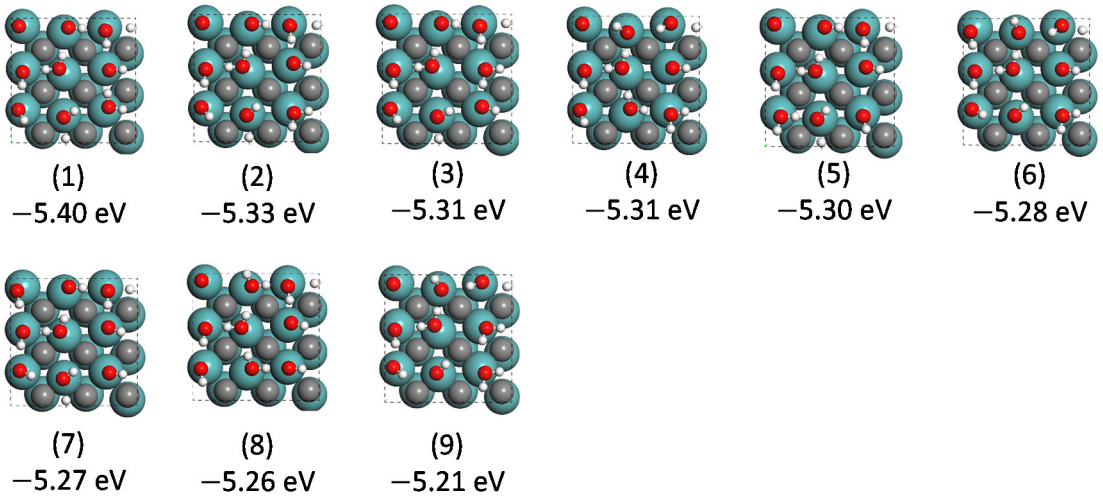

Fig. S48 Configurations of 6OH_3H_2O (mixed 2/3 ML OH and 1/3 ML H_2O) and surface energies without ZPE correction. Gas phase H_2O and H_2 as reference

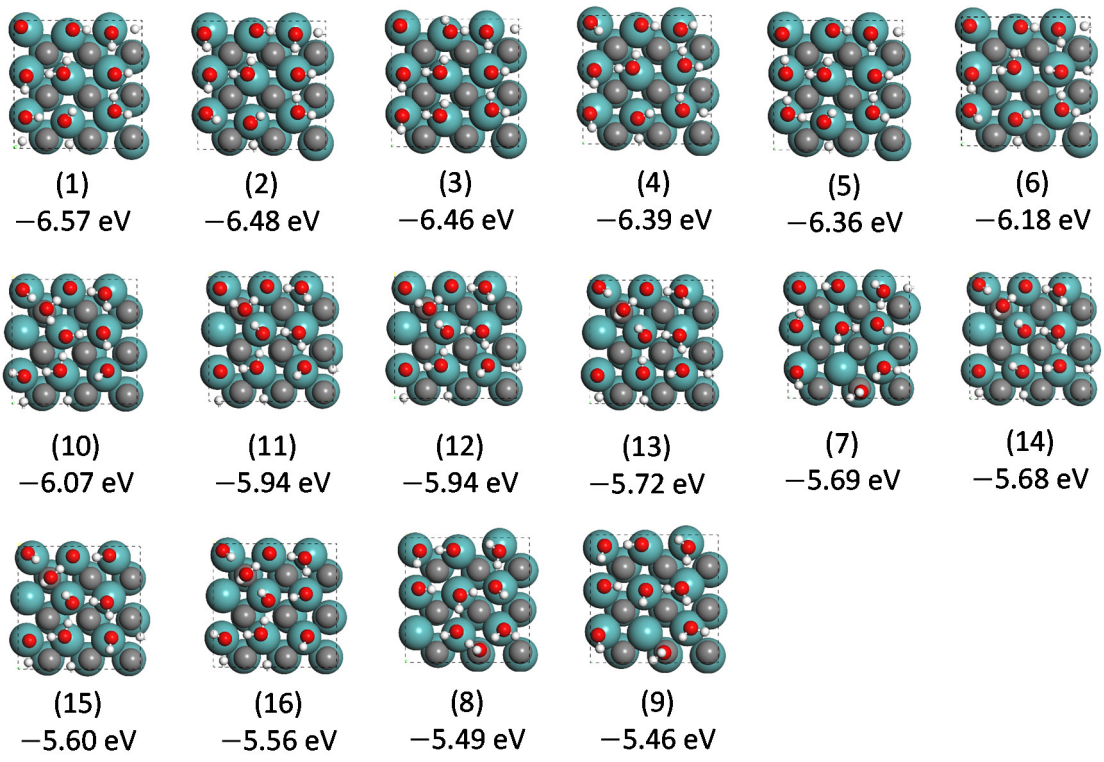

Fig. S49 Configurations of 5OH_4H_2O (mixed 5/9 ML OH and 4/9 ML H_2O) and surface energies without ZPE correction. Gas phase H_2O and H_2 as reference

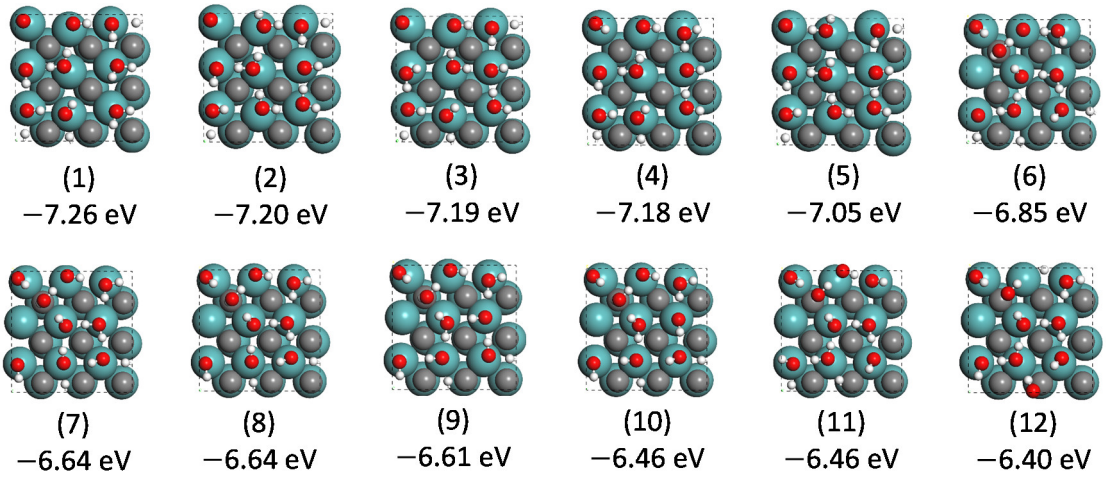

Fig. S50 Configurations of 4OH_5H_2O (mixed 4/9 ML OH and 5/9 ML H_2O) and surface energies without ZPE correction. Gas phase H_2O and H_2 as reference

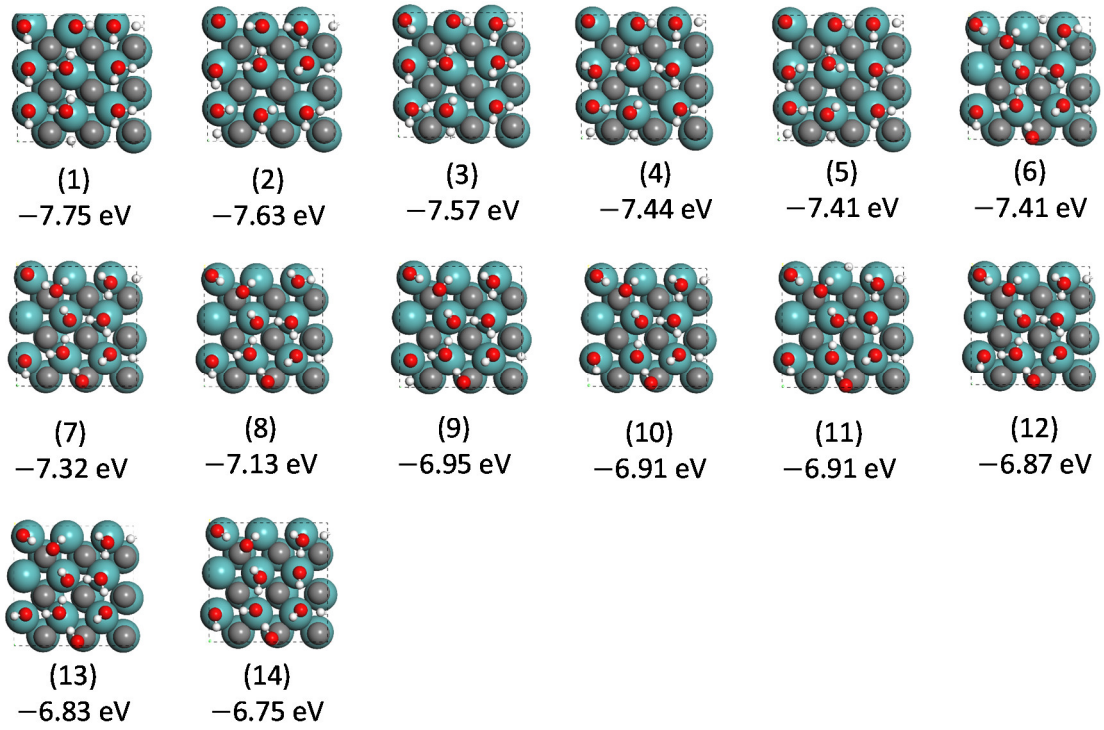

Fig. S51 Configurations of 3OH_6H_2O (mixed 1/3 ML OH and 2/3 ML H_2O) and surface energies without ZPE correction. Gas phase H_2O and H_2 as reference

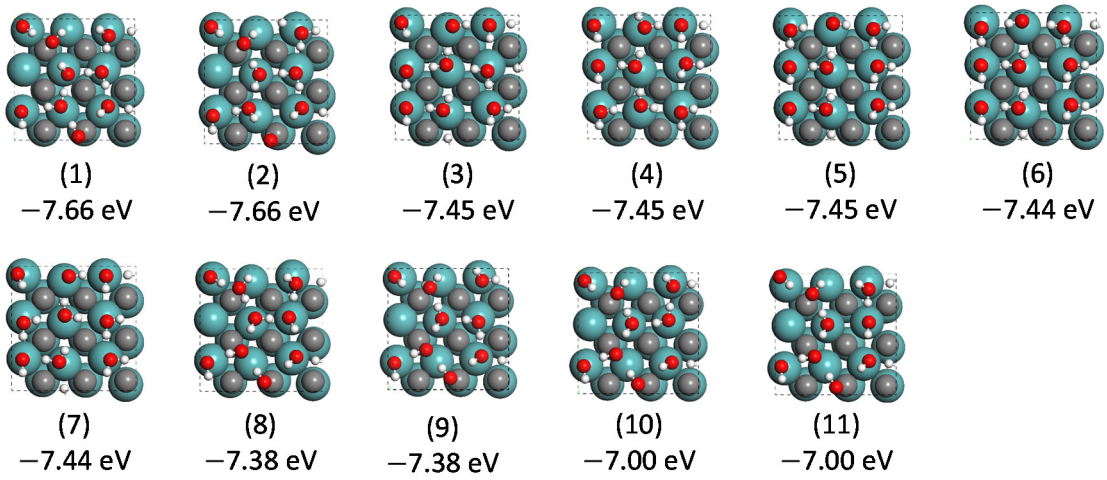

Fig. S52 Configurations of 2OH_7H_2O (mixed 2/9 ML OH and 7/9 ML H_2O) and surface energies without ZPE correction. Gas phase H_2O and H_2 as reference

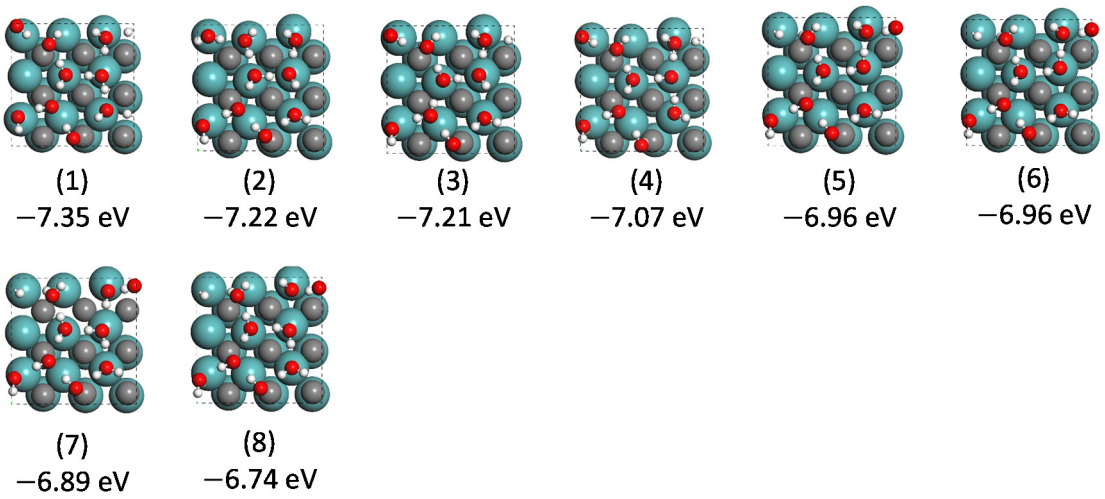

Fig. S53 Configurations of 1OH_8H_2O (mixed 1/9 ML OH and 8/9 ML H_2O) and surface energies without ZPE correction. Gas phase H_2O and H_2 as reference

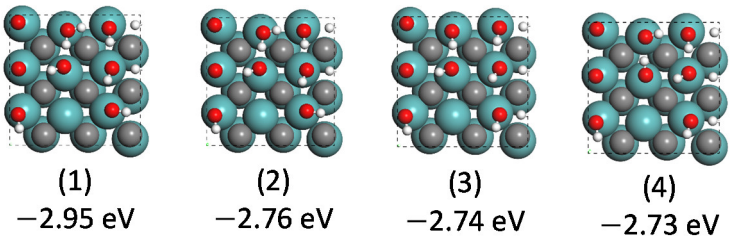

Fig. S54 Configurations of 7OH_1H_2O (mixed 7/9 ML OH and 1/9 ML H_2O) and surface energies without ZPE correction. Gas phase H_2O and H_2 as reference

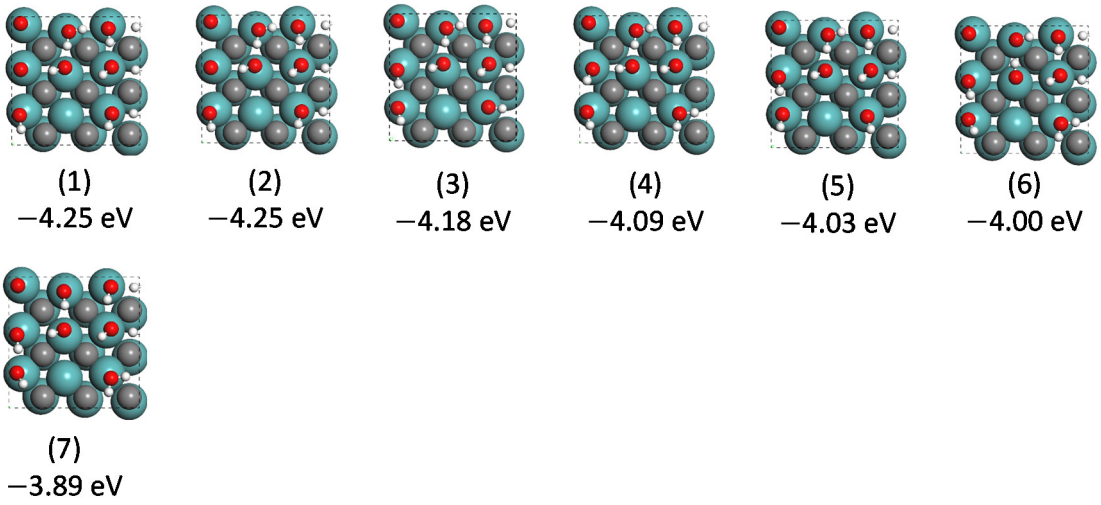

Fig. S55 Configurations of 6OH_2H_2O (mixed 2/3 ML OH and 2/9 ML H_2O) and surface energies without ZPE correction. Gas phase H_2O and H_2 as reference

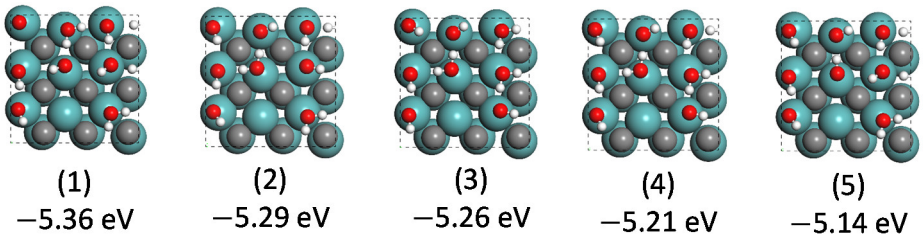

Fig. S56 Configurations of 5OH_3H_2O (mixed 5/9 ML OH and 1/3 ML H_2O) and surface energies without ZPE correction. Gas phase H_2O and H_2 as reference

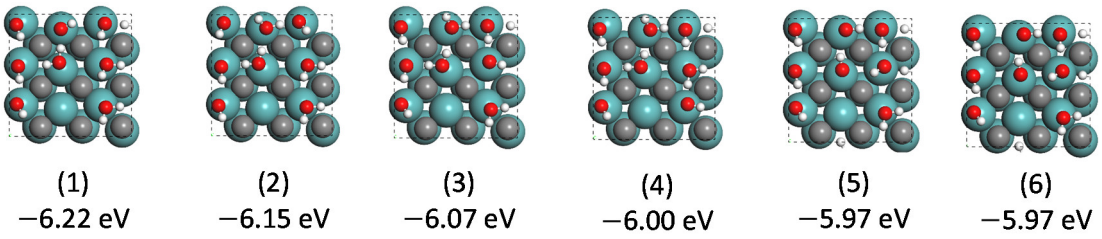

Fig. S57 Configurations of 4OH_4H_2O (mixed 4/9 ML OH and 4/9 ML H_2O) and surface energies without ZPE correction. Gas phase H_2O and H_2 as reference

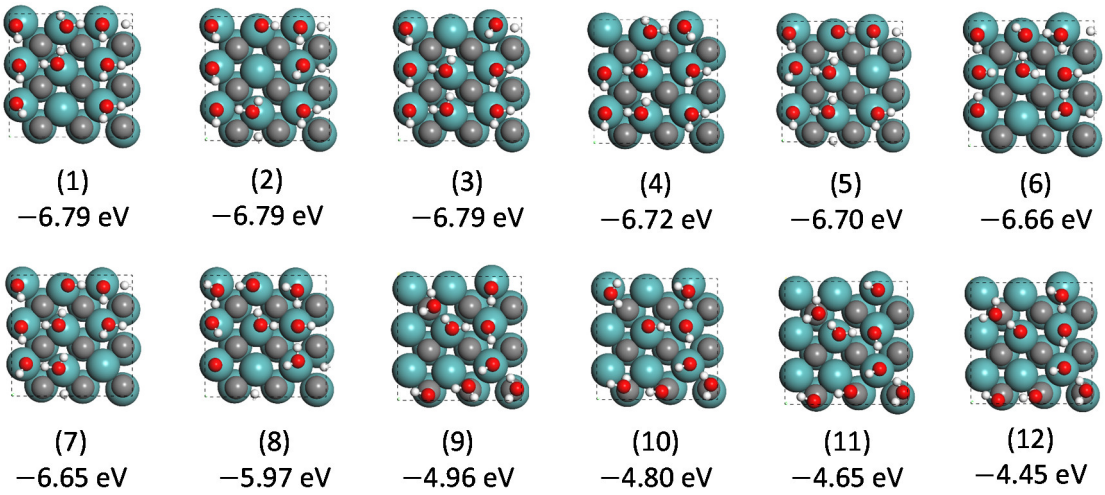

Fig. S58 Configurations of 3OH_5H_2O (mixed 1/3 ML OH and 5/9 ML H_2O) and surface energies without ZPE correction. Gas phase H_2O and H_2 as reference

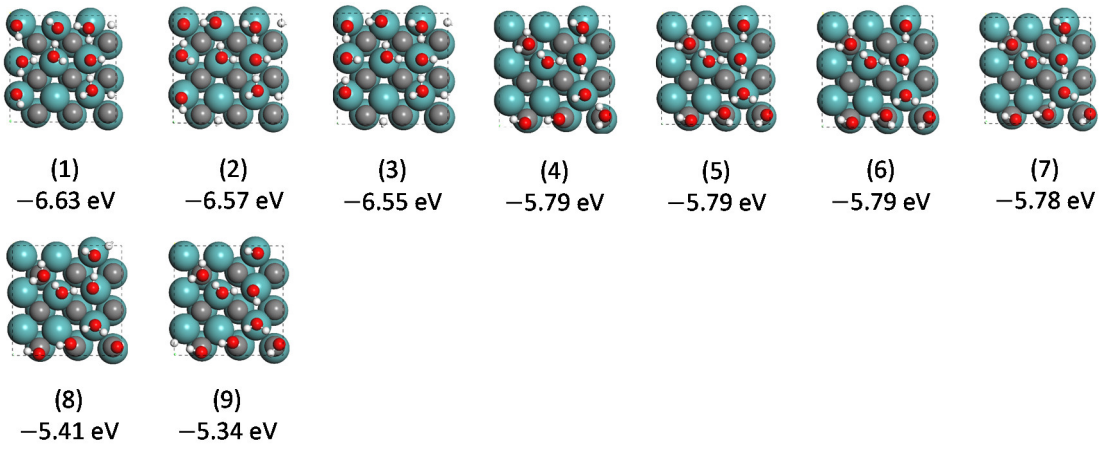

Fig. S59 Configurations of 2OH_6H_2O (mixed 2/9 ML OH and 2/3 ML H_2O) and surface energies without ZPE correction. Gas phase H_2O and H_2 as reference

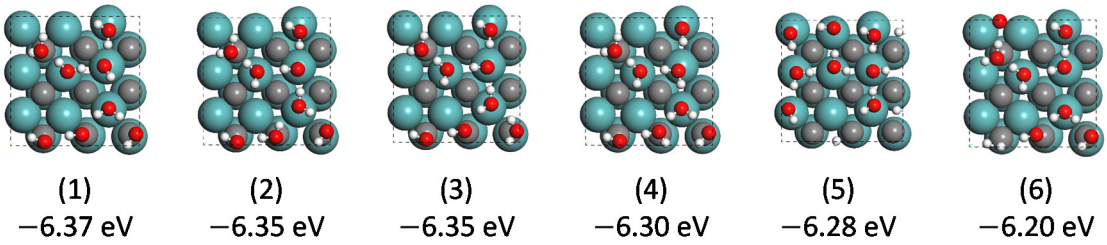

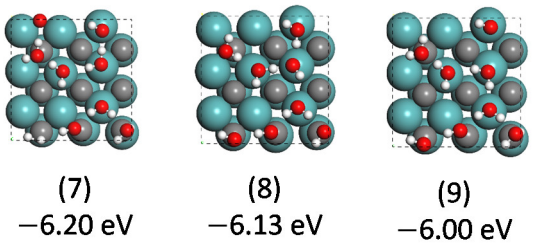

Fig. S60 Configurations of 1OH_7H_2O (mixed 1/9 ML OH and 7/9 ML H_2O) and surface energies without ZPE correction. Gas phase H_2O and H_2 as reference

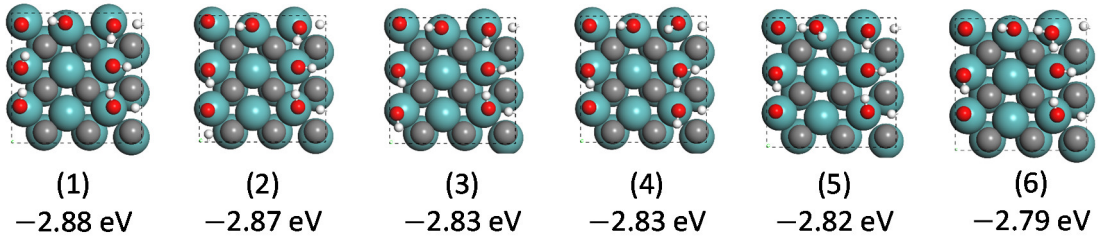

Fig. S61 Configurations of 6OH_1H_2O (mixed 2/3 ML OH and 1/9 ML H_2O) and surface energies without ZPE correction. Gas phase H_2O and H_2 as reference

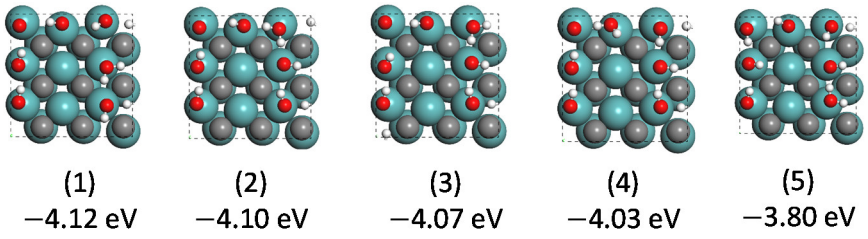

Fig. S62 Configurations of 5OH_2H_2O (mixed 5/9 ML OH and 2/9 ML H_2O) and surface energies without ZPE correction. Gas phase H_2O and H_2 as reference

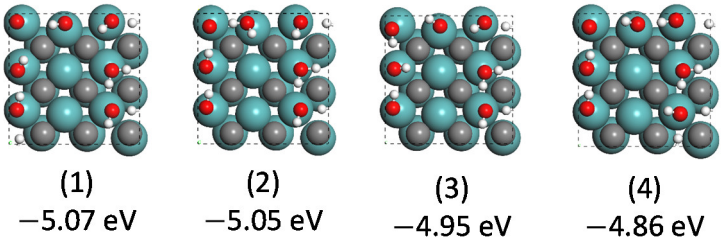

Fig. S63 Configurations of 4OH_3H_2O (mixed 4/9 ML OH and 1/3 ML H_2O) and surface energies without ZPE correction. Gas phase H_2O and H_2 as reference

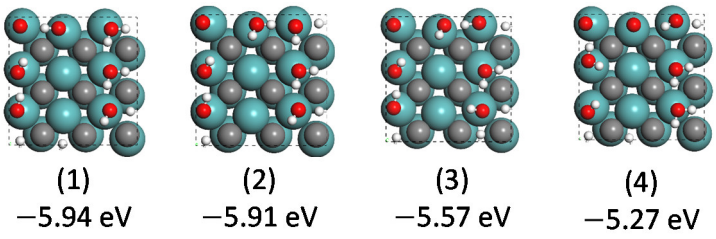

Fig. S64 Configurations of 3OH_4H_2O (mixed 1/3 ML OH and 4/9 ML H_2O) and surface energies without ZPE correction. Gas phase H_2O and H_2 as reference

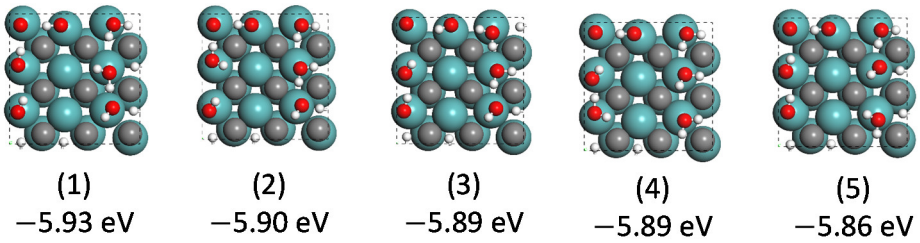

Fig. S65 Configurations of 2OH_5H_2O (mixed 2/9 ML OH and 5/9 ML H_2O) and surface energies without ZPE correction. Gas phase H_2O and H_2 as reference

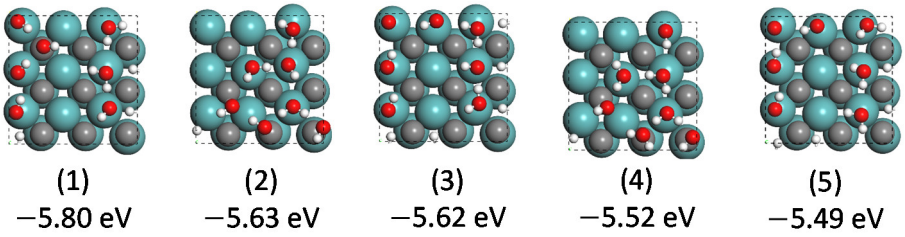

Fig. S66 Configurations of 1OH_6H_2O (mixed 1/9 ML OH and 2/3 ML H_2O) and surface energies without ZPE correction. Gas phase H_2O and H_2 as reference

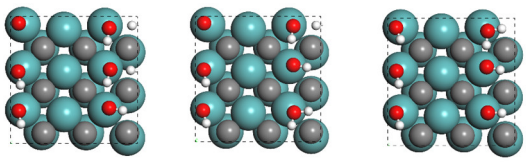

Fig. S67 Configurations of 5OH_1H_2O (mixed 5/9 ML OH and 1/9 ML H_2O) and surface energies without ZPE correction. Gas phase H_2O and H_2 as reference

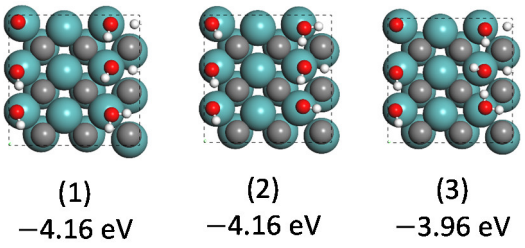

Fig. S68 Configurations of 4OH_2H_2O (mixed 4/9 ML OH and 2/9 ML H_2O) and surface energies without ZPE correction. Gas phase H_2O and H_2 as reference

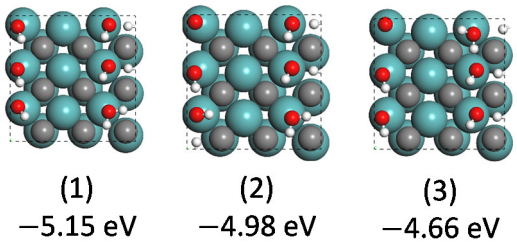

Fig. S69 Configurations of 3OH_3H_2O (mixed 1/3 ML OH and 1/3 ML H_2O) and surface energies without ZPE correction. Gas phase H_2O and H_2 as reference

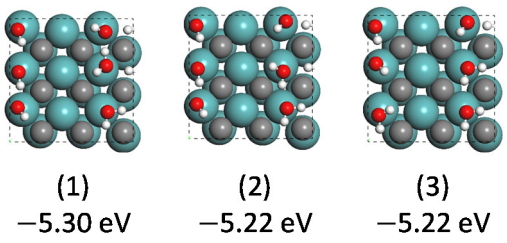

Fig. S70 Configurations of 2OH_4H_2O (mixed 2/9 ML OH and 4/9 ML H_2O) and surface energies without ZPE correction. Gas phase H_2O and H_2 as reference

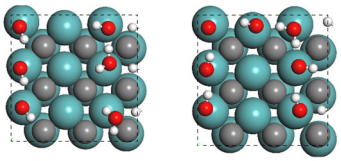

(1) −5.09 eV (2) −5.01 eV

Fig. S71 Configurations of 1OH_5H_2O (mixed 1/9 ML OH and 5/9 ML H_2O) and surface energies without ZPE correction. Gas phase H_2O and H_2 as reference

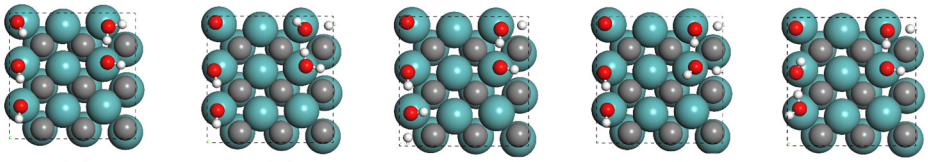

(1) −2.70 eV (2) −2.65 eV (3) −2.62 eV (4) −2.61 eV (5) −2.54 eV

Fig. S72 Configurations of 4OH_1H_2O (mixed 4/9 ML OH and 1/9 ML H_2O) and surface energies without ZPE correction. Gas phase H_2O and H_2 as reference

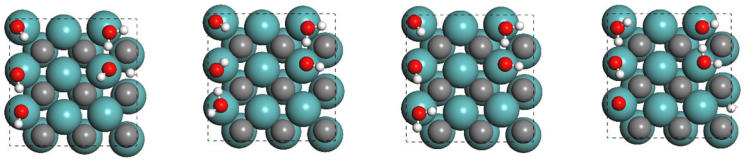

(1) −3.74 eV (2) −3.51 eV (3) −3.48 eV (4) −3.39 eV

Fig. S73 Configurations of 3OH_2H_2O (mixed 1/3 ML OH and 2/9 ML H_2O) and surface energies without ZPE correction. Gas phase H_2O and H_2 as reference

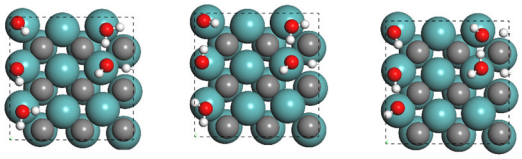

(1) −4.36 eV (2) −4.28 eV (3) −4.15 eV

Fig. S74 Configurations of 2OH_3H_2O (mixed 2/9 ML OH and 1/3 ML H_2O) and surface energies without ZPE correction. Gas phase H_2O and H_2 as reference

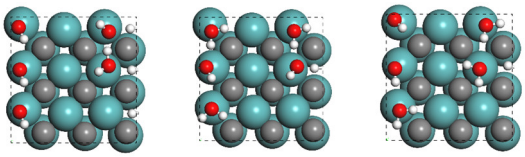

(1)
−4.36 eV

(2)
−4.19 eV

(3)
−3.96 eV

Fig. S75 Configurations of 1OH_4H_2O (mixed 1/9 ML OH and 4/9 ML H_2O) and surface energies without ZPE correction. Gas phase H_2O and H_2 as reference

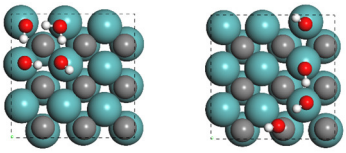

(1)
−2.41 eV

(2)
−1.18 eV

Fig. S76 Configurations of 3OH_1H_2O (mixed 1/3 ML OH and 1/9 ML H_2O) and surface energies without ZPE correction. Gas phase H_2O and H_2 as reference

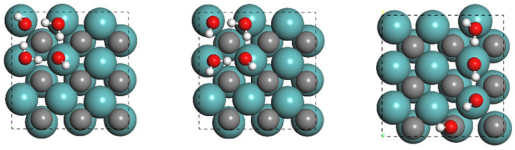

(1)
−3.48 eV

(2)
−3.24 eV

(3)
−2.41 eV

Fig. S77 Configurations of 2OH_2H_2O (mixed 2/9 ML OH and 2/9 ML H_2O) and surface energies without ZPE correction. Gas phase H_2O and H_2 as reference

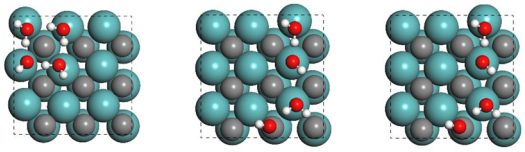

(1)
−3.77 eV

(2)
−3.34 eV

(3)
−3.12 eV

Fig. S78 Configurations of 1OH_3H_2O (mixed 1/9 ML OH and 1/3 ML H_2O) and surface energies without ZPE correction. Gas phase H_2O and H_2 as reference

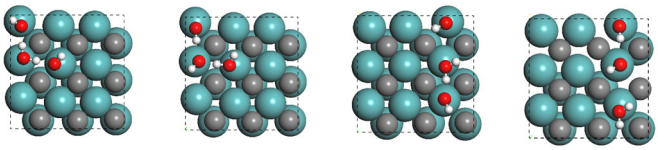

(1)
−1.97 eV

(2)
−1.91 eV

(3)
−1.79 eV

(4)
−1.75 eV

Fig. S79 Configurations of 2OH_1H_2O (mixed 2/9 ML OH and 1/9 ML H_2O) and surface energies without ZPE correction. Gas phase H_2O and H_2 as reference

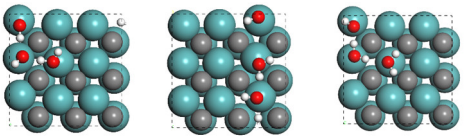

(1)
−2.69 eV

(2)
−2.62 eV

(3)
−2.32 eV

Fig. S80 Configurations of 1OH_2H_2O (mixed 1/9 ML OH and 2/9 ML H_2O) and surface energies without ZPE correction. Gas phase H_2O and H_2 as reference

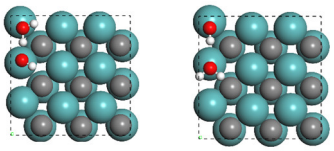

(1)
−1.65 eV

(2)
−1.25 eV

Fig. S81 Configurations of 1OH_1H_2O (mixed 1/9 ML OH and 1/9 ML H_2O) and surface energies without ZPE correction. Gas phase H_2O and H_2 as reference

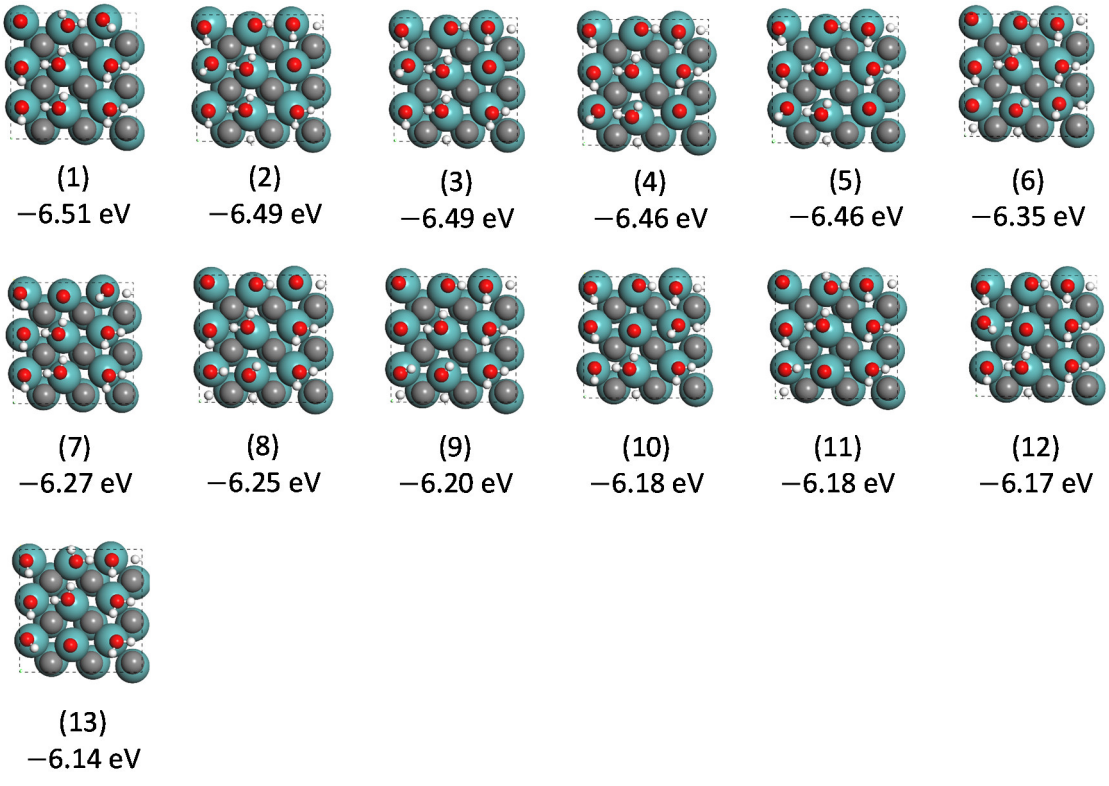

(1)
−6.51 eV

(2)
−6.49 eV

(3)
−6.49 eV

(4)
−6.46 eV

(5)
−6.46 eV

(6)
−6.35 eV

(7)
−6.27 eV

(8)
−6.25 eV

(9)
−6.20 eV

(10)
−6.18 eV

(11)
−6.18 eV

(12)
−6.17 eV

(13)
−6.14 eV

Fig. S82 Configurations of 3OH_5H_2O_1O (mixed 1/3 ML OH*, 5/9 ML H_2O* and 1/9 ML O*) and surface energies without ZPE correction. Gas phase H_2O and H_2 as reference

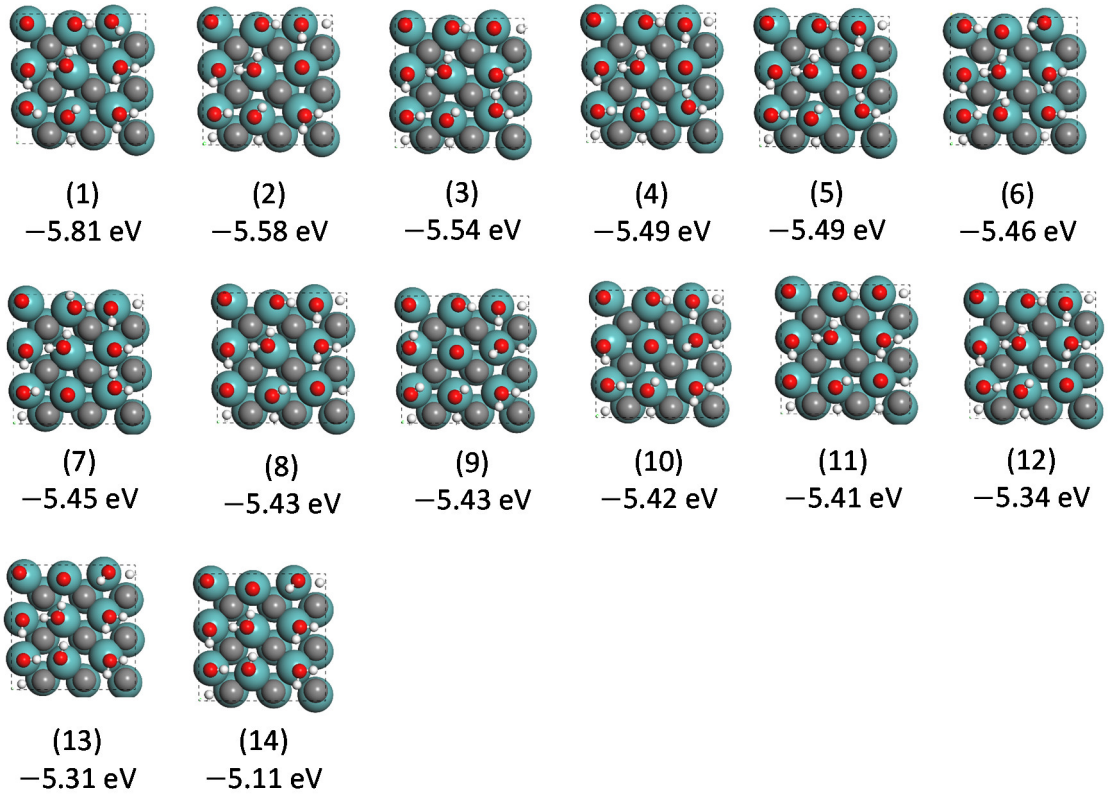

Fig. S83 Configurations of 4OH_4H_2O_1O (mixed 4/9 ML OH*, 4/9 ML H_2O* and 1/9 ML O*) and surface energies without ZPE correction. Gas phase H_2O and H_2 as reference.

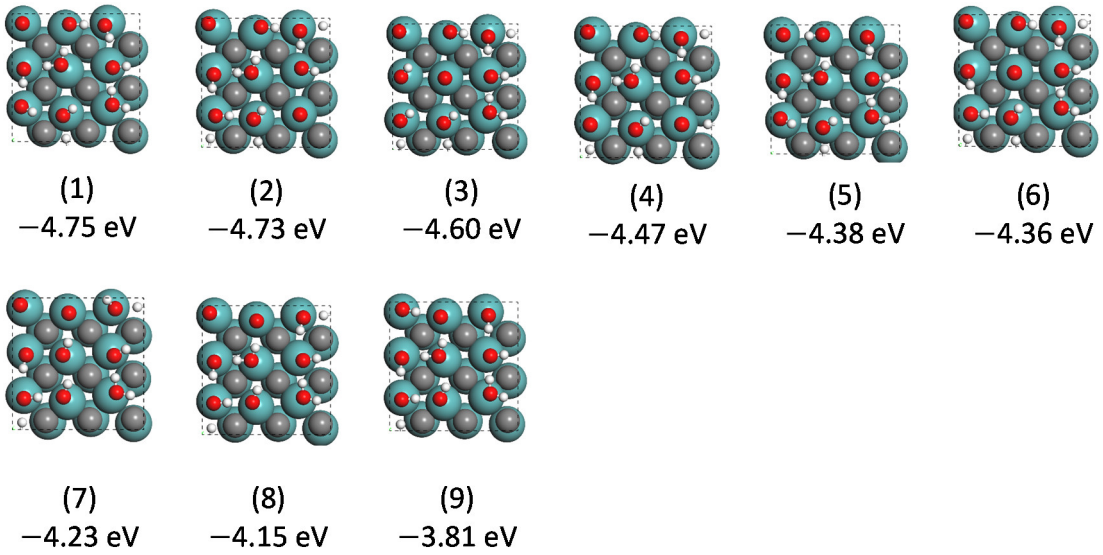

Fig. S84 Configurations of 5OH_3H_2O_1O (mixed 5/9 ML OH*, 1/3 ML H_2O* and 1/9 ML O*) and surface energies without ZPE correction. Gas phase H_2O and H_2 as reference

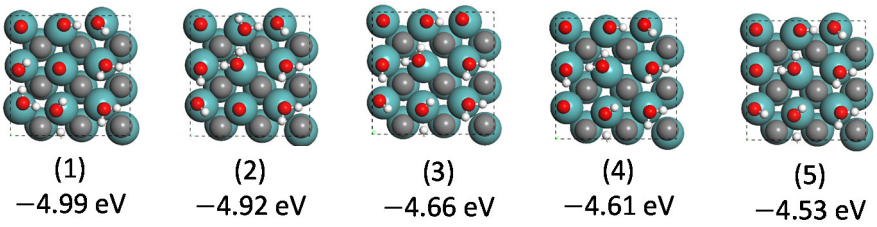

Fig. S85 Configurations of 3OH_4H_2O_2O (mixed 1/3 ML OH*, 4/9 ML H_2O* and 2/9 ML O*) and surface energies without ZPE correction. Gas phase H_2O and H_2 as reference

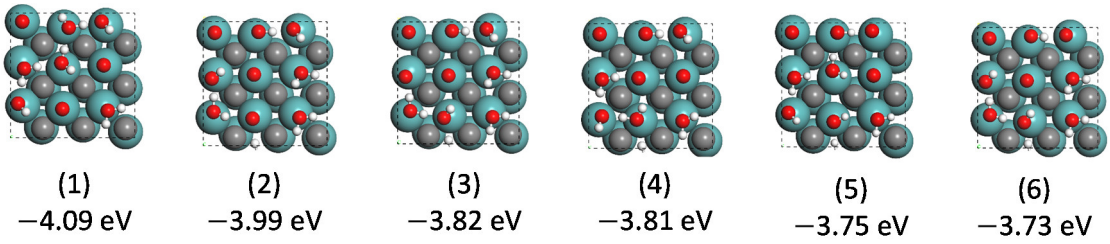

Fig. S86 Configurations of 2OH_4H_2O_3O (mixed 2/9 ML OH*, 4/9 ML H_2O* and 1/3 ML O*) and surface energies without ZPE correction. Gas phase H_2O and H_2 as reference

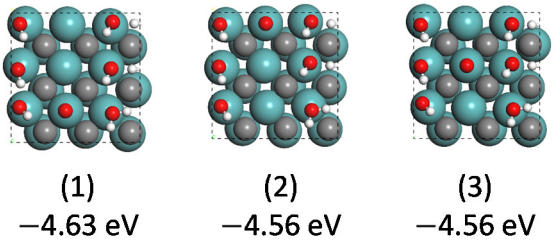

Fig. S87 Configurations of 3OH_3H_2O_1O (mixed 1/3 ML OH*, 4/9 ML H_2O* and 1/9 ML O*) and surface energies without ZPE correction. Gas phase H_2O and H_2 as reference

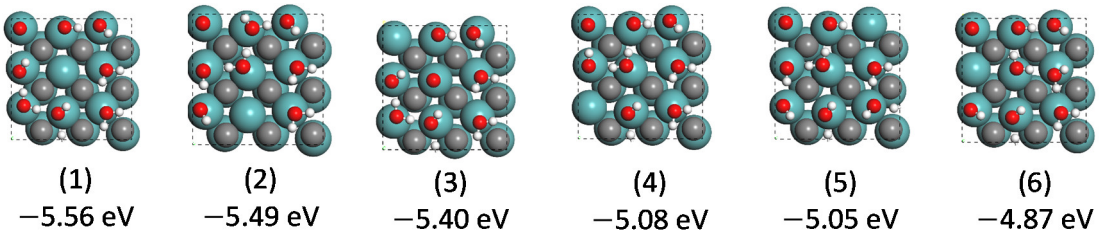

Fig. S88 Configurations of 3OH_4H_2O_1O (mixed 1/3 ML OH*, 4/9 ML H_2O* and 1/9 ML O*) and surface energies without ZPE correction. Gas phase H_2O and H_2 as reference

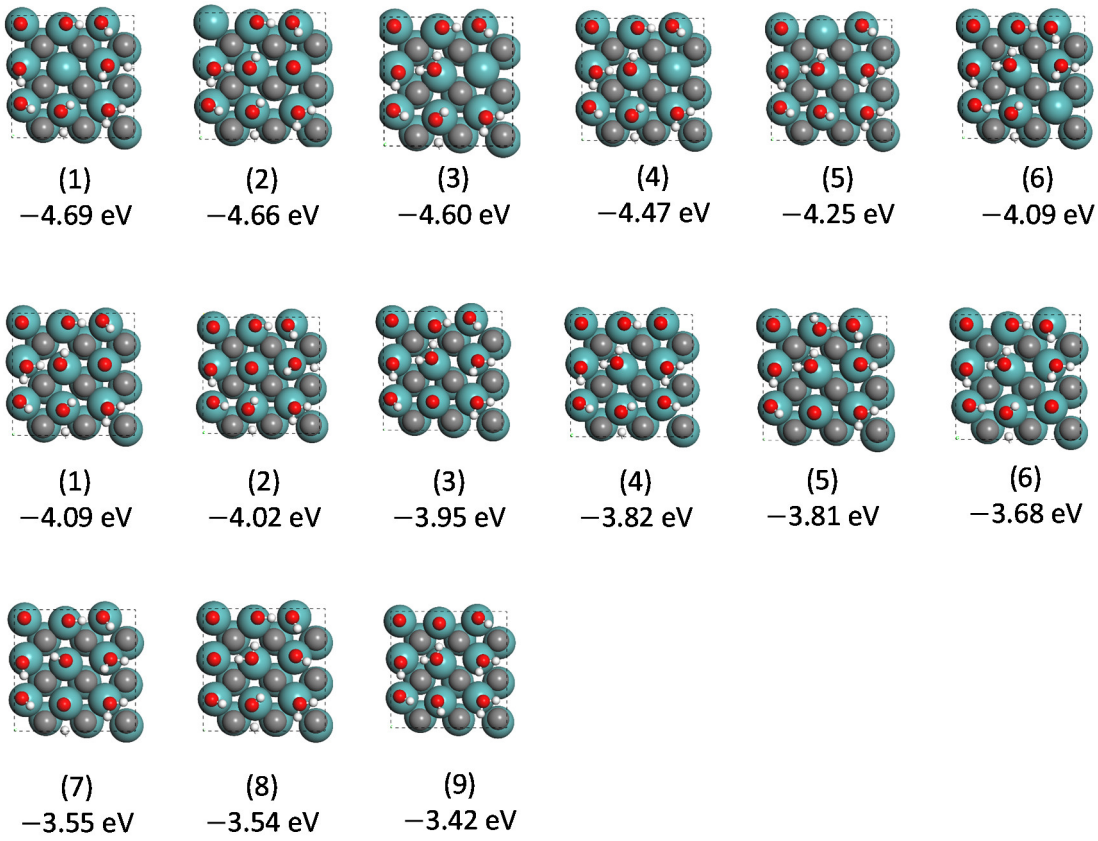

Fig. S89 Configurations of 4OH_3H_2O_1O (mixed 4/9 ML OH*, 1/3 ML H_2O* and 1/9 ML O*) and surface energies without ZPE correction. Gas phase H_2O and H_2 as reference

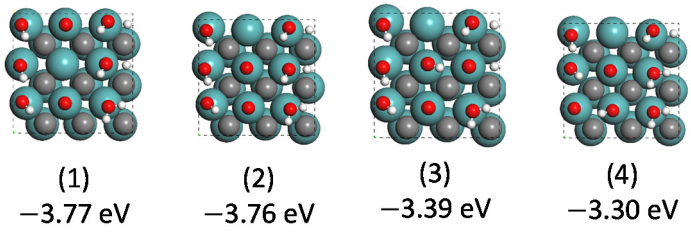

Fig. S90 Configurations of 3OH_3H_2O_2O (mixed 1/3 ML OH*, 1/3 ML H_2O* and 2/9 ML O*) and surface energies without ZPE correction. Gas phase H_2O and H_2 as reference

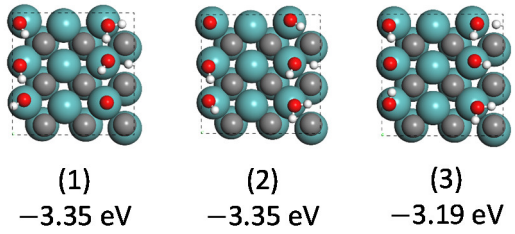

Fig. S91 Configurations of 3OH_2H_2O_1O (mixed 1/3 ML OH*, 2/9 ML H_2O* and 1/9 ML O*) and surface energies without ZPE correction. Gas phase H_2O and H_2 as reference

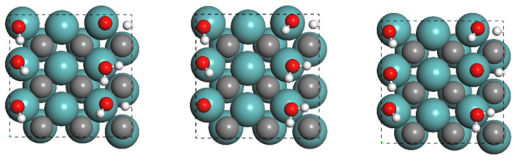

Fig. S92 Configurations of 2OH_3H_2O_1O (mixed 2/9 ML OH*, 1/3 ML H_2O* and 1/9 ML O*) and surface energies without ZPE correction. Gas phase H_2O and H_2 as reference

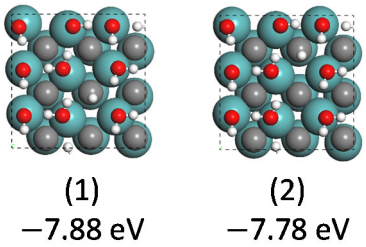

Fig. S93 Configurations of 3OH_6H_2O_1H (mixed 1/3 ML OH*, 2/3 ML H_2O* and 1/9 ML H*) and surface energies without ZPE correction. Gas phase H_2O and H_2 as reference

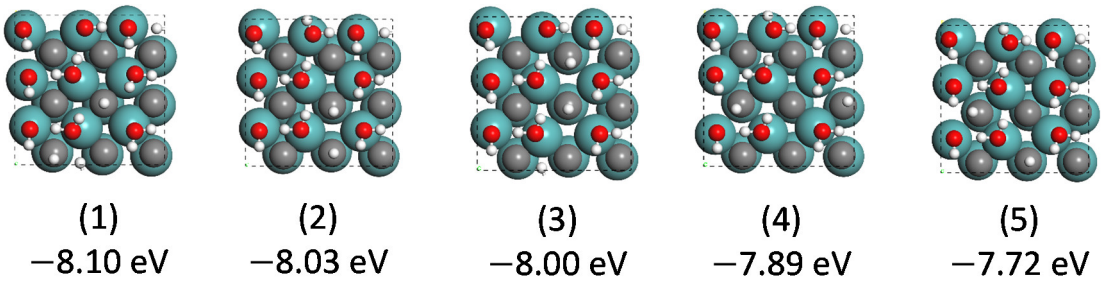

Fig. S94 Configurations of 3OH_6H_2O_2H (mixed 1/3 ML OH*, 2/3 ML H_2O* and 2/9 ML H*) and surface energies without ZPE correction. Gas phase H_2O and H_2 as reference

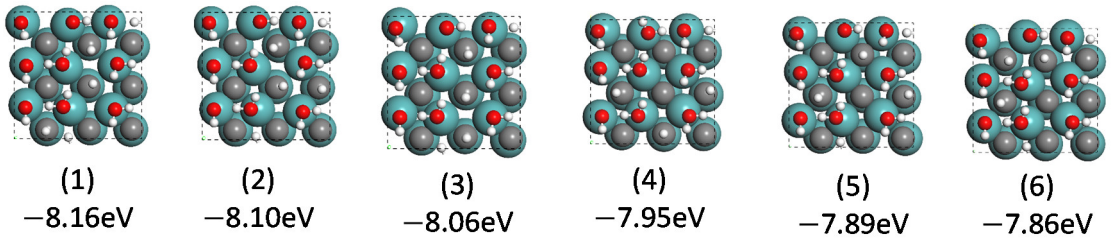

Fig. S95 Configurations of 3OH_6H_2O_3H (mixed 1/3 ML OH*, 2/3 ML H_2O* and 1/3 ML H*) and surface energies without ZPE correction. Gas phase H_2O and H_2 as reference

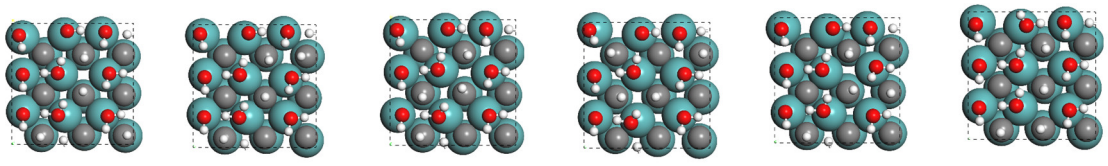

Fig. S96 Configurations of 3OH_6H_2O_4H (mixed 1/3 ML OH*, 2/3 ML H_2O* and 4/9 ML H*) and surface energies without ZPE correction. Gas phase H_2O and H_2 as reference

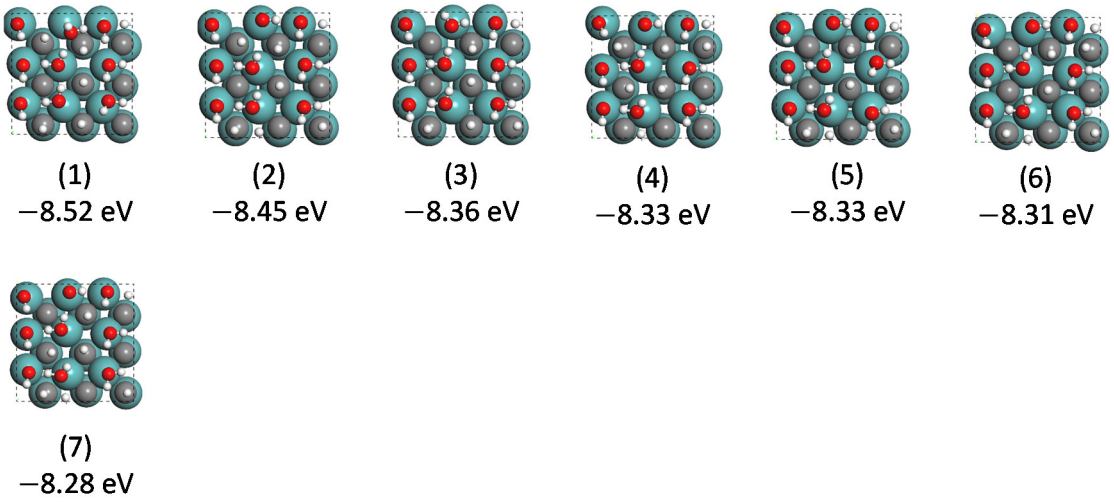

Fig. S97 Configurations of 3OH_6H_2O_5H (mixed 1/3 ML OH*, 2/3 ML H_2O* and 5/9 ML H*) and surface energies without ZPE correction. Gas phase H_2O and H_2 as reference

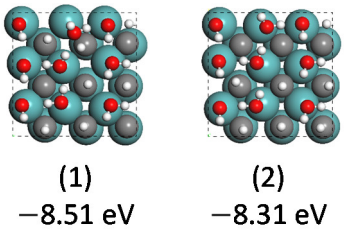

Fig. S98 Configurations of 3OH_6H_2O_6H (mixed 1/3 ML OH*, 2/3 ML H_2O* and 2/3 ML H*) and surface energies without ZPE correction. Gas phase H_2O and H_2 as reference

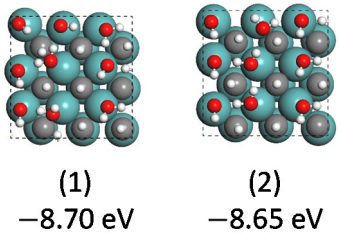

Fig. S99 Configurations of 3OH_6H_2O_7H (mixed 1/3 ML OH*, 2/3 ML H_2O* and 7/9 ML H*) and surface energies without ZPE correction. Gas phase H_2O and H_2 as reference

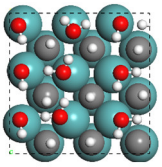

(1)
−8.59 eV

Fig. S100 Configurations of 3OH_6H_2O_8H (mixed 1/3 ML OH*, 2/3 ML H_2O* and 8/9 ML H*) and surface energies without ZPE correction. Gas phase H_2O and H_2 as reference

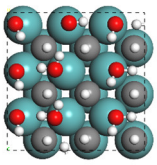

(1)
−8.89 eV

Fig. S101 Configurations of 3OH_6H_2O_9H (mixed 1/3 ML OH*, 2/3 ML H_2O* and 1 ML H*) and surface energies without ZPE correction. Gas phase H_2O and H_2 as reference

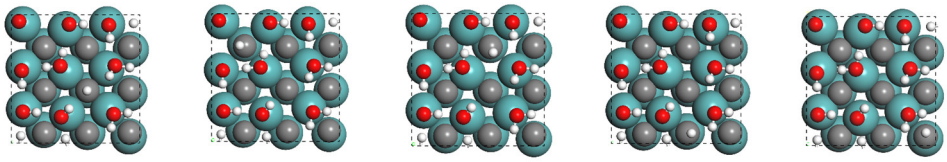

(1)
−7.37 eV

(2)
−7.32 eV

(3)
−7.28 eV

(4)
−7.27 eV

(5)
−7.20 eV

Fig. S102 Configurations of 4OH_5H_2O_1H (mixed 4/9 ML OH*, 5/9 ML H_2O* and 1/9 ML H*) and surface energies without ZPE correction. Gas phase H_2O and H_2 as reference

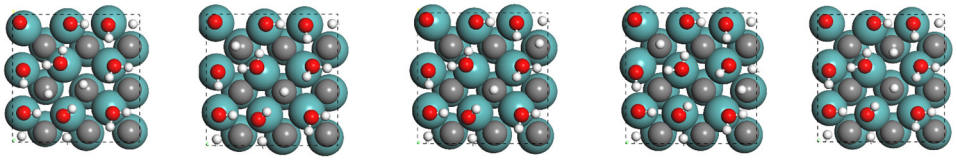

(1)
−7.84 eV

(2)
−7.74 eV

(3)
−7.65 eV

(4)
−7.56 eV

(5)
−7.53 eV

Fig. S103 Configurations of 4OH_5H_2O_2H (mixed 4/9 ML OH*, 5/9 ML H_2O* and 2/9 ML H*) and surface energies without ZPE correction. Gas phase H_2O and H_2 as reference

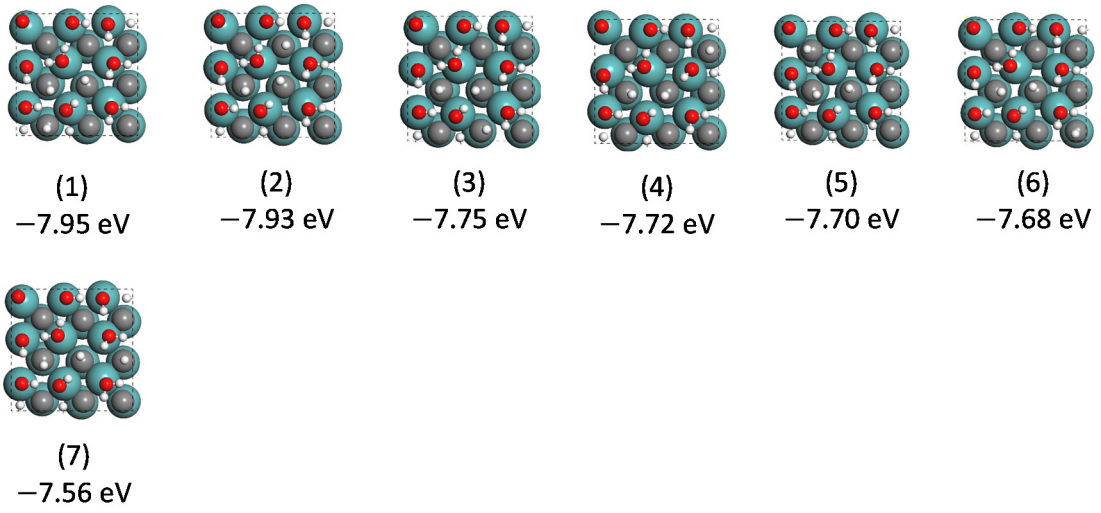

Fig. S104 Configurations of 4OH_5H_2O_3H (mixed 4/9 ML OH*, 5/9 ML H_2O* and 1/3 ML H*) and surface energies without ZPE correction. Gas phase H_2O and H_2 as reference

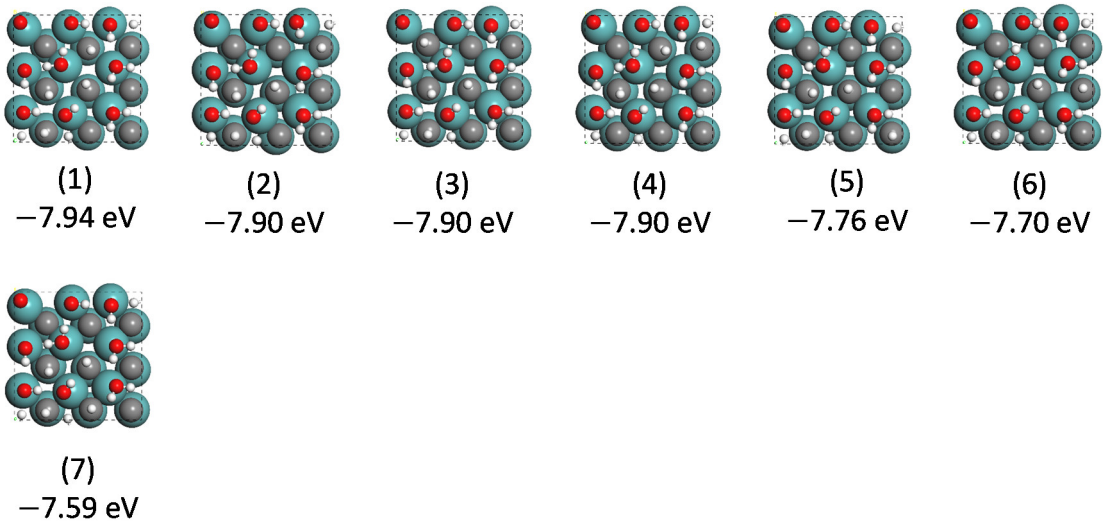

Fig. S105 Configurations of 4OH_5H_2O_4H (mixed 4/9 ML OH*, 5/9 ML H_2O* and 4/9 ML H*) and surface energies without ZPE correction. Gas phase H_2O and H_2 as reference

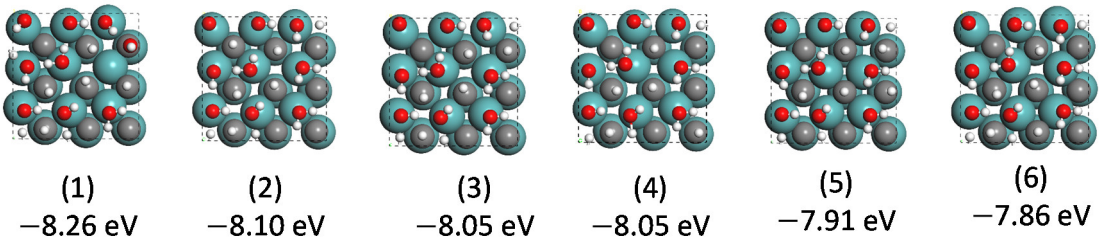

Fig. S106 Configurations of 4OH_5H_2O_5H (mixed 4/9 ML OH*, 5/9 ML H_2O* and 5/9 ML H*) and surface energies without ZPE correction. Gas phase H_2O and H_2 as reference

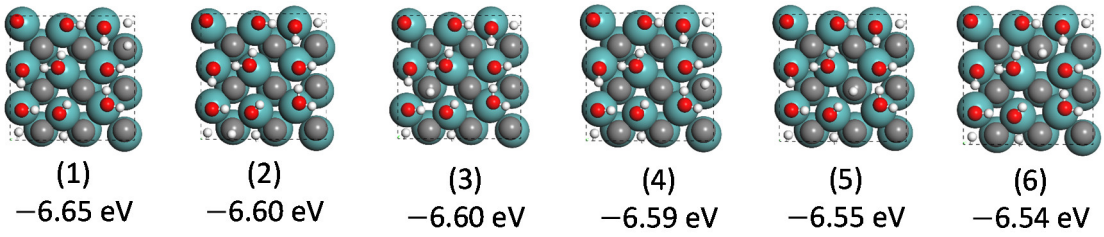

Fig. S107 Configurations of 5OH_4H_2O_1H (mixed 5/9 ML OH*, 4/9 ML H_2O* and 1/9 ML H*) and surface energies without ZPE correction. Gas phase H_2O and H_2 as reference

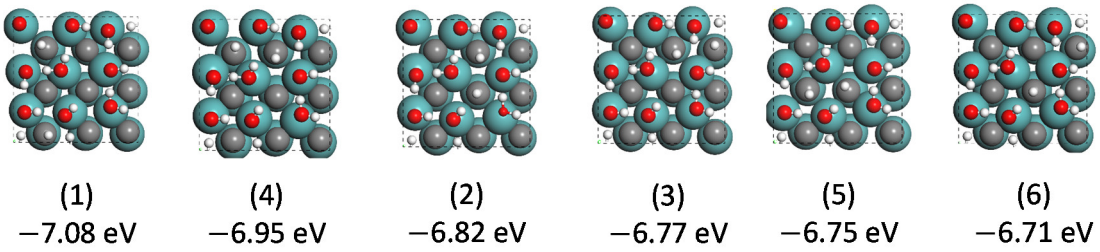

Fig. S108 Configurations of 5OH_4H_2O_2H (mixed 5/9 ML OH*, 4/9 ML H_2O* and 2/9 ML H*) and surface energies without ZPE correction. Gas phase H_2O and H_2 as reference

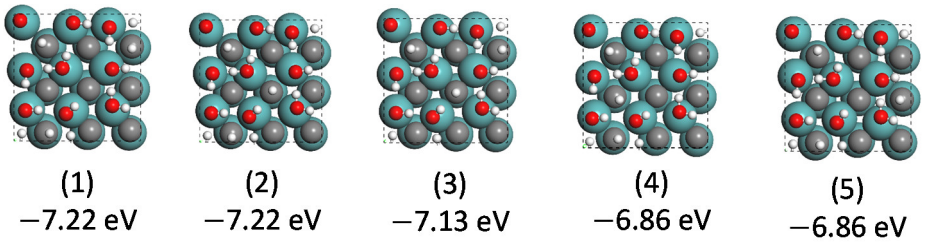

Fig. S109 Configurations of 5OH_4H_2O_3H (mixed 5/9 ML OH*, 4/9 ML H_2O* and 1/3 ML H*) and surface energies without ZPE correction. Gas phase H_2O and H_2 as reference

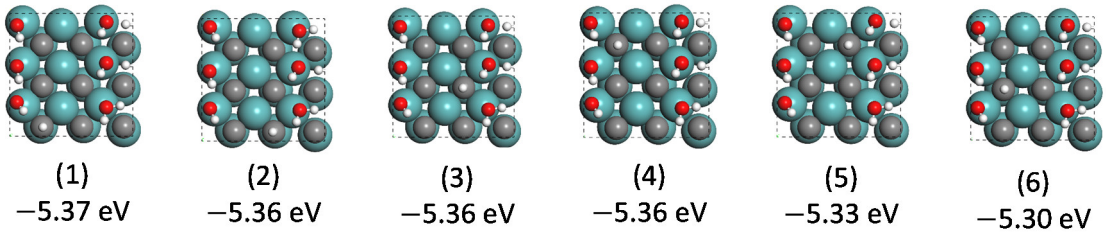

Fig. S110 Configurations of 3OH_3H_2O_1H (mixed 1/3 ML OH*, 1/3 ML H_2O* and 1/9 ML H*) and surface energies without ZPE correction. Gas phase H_2O and H_2 as reference

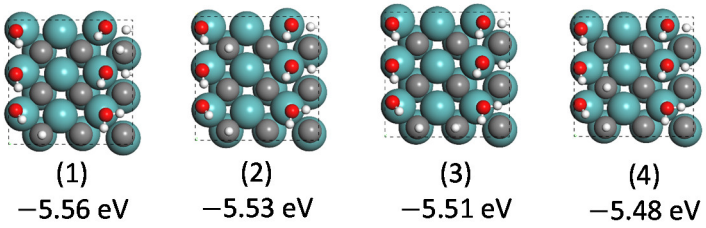

Fig. S111 Configurations of 3OH_3H_2O_2H (mixed 1/3 ML OH*, 1/3 ML H_2O* and 2/9 ML H*) and surface energies without ZPE correction. Gas phase H_2O and H_2 as reference

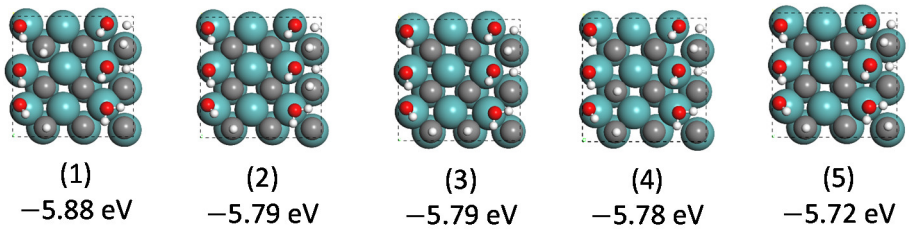

Fig. S112 Configurations of 3OH_3H_2O_3H (mixed 1/3 ML OH*, 1/3 ML H_2O* and 1/3 ML H*) and surface energies without ZPE correction. Gas phase H_2O and H_2 as reference

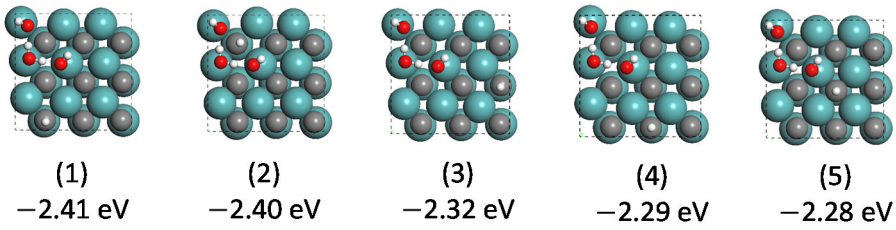

Fig. S113 Configurations of 2OH_1H_2O_1H (mixed 2/9 ML OH*, 1/9 ML H_2O* and 1/9 ML H*) and surface energies without ZPE correction. Gas phase H_2O and H_2 as reference

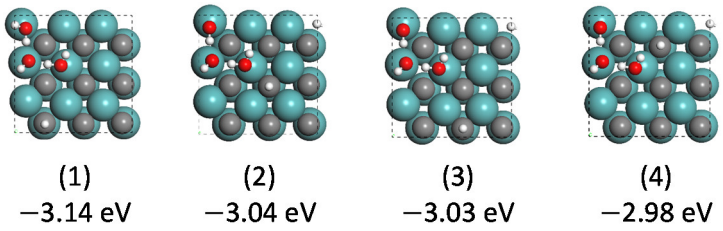

Fig. S114 Configurations of 1OH_2H_2O_1H (mixed 1/9 ML OH*, 2/9 ML H_2O* and 1/9 ML H*) and surface energies without ZPE correction. Gas phase H_2O and H_2 as reference

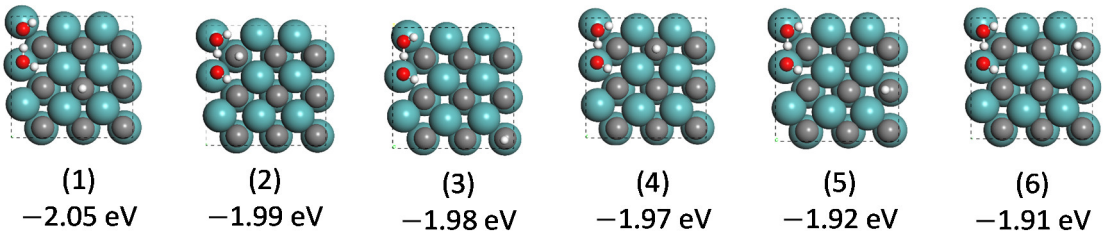

Fig. S115 Configurations of 1OH_1H_2O_1H (mixed 1/9 ML OH*, 1/9 ML H_2O* and 1/9 ML H*) and surface energies without ZPE correction. Gas phase H_2O and H_2 as reference

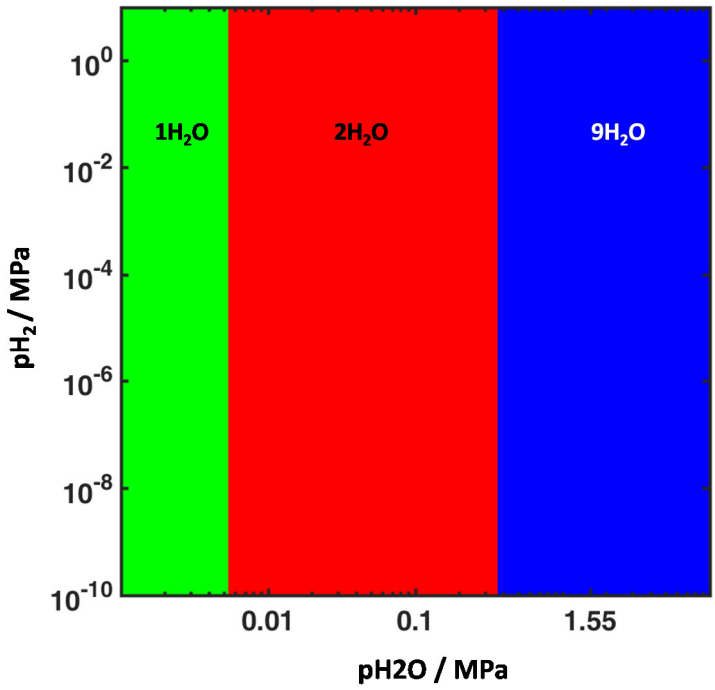

Fig. S116 Surface phase structures of fcc MoC (001) surface under H_2O/H_2 environment at 473.15 K (only molecular H_2O adsorption structures were considered).

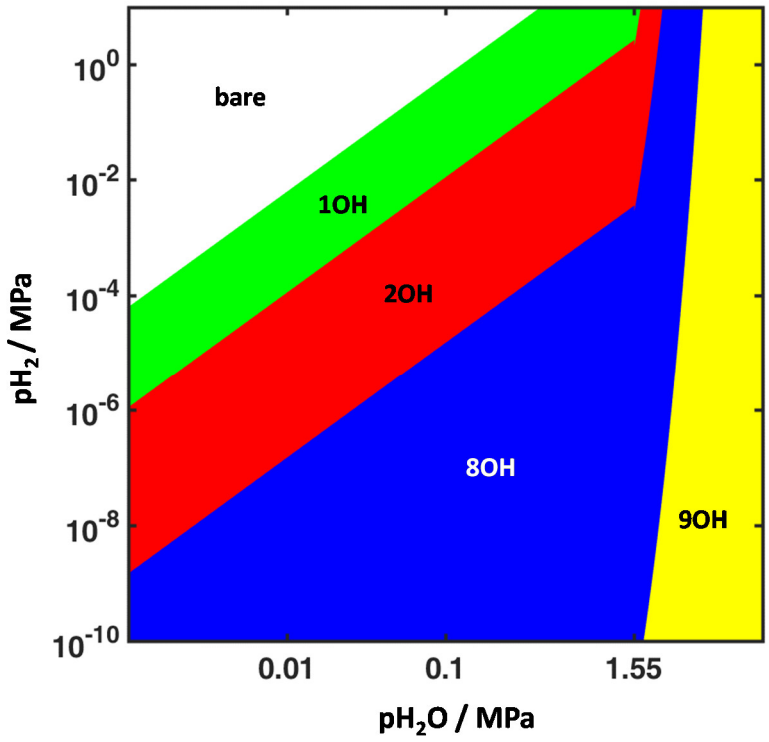

Fig. S117 Surface phase structures of fcc MoC (001) surface under H_2O/H_2 environment at 473.15 K (only surface OH* structures were considered).

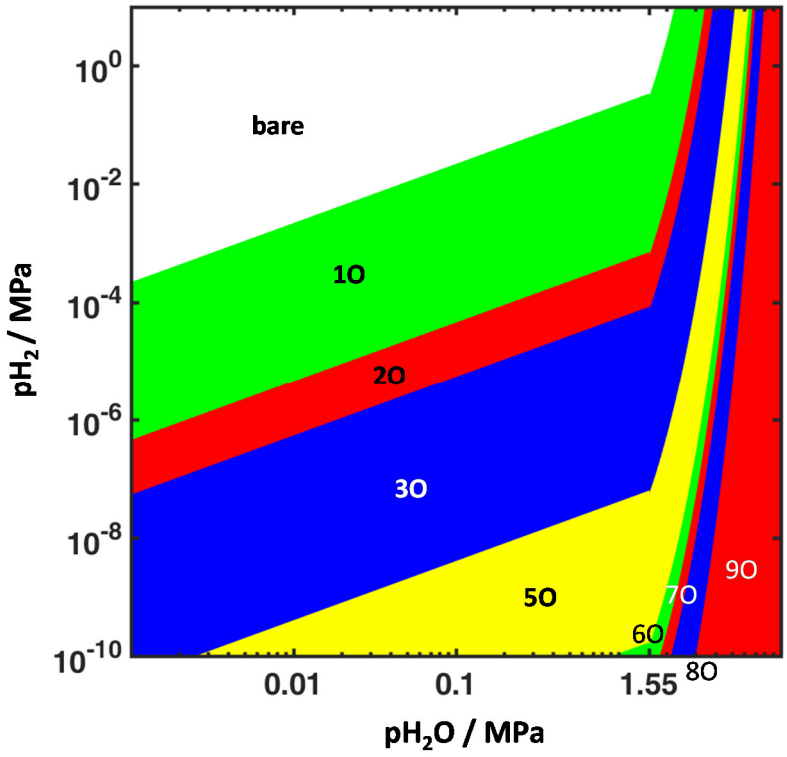

Fig. S118 Surface phase structures of fcc MoC (001) surface under H_2O/H_2 environment at 473.15 K (only surface O* structures were considered).

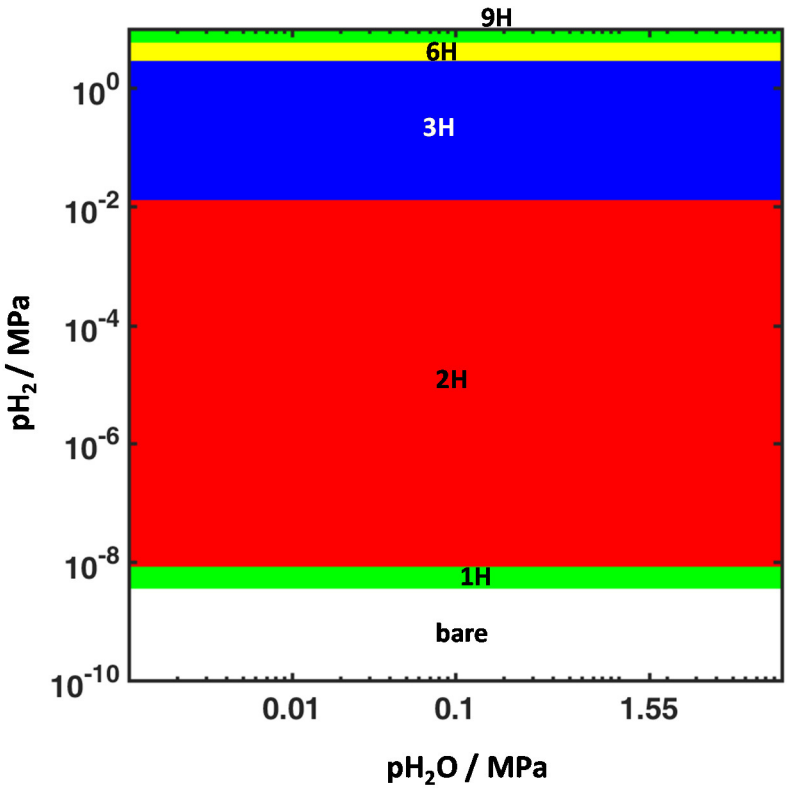

Fig. S119 Surface phase structures of fcc MoC (001) surface under H_2O/H_2 environment at 473.15 K (only surface H* structures were considered).

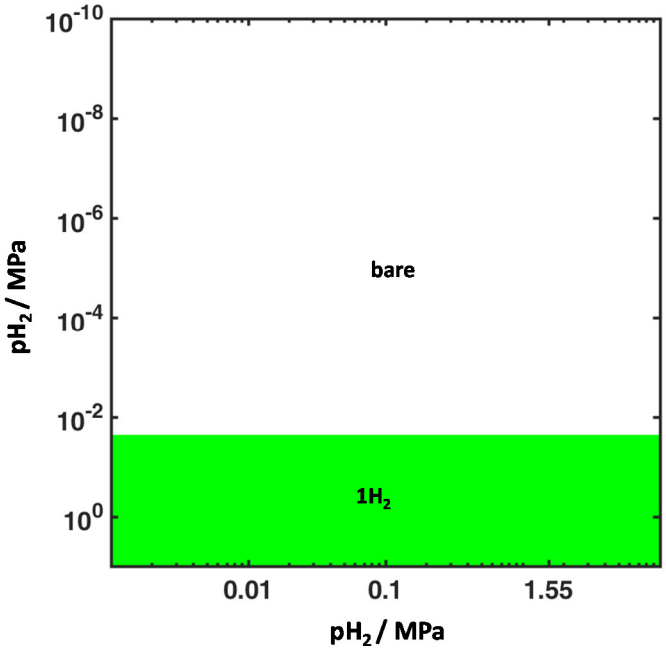

Fig. S120 Surface phase structures of fcc MoC (001) surface under H_2O/H_2 environment at 473.15 K (only surface H_2* structures were considered).

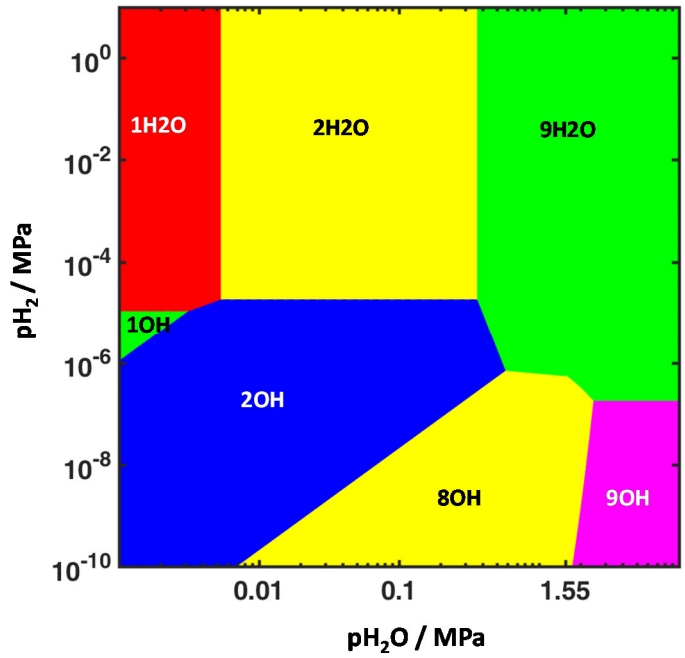

Fig. S121 Surface phase structures of fcc MoC (001) surface under H_2O/H_2 environment at 473.15 K (only pure surface H_2O* and pure surface OH* structures were considered without considering their mixtures).

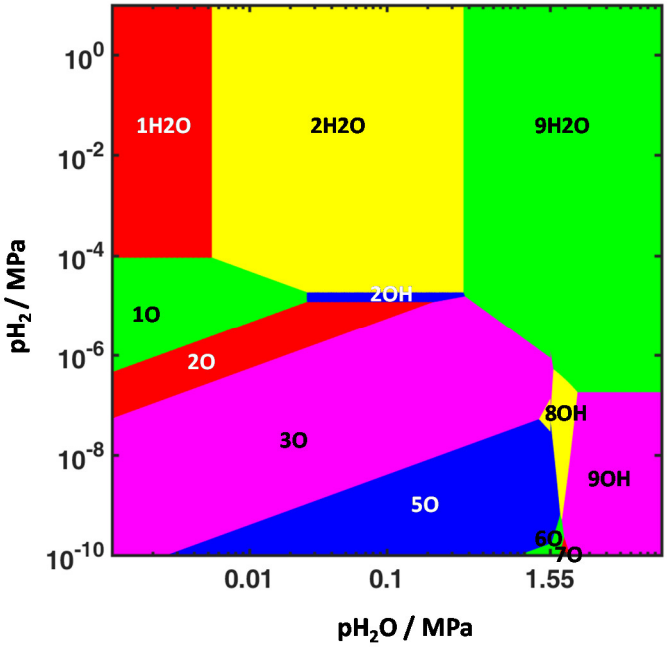

Fig. S122 Surface phase structures of fcc MoC (001) surface under H_2O/H_2 environment at 473.15 K (only pure surface H_2O*, pure surface OH* and pure surface O* structures were considered without considering their mixtures).

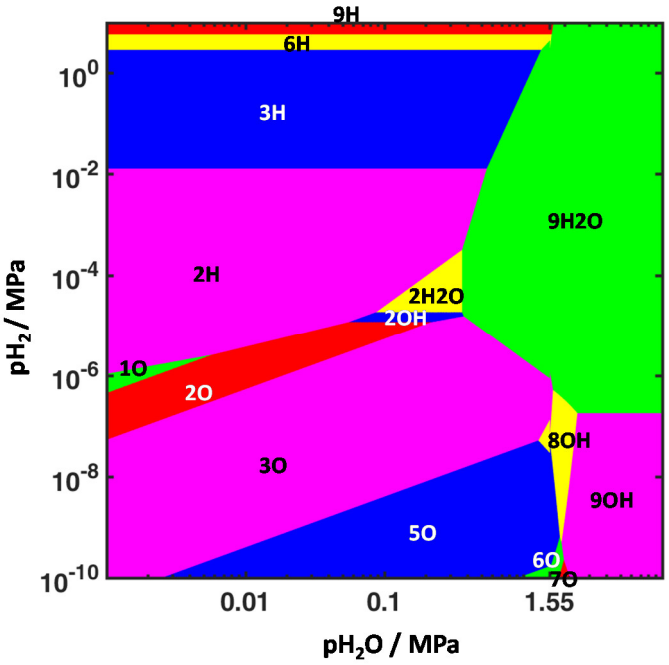

Fig. S123 Surface phase structures of fcc MoC (001) surface under H_2O/H_2 environment at 473.15 K (only pure surface H_2O*, pure surface OH*, pure surface O*, pure surface H* and pure surface H_2* structures were considered without considering their mixtures).

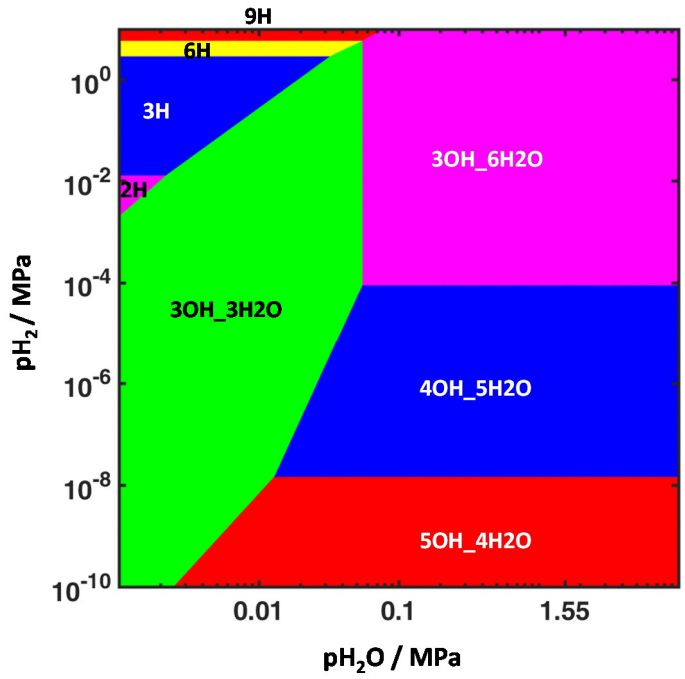

Fig. S124 Surface phase structures of fcc MoC (001) surface under H_2O/H_2 environment at 473.15 K (only pure surface H_2O*, pure surface OH*, pure surface O*, pure surface H*, pure surface H_2* and the mixtures of H_2O*/OH* structures were considered).

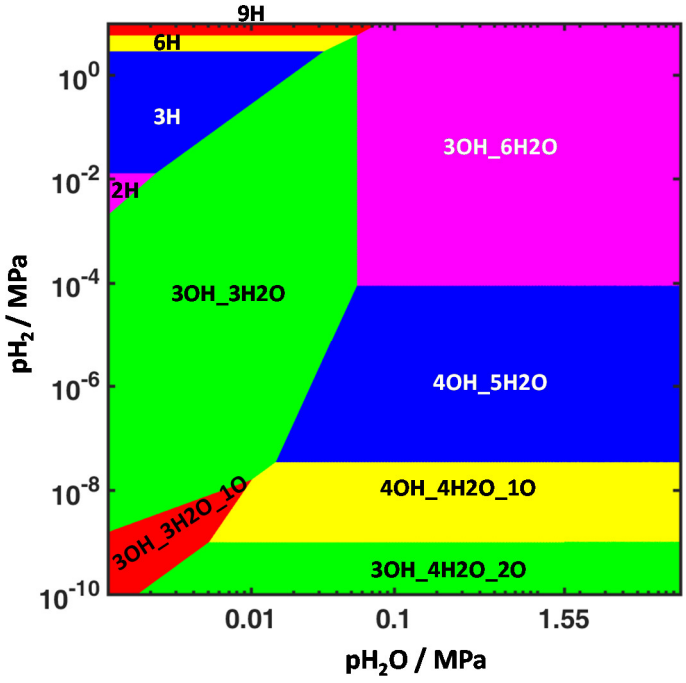

Fig. S125 Surface phase structures of fcc MoC (001) surface under H_2O/H_2 environment at 473.15 K (only pure surface H_2O*, pure surface OH*, pure surface O*, pure surface H*, pure surface H_2*, the mixtures of H_2O*/OH*, H_2O*/OH*/O*, H_2O*/OH*/H* structures were considered).

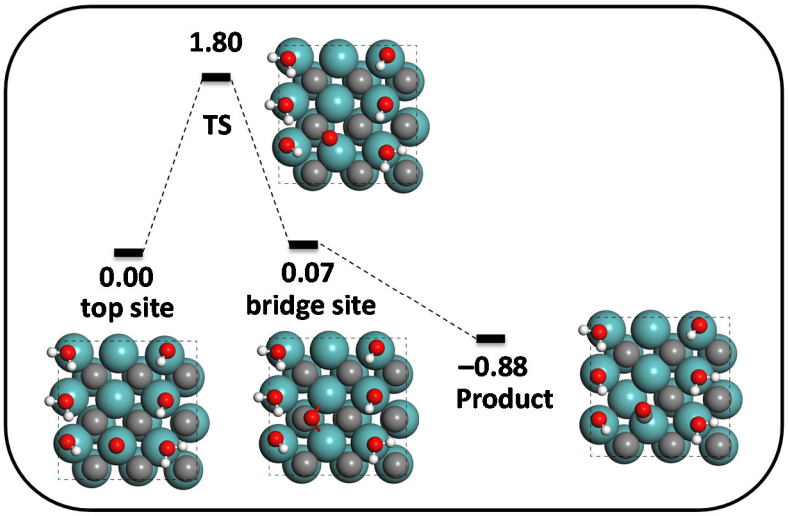

3OH_3H_2O_1O

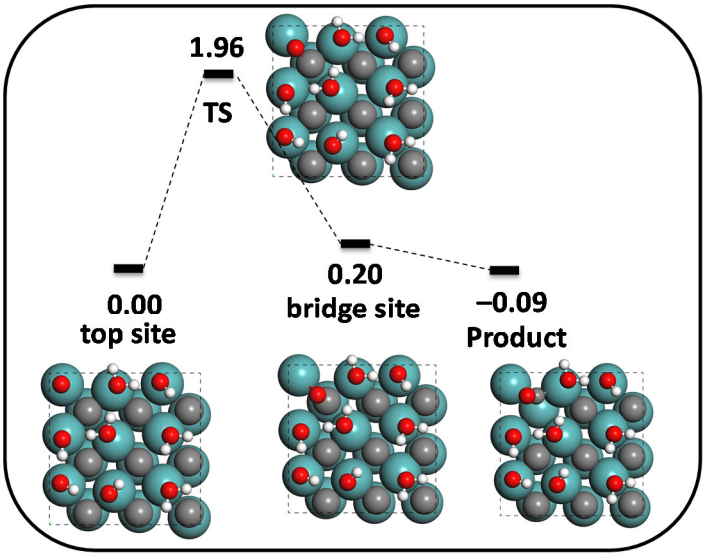

4OH_4H_2O_1O

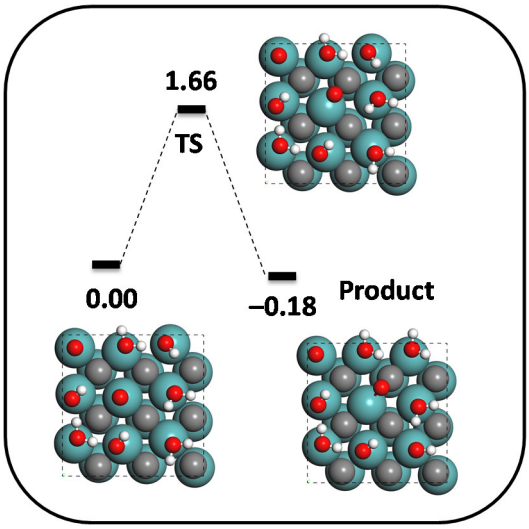

3OH_4H_2O_2O

Fig. S126 The potential energy profiles for the transformation of top site O* to a bridge site O* on stable surface phases.

We tried the bridge site configuration on MoC (001) surface by initially placing the O atom at the bridge site and letting it be optimized subsequently. It turned out that the O atom is prone to bond with the surface C site with C-O bond lengths of 1.24 - 1.28 Å indicating a carbon monoxide-like species formation, while the interaction between the Mo and O is rather weak. As we have well confirmed in edition_1 that "no matter the direct deprotonation pathway or the hydroxyls disproportionation pathway, the initial configuration of generated O* had the top site configuration, where the O* bonded with only one Mo site with the Mo-O bond directing perpendicular with the (001) surface." Thus, the emergence of bridge site O* should be from the further transformation of top site O*. Now we provide the potential energy profiles for bridge site O* formation as shown in the figure below. For example, as for the potential energy profile on the '3OH_3H2O_1O' phase structure (the 3OH_3H2O_1O structure emerges as a stable phase shown in Figure 7 of the manuscript), the bending of the vertical Mo-O bond in top site O* will result in a C-O bond formation with length of 1.24 Å. The initial Mo-O bond in the top site O* totally break up in the transformation process, where the Mo···O distance increased from 1.71 Å in the top site O* to about 2.70 Å in the bridge site O* (The Mo···O distance in the molecular H_2O adsorption on the Mo site is around 2.30 Å). The energy barrier for the above transformation is 1.80 eV which is too high for its happening under methanol steam reforming environment (reaction temperature≤ 200°). Besides, the bridge site CO* species is relatively unstable which would move out from the lattice carbon site to form a structure resembling a carbon monoxide molecule adsorbing near the surface carbon vacancy. Similarly, the energy barriers for the further transformation of top site O* to the bridge site O* on the other surface phase structures are too high to happen under methanol steam reforming temperatures. Since the formation of bridge site O* species will hardly happen due to the significant energy barriers (1.7 – 2.0 eV) under methanol steam reforming temperatures and would probably resulted in surface vacancies leading to surface stability problems which was beyond the scope of this manuscript, thus the bridge site O* is not considered in this manuscript here.

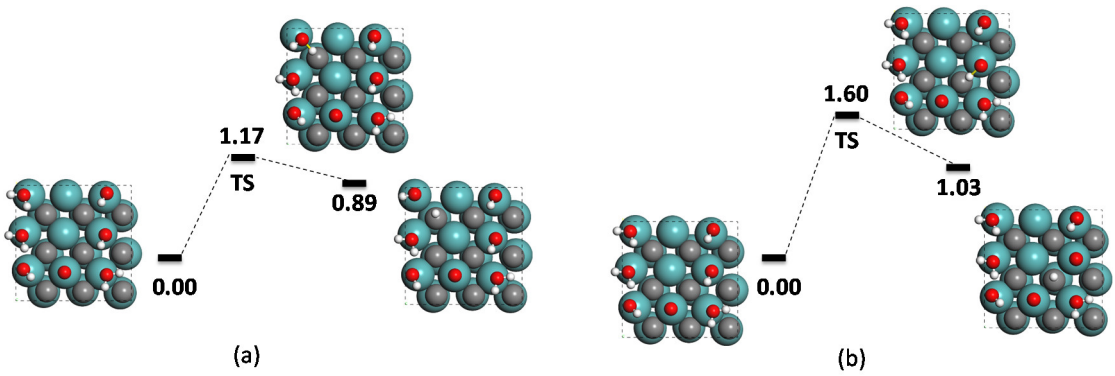

Fig. S127 The potential energy profiles for the H_2O dissociation to generate surface OH* (a) and OH* direct deprotonation to generate O* (b) on 3OH_3H_2O_1O surface structure.

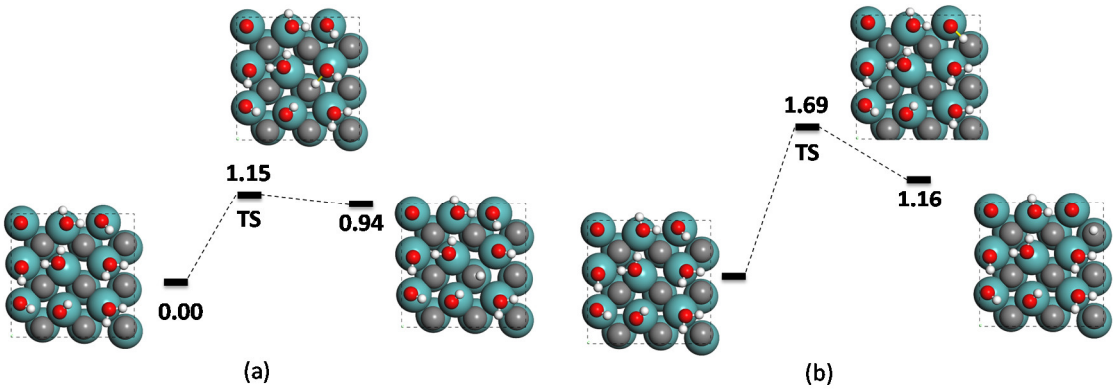

Fig. S128 The potential energy profiles for the H_2O dissociation to generate surface OH* (a) and OH* direct deprotonation to generate O* (b) on 4OH_4H_2O_1O surface structure.

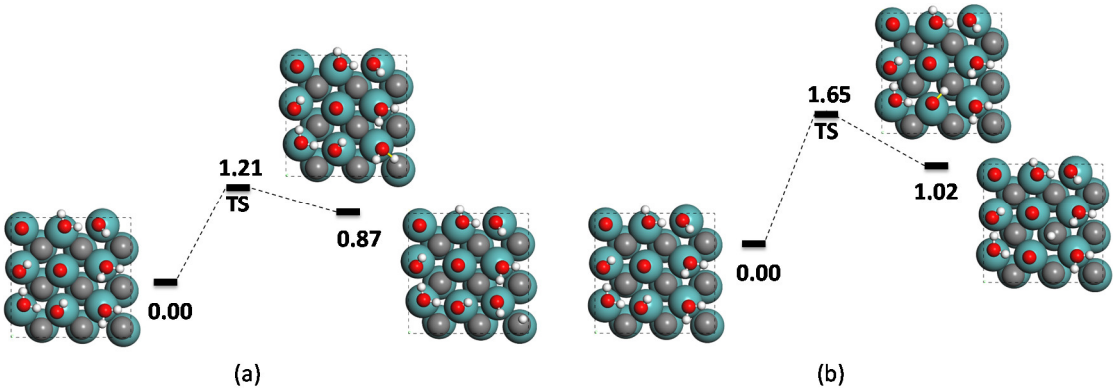

Fig. S129 The potential energy profiles for the H_2O dissociation to generate surface OH* (a) and OH* direct deprotonation to generate O* (b) on 3OH_4H_2O_2O surface structure.

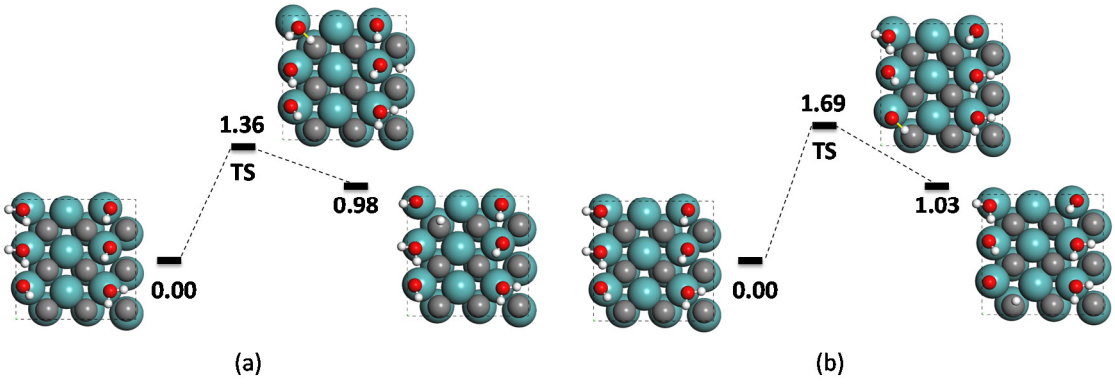

Fig. S130 The potential energy profiles for the H_2O dissociation to generate surface OH* (a) and OH* direct deprotonation to generate O* (b) on 3OH_3H_2O surface structure.

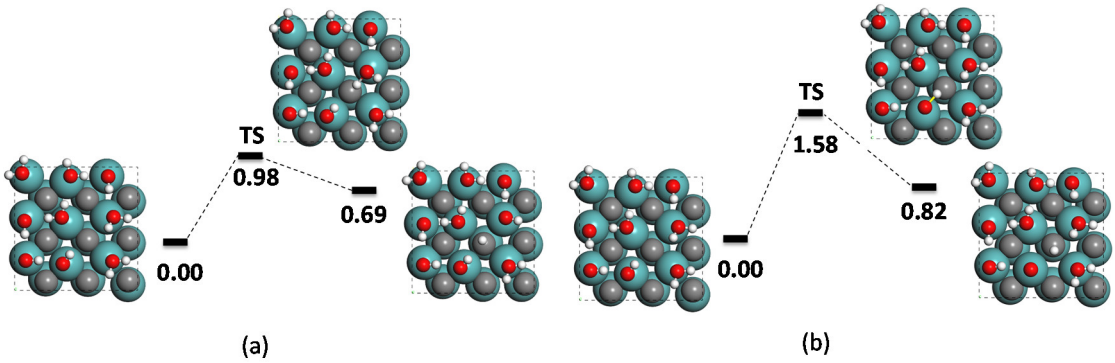

Fig. S131 The potential energy profiles for the H_2O dissociation to generate surface OH* (a) and OH* direct deprotonation to generate O* (b) on 4OH_5H_2O surface structure.

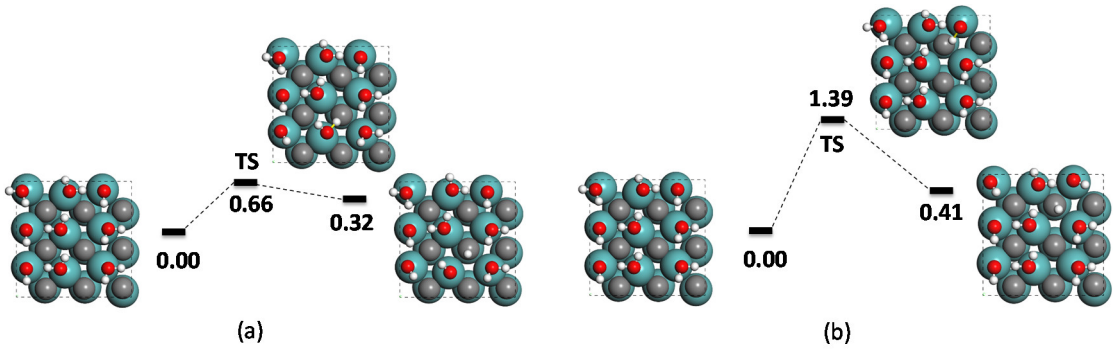

Fig. S132 The potential energy profiles for the H_2O dissociation to generate surface OH* (a) and OH* direct deprotonation to generate O* (b) on 3OH_6H_2O surface structure.

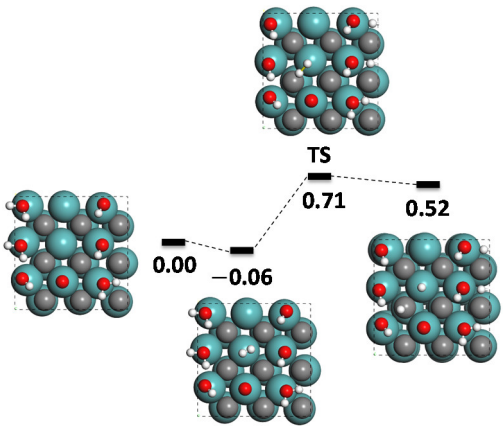

Fig. S133 The potential energy profiles for the H_2 dissociation to generate surface H* on 3OH_3H_2O_1O surface structure.

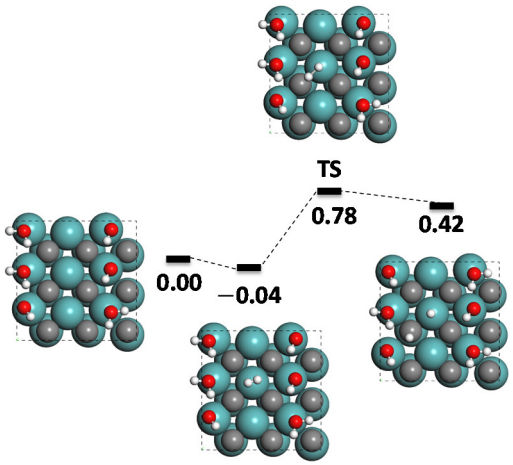

Fig. S134 The potential energy profiles for the H_2 dissociation to generate surface H* on 3OH_3H_2O surface structure.

Table S1 Energetic aspects of surface H_2O^* dissociation with n adsorbing H_2O^* (n = 1-9), $\Delta E_{TS,ZPE}^{\neq}$ and $\Delta E_{TS}^{\neq}$ were energy barriers of H_2O^* dissociation with or without ZPE correction, respectively; $\Delta E_{r,ZPE}$ and ΔE_r were reaction energies of H_2O^* dissociation with or without ZPE correction, respectively; σ_{TS}^{i} were imaginary frequencies of transition states for H_2O^* dissociation; $d_{O\cdots H}^{\neq}$ and $d_{C\cdots H}^{\neq}$ were the lengths of breaking O-H bond of $H_2O^*$and lengths of forming C-H bond of C site in the transition state, respectively. Energies were in eV with H_2O^* adsorption states as reference, distances were in Å and frequencies were in cm^{-1}

	$nH_2O^* \rightarrow (n-1)H_2O^* + OH^* + H^*$						
n	$\Delta E_{TS,ZPE}^{\neq}$	$\Delta E_{TS}^{\neq}$	$\Delta E_{r,ZPE}$	ΔE_r	σ_{TS}^{i}	$d_{O\cdots H}^{\neq}$	$d_{C\cdots H}^{\neq}$
1	0.22	0.38	0.01	0.07	1167	1.313	1.335
2-a	0.30	0.42	-0.26	-0.20	1291	1.257	1.416
2-b	0.50	0.65	0.28	0.34	1002	1.385	1.290
3-a	0.32	0.45	-0.46	-0.44	1291	1.317	1.373
3-b	0.30	0.43	-0.39	-0.37	1296	1.297	1.390
3-c	0.32	0.46	-0.47	-0.45	1269	1.369	1.321
4-a	0.48	0.64	-0.26	-0.23	1286	1.357	1.350
4-b	0.41	0.55	0.00	0.09	1239	1.351	1.348
5-a	0.46	0.61	-0.08	0.01	1257	1.354	1.351
5-b	0.50	0.67	-0.10	-0.02	1203	1.284	1.372
5-c	0.44	0.63	-0.21	-0.14	1192	1.310	1.349
6-a	0.48	0.63	0.01	0.09	1235	1.357	1.347
6-b	0.49	0.64	-0.03	0.04	1173	1.303	1.353
7-a	0.33	0.48	-0.33	-0.27	1325	1.293	1.388
7-b	0.55	0.71	-0.05	0.01	1298	1.317	1.382
8-a	0.69	0.85	-0.14	-0.10	1379	1.358	1.355
8-b	0.52	0.67	-0.18	-0.12	1357	1.327	1.363
9	0.62	0.76	-0.02	0.04	1214	1.307	1.356

Table S2 Energetic aspects of surface H_2O^* dissociation with n adsorbing OH* (n = 1-8), $\Delta E_{TS,ZPE}^{\neq}$ and $\Delta E_{TS}^{\neq}$ were energy barriers of H_2O^* dissociation with or without ZPE correction, respectively;

$\Delta E_{r,ZPE}$ and ΔE_r were reaction energies of H_2O^* dissociation with or without ZPE correction, respectively; σ_{TS}^{i} were imaginary frequencies of transition states for H_2O^* dissociation; $d_{O\cdots H}^{\neq}$ and $d_{C\cdots H}^{\neq}$ were the lengths of breaking O-H bond of $H_2O^*$and lengths of forming C-H bond of C site in the transition state, respectively. Energies were in eV with H_2O^* adsorption states as reference, distances were in Å and frequencies were in cm^{-1}

	n*HO* + H_2O* → (*n* + 1)HO* + H						
n	$\Delta E_{TS,ZPE}^{\neq}$	$\Delta E_{TS}^{\neq}$	$\Delta E_{r,ZPE}$	ΔE_r	σ_{TS}^{i}	$d_{O\cdots H}^{\neq}$	$d_{C\cdots H}^{\neq}$
1-a	1.00	1.15	0.71	0.78	1219	1.354	1.321
1-b	0.43	0.58	0.19	0.23	1020	1.345	1.295
1-c	0.35	0.49	0.11	0.19	1169	1.356	1.325
2-a	1.28	1.45	0.77	0.83	1232	1.361	1.311
2-b	0.72	0.86	0.33	0.36	985	1.405	1.267
2-c	0.46	0.60	0.15	0.18	1210	1.330	1.334
3-a	1.02	1.17	0.75	0.77	1172	1.368	1.301
3-b	0.96	1.11	0.73	0.79	1074	1.335	1.302
3-c	0.68	0.83	0.21	0.26	1213	1.377	1.315
4-a	1.53	1.69	0.91	0.98	897	1.468	1.250
4-b	0.96	1.14	0.87	0.95	853	1.458	1.260
4-c	0.82	0.99	0.61	0.68	1175	1.371	1.308
5-a	1.41	1.57	1.13	1.19	1059	1.429	1.272
5-b	1.06	1.23	0.95	1.02	851	1.464	1.260
5-c	1.02	1.19	0.77	0.85	914	1.442	1.267
6-a	1.67	1.86	1.18	1.27	1212	1.378	1.301
6-b	1.63	1.80	1.32	1.39	665	1.526	1.231
7	1.71	1.87	1.43	1.52	821	1.486	1.231
8	1.35	1.53	1.41	1.49	942	1.444	1.266

Table S3 Reaction rate constants k (s^{-1}) of elementary reactions at different surface coverage at 473.15 K; the reaction pathway with lowest energy barrier at each coverage was selected. (In order to cancel the error with low frequency mode in calculating the vibrational partition functions, frequencies below 200 cm^{-1} were shifted to 200 cm^{-1})

	surface OH* formation		**surface O* formation**			**surface H* formation**	
n	*n*H_2O*	*n*OH*	*n*OH*_deprotonation	*n*OH*_condensation $r_{forward}$	*n*OH*_condensation $r_{reverse}$	*n*H_2*	*n*H*
1	1.4×10^{10}	3.9×10^{8}	8.7×10^{4}	—	—	1.8×10^{10}	4.7×10^{9}
2	1.5×10^{9}	2.4×10^{7}	1.2×10^{2}	6.3×10^{12}	5.6×10^{11}	5.3×10^{7}	8.6×10^{5}
3	1.6×10^{9}	1.4×10^{5}	3.6×10^{-2}	6.0×10^{12}	4.4×10^{12}	1.6×10^{6}	1.8×10^{3}
4	1.4×10^{8}	5.5×10^{3}	4.9×10^{-2}	6.9×10^{12}	4.1×10^{10}	4.7×10^{6}	3.0×10^{4}
5	8.8×10^{7}	4.1×10^{1}	9.0×10^{-3}	8.0×10^{12}	1.6×10^{11}	1.2×10^{7}	1.9×10^{4}
6	2.9×10^{7}	3.7×10^{-5}	2.1×10^{-7}	2.4×10^{12}	1.0×10^{11}	2.5×10^{7}	1.9×10^{1}
7	9.2×10^{8}	3.7×10^{-6}	3.3×10^{-5}	6.8×10^{12}	1.9×10^{10}	9.9×10^{6}	5.8×10^{5}
8	2.1×10^{7}	1.3×10^{-2}	2.3×10^{-4}	8.9×10^{12}	3.6×10^{9}	2.6×10^{7}	8.8×10^{4}
9	1.6×10^{6}	—	9.1×10^{-4}	4.3×10^{12}	9.2×10^{9}	1.6×10^{7}	—

1

2

3

4

5

6

7

8

9

10

11

12

13

14

15

16

17

18

19

20

21

22

23

24

25

26

27

28

29

30

31

32

33

34

35

36